Aix*Marseille université
Initiative d'excellence

NNT/NL : 2020AIXM0001/001ED000

THÈSE DE DOCTORAT

Soutenue à Aix-Marseille Université
le 18 novembre 2020 par

Léandre VARENNES-PHILLIT

Visuomotor control of the fly when chasing a dummy target.

Discipline
Sciences du Mouvement Humain

Spécialité
Biorobotique

École doctorale
ED 463 SCIENCES DU MOUVEMENT HUMAIN

Faculté des sciences du sport de Luminy
UMR 7287 Institut des Sciences du Mouvement
163 Av de Luminy, 13009 Marseille, France

Deparment of Bioengineering
Imperial College London

Composition du jury

Prof. Karin Nordström Flinders Health and Medical Research Institute, Adelaide, Australia.	Rapporteure
Prof. Martin Egelhaaf Department of Neurobiology, Bielefeld University, Germany	Rapporteur
Prof. Reinoud Bootsma Aix Marseille Univ, ISM, Marseille, France.	Président du jury
Dr. Stéphane VIOLLET Aix Marseille Univ, CNRS, ISM, Marseille, France.	Directeur de thèse
Prof. Holger G. Krapp Department of Bioengineering, Imperial College London, United-Kingdom.	CoDirecteur de thèse

DGA

Imperial College London

I, undersigned, Léandre Varennes-Phillit, hereby declare that the work presented in this manuscript is my own work, carried out under the scientific direction of Stéphane Viollet and Holger Krapp, in accordance with the principles of honesty, integrity and responsibility inherent to the research mission. The research work and the writing of this manuscript have been carried out in compliance with both the french national charter for Research Integrity and the Aix-Marseille University charter on the fight against plagiarism.

This work has not been submitted previously either in this country or in another country in the same or in a similar version to any other examination body.

Marseille, November 4th 2020.

Résumé

Certaines mouches mâles pourchassent d'autres mouches en vol. Le projet de thèse vise à construire un modèle de contrôle sensorimoteur de ce comportement de poursuite. Une cible factice mobile induit le comportement de poursuite chez les mouches males. J'ai développé une plate-forme expérimentale où la position et l'orientation 3D de la mouche sont enregistrées pendant qu'elle poursuit la cible dont la trajectoire est contrôlée par ordinateur. L'analyse des trajectoires de vol a permis de caractériser le contrôle du changement de cap du poursuivant dans les trois dimensions. Plusieurs trajectoires de cible ont été utilisées dans le but d'étudier les stratégies cinématiques de la poursuite. J'ai découvert que le male de l'espèce *Lucilia* utilise le suivi de cible dans le plan horizontal et l'interception dans le plan vertical. Dans cette thèse je présente les structures neuroanatomiques impliquées dans ces différences de stratégie. J'ai également installé une caméra embarquée, située à proximité de la cible pour observer la rotation de la mouche autour de son axe longitudinal (angle de roulis). Cela a permis de valider l'hypothèse d'un vol coordonné et d'une réaction de type atterrissage dans les derniers instants de la poursuite. Dans ce projet, j'ai caractérisé les stratégies de poursuite de la mouche Lucilia. J'ai montré l'implication du roulis du corps pendant les virages serrés, enfin j'ai discuté du contrôle de l'orientation de la tête - ou de la coordination tête-corps -, qui est essentiel lors de l'exécution d'un comportement visiomoteur.

Mots clés: poursuite aérienne, mouche, insecte, stratégie de capture, stratégie d'interception, vision, neuroéthologie, orientation du corps, dynamique de vol.

Abstract

Short Abstract

Male blowflies chase and catch other flies in fast acrobatic flights. The project aims to construct model of the sensorimotor control of such chasing behaviour. A moving dummy target (a small sphere) induces chasing flights in freely flying flies. I designed an experimental platform where the 3d position and orientation of the fly was recorded while chasing the actuated dummy target. The analysis of the flies' trajectories helped to characterize the steering control of the pursuer, in the three dimensions. Changes of the trajectory of the dummy target were used to study chasing strategies through body kinematics. I discovered that the male *Lucilia* employs tracking in the horizontal plane and interception in the vertical plane. I discussed the neuroanatomical structures implicated in these differences. I also installed a camera close to the target to observe the rotation of the fly around its longitudinal axis (roll-angle). This validated the hypothesis of coordinated flight, and a landing-like response just before capturing the target. In this project I characterized blowfly pursuit strategies, argued the necessity of body roll during sharp turns, and discussed the control of head orientation – or head-body coordination –, which is essential when performing visuomotor task.

Key words: aerial pursuit, fly, insect, capture strategy, interception strategy, vision, neuroethology, body orientation, flight dynamics.

Long Abstract

It is difficult to swat a fly and completely unthinkable to catch it on the wing. However, in several species of Diptera, the male detects, pursues, and catches the female in flight, a crucial achievement for the survival of the species. Flies may be found in every habitat, from cities to countryside. Males are on the alert, the pursuit can take place anywhere, even in very cluttered places such as undergrowth. This behaviour is both extremely fast and robust - i.e. indifferent to external conditions. The fact that this formidable reflex is carried out by an animal with a brain structure smaller than a pinhead is of interest to scientists of all kinds, biologists, behaviourists, neuroscientists, engineers, from civil society and the military. Dipteran flies have very diverse morphologies. Millions of years of evolution have given each pursuer the best assets to succeed in capturing the target that suits him. The morphological variations echo with behavioural diversities. Indeed, each species has its own pursuit style. Inter-species variations are, for the most part, the result of neuroanatomical disparities. Several vision-guided reflexes have been identified in the fly. These reflexes have independent visual information processing mechanisms, but they are undeniably linked at the level of motor neurons. I will present those that can interact with the pursuit reflex: optomotor response, looming response, and object fixation. In each case I will present experiments performed on flies, and how the results of these experiments contributed to the understanding of these visual reflexes. In this thesis I am interested in the sensorimotor control of chasing behaviour of the blowfly *Lucilia*. For the male to succeed in its mission, each of the three phases must be passed, target detection, tracking, and of course capture. The male blowfly pursues a dummy target (small black sphere) in the laboratory as if it were a female in the wild. I have developed an experimental setup in which the male blowfly pursues the dummy target whose trajectories are controlled by computer. The scene is under the coverage of two high-speed cameras. After 2d tracking of the actors' positions on the images of the two films, the positions of the target and the fly are reconstructed in 3D, as well as the orientation of the longitudinal body-axis of the pursuer. Positions and orientations will serve as a support to identify the sensorimotor control loops responsible for the chasing reflex.

Two target trajectories are presented to the males, one circular, the other following a spring-shaped path. These trajectories cover rather diverse possible combinations of translations and rotations of the target at different speeds. The analysis of the chaser's movements brings to light very interesting behaviour. First, the pursuit strategies differ according to the plane of approach. In the horizontal plane the fly executes a tracking strategy, while in the vertical plane I observe an interception strategy. Behavioural data suggest a mixed steering control, based on a combination of error angle (θ_E, the angle formed between the speed vector and the line of sight: the line connecting the fly and the target), and on the bearing angle rate ($\mathrm{d}\theta_A/\mathrm{dt}$ or Ω_A being the rate of the angle formed between line of sight and line between the fly and a stationary point in the environment), each with a gain, k and N, respectively. This mixed control strategy between θ_E and Ω_A has been documented for one hawk species (Brighton and Taylor

2019). I implemented a kinematic model of pursuit based on the behavioural data just recorded. The behaviour of this virtual fly shows that the angular velocity component of this control law ($N.\omega_A$) does not participate significantly to improve the pursuer's trajectory under the tested conditions. I conclude that this control block is probably not used by the system. Thus, two simple proportional laws command the steering, one in azimuth and one in elevation, with their own gain ($k_H = 26\ s^-1$ and $k_V = 10$ s^-1) and time delay ($\Delta t_H = 10$ ms and $\Delta t_V = 21$ ms). Note that the a time delay of 10 ms is the fastest ever encountered in a pursuit behaviour so far.

In my model, the difference between tracking and interception resides in the offset value the system applies in elevation. The hypothesis is reinforced by the fronto-dorsal position of an area of the male's retina which is known to be related to the chasing behaviour. This acute zone, also known as the love spot in males, present better properties than the rest of the surface of the compound eye - better optics, photoreceptor's action potential faster and with higher amplitude, and neural connections feeding into sex specific pathway. In the horizontal plane, the velocity vector and the longitudinal body axis are not always aligned, which evokes the presence of side-slips. In the vertical plane, however, the body is never aligned with the velocity vector, but remains equal to a constant angle different from zero. In my experimental conditions, this angle is kept constant, which shows the absence of side-slips in the vertical plane.

The installation of a third camera embedded in the pursuit and filming the final phase as close as possible to the target provides another view of the scene. I observe that the body of the fly is often in rotation around its longitudinal axis (body-roll). In a similar way than fixed wing aircraft, during pursuit the fly changes its flight direction by mean of banked turns. The analysis of the translational velocity profiles shows that during sharp turns the fly considerably reduces its forward speed before turning. The presence of a banked turn coupled with a reduction in the forward speed is in favour of coordinated flight. The latter ensures minimum energy expenditure by keeping the centrifugal force low. This point is not documented for insects in aerial pursuit, so far.

Flying insects, like almost all visually oriented animals, tend to maintain a default orientation of their eyes to the environment. Gaze stabilization serves a number of functions, including: 1- simplifying the estimation of translational self-motion, 2- aligning head-based sensory systems with the inertial vector that facilitates the transformation of sensory signals into motor commands, and 3- reducing motion blur in visual input. The embedded module provides series of images of the pursuit during which the pursuer's head is not aligned with the body nor with the external horizon. Why would the gaze stabilization be paused or reduced during pursuit? We will wonder about the movements of the head in reaction to the rather important rotations of the body along its 3 axes. The control of the pursuit is entirely based on the projection of the target on the pursuer's retina. Any movement of the head will have consequences on the retinal image and thus on the tracking behaviour. During the last moments of the pursuit, when the male is within a very short distance of the target, he performs a last acrobatic manoeuvre. While pulling up, the male extends its legs to catch the target. This behaviour looks like the landing response triggered by

the sight of an approaching object in tethered flies' experiments. I will finish my thesis by giving for each phase of the pursuit, future directions, questions, or experiments to explore.

Acknowledgements

Thank you to my supervisors, Stephane Viollet and Holger Krapp, for inspiring this project.

Thank you Stephane for always caring, and being positive. Thank you for quickly changing direction in front of a dead end road. You really helped me to move forward.

Than you Holger for encouragement at every step. Thank you for bringing back the meaning and importance of the project. Thank you for hiring me and pushing the challenge to follow two projects in parallel. Also thank you for patiently improving my writings.

I am very grateful to have been part of the two extraordinary teams. Thank you to every member of the Biorobotic team in Marseille, with special thanks to Julien Diperi for his great work and for making things fun. Thank you to Ben Hardcastle, Jiaqi Huang and Martina Wicklein in Imperial, for welcoming me and showing me the way. You patiently showed me the basics of studying fly behaviour, thank you.

Thank you to lab mates Valentin Riviere, Roman Goulard and Martin Bossard for invaluable advice and company through many late nights.

Doctoral school staff Gilles Montagne and Nathalie Roustan have kept me on track, thank you too.

Thank you to members of my examination jury, my thesis reviewers, Karin Nordstrom and Martin Egelhaaf, for manuscript improvements, as well as Nicolas Franceschini and Reinoud Bootsma for advice and discussion. Thanks to Remy Casanova for taking an interest in my work.

Thanks to Veronique Serfaty, at DGA and Victoria Cox at DSTL, for offering additional lines of support and for the opportunities to travel and present my work regularly.

Thank you to the DGA for financial support.

Finally, thank you to the friends I have made along the way, Jerem, Anna, Grantoine, Aude and Raph. Special thanks to older friends for their unconditional support, and their help to cross the final line.

Thank you to my family, you kept me going. Thank you the Falque family for offering me the best working conditions. Merci Mam pour tous les sacrifices.

Thank you Charlotte for making this thesis better such as everything you touch. Thank you for your presence all along the bumpy path. Most of all, thank you for giving birth to my hero, Marius.

Léandre P. Varennes | *Dr (soon), MEng, PharmD*

20 Rue Saint Savournin – 13001 Marseille, France

leandrev@hotmail.fr • DoB: 30-08-1988

Research Assistant

Imperial College London, Oct 2017- March 2019

Electrophysiology experiments. I focused on extracellular recordings from optic flow processing inter-neurons in the fly motion vision pathway. I developed the experimental procedure, upgraded and changed technical components, performed and analyzed quantitative electrophysiological experiments.

Implementation of the visual display a data projector-based device (DLP) with Python. Configuration for multiple electrophysiological experiments with flies. Creation of a platform to generate desired visual stimuli with Matlab. I also designed the implementation of the DLP with rotating polarization filters. These experiments will give valuable information on how polarized light is processed in various species of flies.

PhD scheme

Sept 2014–Oct 2017, Validated in Nov 2020

Head Body Movements In Free Flying Flies When Chasing A Dummy Target.
Supervisors: Dr. Stéphane Viollet (Aix Marseille Université) and Prof. Holger G Krapp (Imperial College London)

- **Aix Marseille Université, Equipe Biorobotique** — **Marseille (Fr)**
  Building setup, method paper and pursuing flies data analysis — *Aug 2015–Aug 2017*
  Designing synthetic trajectories of the target. Upgrading the experimental arena with an embedded observation point. Building this dedicated microendoscope to observe a pursuing fly during its final approach. Validation of capabilities.

- **Imperial College Bioengineering Department** — **London (UK)**
  Initial state — *Oct 2014–Jul 2015*
  Literature review on insects vision. Defining the requirements of the experimental setup. Validation of the first prototype and first experiments on pursuit flights. 3D actuation of the target that is pursued by a male fly. Skills on high speed videography and quantitative behavioral data analysis

Publications

Two pursuit strategies for a single sensorimotor control task in blowfly. — **Scientific Reports**
L. Varennes, H. Krapp, S. Viollet, — *2020*

Implementation of a 1440Hz DLP for calibrating Optic Flow sensors — **IEEE MED'2020**
C. Viel, L. Varennes, S. Viollet, — *2020*

How do hoverflies use their righting reflex? — **Journal of Experimental Biology**
A. Verbe, L. Varennes, J.L Vercher, S. Viollet, — *2020*

A novel setup for 3D chasing behavior analysis in flies — **Journal of Neuroscience Methods**
L. Varennes, H. Krapp, S. Viollet, — *2019*

Conferences

- Talks:

DSTL UK-French PhD Scheme Conferences — **Portsmouth (UK)**
A new setup for 3D chasing behavior analysis in flies — *2017*

DSTL UK-French PhD Scheme Conferences — **Salisbury (UK)**
Gaze stabilization in free flying flies when chasing a dummy target — *2015*

- Posters:

35th International Ethological Conference, Behavior 2017 **Estoril(Pt)**
A new setup for 3D chasing behavior analysis in flies (2) *2017*

Gordon Research Conference, Neuroethology 2017 **Les Diablerets(Ch)**
A new setup for 3D chasing behavior analysis in flies (2) *2017*

DGA Fr-UK conference 2016 **Paris(Fr)**
A new setup for 3D chasing behavior analysis in flies (1) *2016*

DSTL UK-French PhD Scheme Conferences: 2015 **Salisbury(UK)**
Gaze stabilization in free flying flies when chasing a dummy target *2015*

Education

Academic Qualifications

- **MINELEC Université de Provence** **Marseille (Fr)**
  MScRes Nanotechnologies *2013*
- **Ecole des Mines** **St Etienne (Fr)**
  MEng Electrical and Electronic Engineering , Intelligent systems, Bioelectronics *2011–2013*
- **Université Lyon 1** **Lyon (Fr)**
  PharmD, BSc and MSc Pharmacy (Biology, Zoology, statistics, social behavior, cell culture) *2006–2014*

Notable Projects

- **PharmD (French Doctor of Pharmacy)** **Université Claude Bernard Lyon 1 (Fr)**
  Defended thesis. Jury : Prof Hartmann, Prof Goffette, Dr Boeuf *2014*
  'Electrical and implantable devices, from functional stimulation to the increase of human capabilities.'
- **MScRes Project: Monash University** **Melbourne (Aus)**
  Internship in Biochemistry lab of Pr Winther Jensen. *2013*
  'Increase properties of polymer PEDOT-PSS-Gelatin for electrode creation in a bionic eye application.'

Technical and Personal skills

- **Biology**: Animal vision, polarization vision, behavior analysis, neuroethology, electrophysiology, extracellular recordings, animal preparation, dissection, media preparation, pharmacology.
- **Computing**: image processing and high speed videography, DLT and 3D reconstruction, signal processing, neuronal activity analysis, statistics, model of dynamic behavior and its control. Proficient in: Matlab, Arduino, C.
- **Optics**: polarized filters, microscopy, fiber optics, high speed cameras and objectives, stereocameras.
- **Others**: CAD, 3D printing, laser cutting.
- **Previous jobs: Pharmacist** (1000h), quality and validation and delivery of medicines. production in hospital and industry. Team manager, and teacher in University. I've been working since I was 16.
- **Other:** Trail, Literature, Music.

Formations *(en Français)*

Méthode, Outils, Language: 34h

- **Enregistrement et traitement des signaux** — **Faculté des sciences du sport Luminy Marseille**
  Valid: Sciences du Mouvement Humain — *18h*
- **Lecture rapide et efficace** — **Campus St Charles, Marseille**
  Valid: Sciences du Mouvement Humain — *16h*

Insertion Professionnelle: 34h

- **Docteur et fonction publique : perspectives et reconnaissances?** — **Campus St Charles, Marseille**
  Valid: Collège Doctoral Aix- Marseille Université — *10h*
- **Innovations, intégrations, technologies: les limites du corps** — **Université Paris 1 Panthéon Sorbonne**
  Valid: Sciences du Mouvement Humain — *7h*
- **Normes usages et detournements** — **UPMC Sorbonne Universités ISIR**
  Valid: Sciences du Mouvement Humain — *7h*
- **Rendez-vous de la cohorte : poursuite de carrière** — **Campus Saint Charles, Marseille**
  Valid: Sciences de la Vie et de la Santé — *6h*
- **Prendre ses fonctions de doctorant** — **Campus Luminy, Marseille**
  Valid: Collège Doctoral Aix- Marseille Université — *4h*

Ouverture Scientifique: 61h

- **Posture Ethique du Chercheur et Communication** — **Belle de Mai et campus Saint-Charles, Marseille**
  Valid: Collège Doctoral Aix- Marseille Université — *24h*
- **Zététique et autodéfense intellectuelle** — **campus Saint-Charles, Marseille**
  Valid: Collège Doctoral Aix- Marseille Université — *16h*
- **Nuit des Chercheurs 2016** — **Marseille**
  Valid: Sciences du Mouvement Humain — *6h*
- **De la théorie à la métathéorie. Approches des formes du savoir** — **IMéRA, Aix-Marseille**
  Valid: Collège Doctoral Aix- Marseille Université — *6h*
- **Biomimétisme et Bio-inspiration** — **IMéRA, Institut d'études avancées d'Aix-Marseille**
  Valid: Sciences du Mouvement Humain — *4h*
- **Epistémologie et sociologie des sciences : stage de réflexion** — **campus Saint-Charles, Marseille**
  Valid: Collège Doctoral Aix- Marseille Université — *3h*
- **LaTeX** — **campus Saint-Charles, Marseille**
  Valid: Collège Doctoral Aix- Marseille Université — *2h*

Contents

Résumé 3

Abstract 7

Acknowledgements 8

CV 12

Contents 12

List of Figures 15

List of Tables 17

List of acronyms 18

Glossary 19

1 Fly's aerial pursuit as a visual behaviour, and how nature optimised the chaser's physiology. 21
- 1.1 Introduction . . . 23
- 1.2 Fly vision . . . 25
  - 1.2.1 Compound eyes . . . 25
  - 1.2.2 Motion vision . . . 27
- 1.3 Visually evoked behaviors, and experiments . . . 30
  - 1.3.1 Optomotor response . . . 30
  - 1.3.2 Responses to looming stimuli . . . 32
  - 1.3.3 Following an object: object fixation or target pursuit? . . . 35
  - 1.3.4 Object fixation . . . 35
- 1.4 Target Pursuit . . . 38
  - 1.4.1 Target detection . . . 38
  - 1.4.2 Tracking . . . 43
  - 1.4.3 Final approach and capture . . . 44

2 A novel setup for the analysis of free flight chasing behavior. 45
- 2.1 Introduction . . . 47
- 2.2 System description . . . 49
  - 2.2.1 Principle of operation: . . . 49

2.2.2 Accuracy of generating and reconstructing target trajectories: . 54
2.2.3 Spatial resolution of the cameras 56
2.3 Analysing 3D chasing flights 59
2.3.1 Parameters describing strategies of catching targets 59
2.3.2 Parameters describing the orientation of the fly during pursuit flights 63
2.4 Discussion 65
2.5 Latest system upgrades 68

3 Two pursuit strategies for a single sensorimotor control task in blowfly. 78
3.1 Introduction 80
3.2 Pursuit strategies in flying animals 82
3.2.1 Constant target heading angle 82
3.2.2 Constant bearing angle 84
3.2.3 Mixed pursuit 84
3.3 Analysis of blowfly's pursuit 85
3.3.1 Experimental conditions 85
3.3.2 Distribution of invariant parameters 86
3.3.3 Kinematics: control of steering 88
3.3.4 Limits of the constant target altitude 90
3.4 Developing kinematic models 91
3.5 Developing dynamic models 95
3.6 Conclusion 97

4 Discussion 99
4.1 Introduction 101
4.2 Neuroanatomical structures of the pursuit 102
4.2.1 Love spot in *Lucilia* 102
4.2.2 Neurons implicated in pursuit 102
4.2.3 Body shape and horizontal side-slip 108
4.3 Coordinated flight 110
4.3.1 Banked turns 110
4.3.2 Forward speed 112
4.3.3 Horizontal steering influences vertical steering 113
4.4 Head-body movements while chasing 115
4.4.1 Gaze stabilization 115
4.4.2 The head is not locked to horizon 117

5 Conclusion 119
5.1 Concluding remarks 120
5.2 Future directions 121

Conclusion 122

Bibliography **123**

ANNEXE **145**

List of Figures

1.1 Minimum energy cost of transportation. 24
1.2 Fly's vision: compound eyes and optic lobes. 26
1.3 Global structure of translatory and rotatory optic flow fields, and local analysis of visual motion. 28
1.4 General principles of 3 visually driven behaviours in *Drosophila*. 30
1.5 Optomotor response analysis in flies under free flight conditions. . . . 31
1.6 Fly's response to looming stimulus. 33
1.7 Optomotor response and figure (object) fixation. 36
1.8 Retinal profile of the target. 39
1.9 The 'love spots' of flies. 40

2.1 Schematic view of the chasing arena. 50
2.2 Pictures of the chasing arena. 51
2.3 Precision of a circular target trajectory across 11 trials. 53
2.4 Precision of a ellipsoidal target trajectory across 11 trials 55
2.5 Validation of the 3D trajectory reconstruction method. 57
2.6 Preliminary results: Example of fast capture and long pursuit characterization 60
2.7 Preliminary results: Analysis of dynamics in a capture 61
2.8 Embedded pictures of the target and the pursuer 66
2.9 Improvements of the videography and calibration. 68
2.10 Latest version of the microendoscope. 70
2.1 List of equipment: arena and actuation 72
2.2 List of equipment: Observation, first version 73
2.3 System representation as functional schematics 74
2.4 Stereovision, record and track 75
2.5 3D reconstruction and positions analysis. Example of a very long pursuit characterization 76
2.6 Analysis of the mechanical repeatability 77

3.1 Definition of angular parameters during pursuit, and planar pursuer's trajectories with different control strategies. 81
3.2 Graphical definition of the angular parameters in the horizontal and the vertical plane. 86
3.3 Distribution of the angular parameters: mean vector and standard deviation. 87
3.4 Impact of angular and angular rate parameters on the heading. 89

3.5 Optimization of gains for the three steering control models. 92
3.6 Experimental and model trajectories. 93
3.7 Models of chasing behaviour. 96

4.1 Organization of the male specific neuronal pathway. 103
4.2 Wide-field motion-sensitive neurons, optomotor response and pursuit. 105
4.3 Final approach and target's projection on fly's retina. 107
4.4 View from the embedded camera and banked turn 111
4.5 Looking for relationships between horizontal speed and other variables 112
4.6 Relationship between horizontal and vertical steering. 114
4.7 In head-fixed model, two approaches may bring back the target into the love spot 116
4.8 Capture of the target, recorded by a Awaiba microcamera. 117

List of Tables

1.1 General optomotor properties in flies 34
1.2 General collision avoidance properties in flies. 35
1.3 General properties of object fixation in flies. 37

3.1 Equations governing steering for different pursuit strategies. 83

List of acronyms

BP
Biased pursuit. 81–83, 88, 91–93

CBA
Constant bearing angle. 83

CTHA
Constant target heading angle. 83

DTT
Distance to target. 39, 62, 63

LoB
Line of body. 56, 57, 62–65, 101, 109, 110, 113

LoF
Line of flight. 62, 64, 65, 80, 81, 85, 101, 109, 110

LoS
Line of sight. 56, 57, 62–64, 80, 81, 85, 94, 101, 109, 113

MP
Mixed pursuit. 83, 91–93

PN
Proportional navigation. 81, 83, 84, 87, 88, 91, 92

PP
Pure pursuit. 81–84, 88

Glossary

θ_A
: Bearing angle: angle formed between line of sight and reference frame. 5, 62, 80, 81, 83–89, 91

θ_{AH}
: Horizontal component of the bearing angle. 56, 57, 62, 63, 85, 87

θ_{AV}
: Vertical component of the bearing angle. 56, 57, 63, 85, 87, 90

θ_B
: Fly longitudinal body angle: angle formed between line of body and reference frame. 62

θ_{BH}
: Horizontal component of the fly longitudinal body angle, or Yaw-angle. 56, 57, 62, 63

θ_{BV}
: Vertical component of the fly longitudinal body angle, or Pitch-angle. 56, 57, 63

θ_E
: Flight error angle, or just error angle, is also referred as target heading angle: angle formed between line of flight and line of sight. 5, 62, 63, 80–84, 86–91, 95, 96, 109, 112

θ_{EB}
: Body error angle: angle formed between line of body and line of sight. 62–64, 109, 113

θ_{EBH}
: Horizontal component of the body error angle. 62, 64

θ_{EBV}
: Vertical component of the body error angle. 62, 64

θ_{EH}
: Horizontal component of the target heading angle. 62, 64, 85, 87, 89, 113

θ_{EV}
: Vertical component of the target heading angle. 62, 64, 85, 87–90

θ_P

Heading angle: angle formed between line of flight and reference frame. 62, 81, 84–89

θ_{PH}

Horizontal component of the heading angle. 62, 85, 87

θ_{PV}

Vertical component of the heading angle. 85, 87

1 Fly's aerial pursuit as a visual behaviour, and how nature optimised the chaser's physiology.

Sommaire

1.1 Introduction . . . 23
1.2 Fly vision . . . 25
1.2.1 Compound eyes . . . 25
1.2.2 Motion vision . . . 27
1.3 Visually evoked behaviors, and experiments . . . 30
1.3.1 Optomotor response . . . 30
1.3.2 Responses to looming stimuli . . . 32
1.3.3 Following an object: object fixation or target pursuit? . . . 35
1.3.4 Object fixation . . . 35
1.4 Target Pursuit . . . 38
1.4.1 Target detection . . . 38
1.4.2 Tracking . . . 43
1.4.3 Final approach and capture . . . 44

1.1 Introduction

Chapter outline. This first chapter aims to present the context of the thesis and the question will be raised whether the pursuit in blowfly *Lucilia* could be modeled as a visuomotor control. During my PhD project thesis I realised behavioural experiments, I analysed series of parameters during the pursuit, and the data I obtained served to create models of chasing response of blowfly. In the introduction I will provide a motivation for flies often being used as model organisms in neuroethology to study the neuronal basis of behaviour and how they may inspire novel approaches in engineering. In the next part I will describe fly vision, starting with the morphology of the compound eye and then showing the importance of visual wide-field motion, or optic flow, used to estimate the fly's self motion in a textured environment. In the third part I will present three visually evoked behaviors: optomotor response, looming detection and object fixation. I will focus on the description of simple behavioral experiments that allowed neuroethologists to derive models of sensorimotor control. Optomotor reflexes stabilize the animal's head and body orientation against external perturbations in a visually structured environment. Looming stimuli elicit collision avoidance, escape or landing responses. And during object fixation the fly follows movements of an object while ignoring the background motion. In the last part I will focus on the aerial pursuit of small targets. Pursuers use vision to control their chasing flight. Aerial pursuit can be divided in 3 phases: detection, tracking and capture. For each of these phases I will present some useful anatomical and physiological adaptations that improve the pursuer's chasing performance.

Fly's generalities. Among invertebrates, insects, characterized by a segmented body plan, are not only the largest taxon of arthropods, but the most numerous in the whole animal kingdom with 6 to 10 millions of extant species. They can be found almost all over the world with diverse body size and shapes especially adapted to their habitat. Many insects show highly complex adaptive behaviors, from simple reflexes such as optomotor response, avoiding collision or catching evasive prey, up to solving cognitive tasks such as learning abilities, and social interactions. Spatial orientation skills also stay reminiscent of the abilities of vertebrates and even humans.

Insects are the only invertebrates that have developed flight. As far as we know, flapping-wing flight appeared only four times in the animal kingdom: insects, Pterosaurs, birds and bats. Insects were the first to develop flight about 350 million years ago during the Carboniferous, and their incredible adaptability has kept them alive and evolving until today. Besides the advantages that flight offers in terms of locomotion and escape, it is 10 times more energy efficient than walking when looking at the energy costs: the minimum energy used to move mass per distance, see Figure 1.1.

Inside the insect class, true flies or Dipteran (wearing 2 wings) flies are arguably one of the most diverse orders in the animal kingdom. The only thing they all have in common is that they have 2 wings, 3 body segments and 6 legs. However, moving in three dimensions while avoiding obstacles or chasing a target requires a very fast

and efficient sensorimotor control to survive. Their small size, comparatively simple nervous systems and highly efficient compound eyes make flies an ideal model system to study how animals use vision-based information to control behavior (Land and D.-E. Nilsson 2012). Their brain, often referred to "minute structures controlling complex behaviors" (Kinoshita and Homberg 2017) make them a great source of inspiration for engineers.

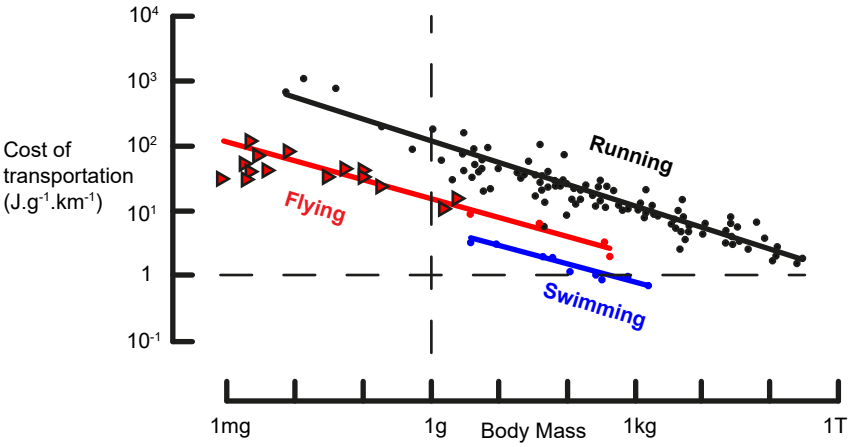

Figure 1.1 – **Minimum energy cost of transportation (COT) for running, flying and swimming animals as a function of their body mass.** Data are plotted on double logarithmic scales. Flying insects are presented by triangles. This figure was adapted from Butler 2016.

Behavioural studies in Diptera. With their small brain (Strausfeld 1976), insects are often considered to be "simple reflex machines", or "deterministic systems" (Nicolas Franceschini 2014; Chittka 2016). In the manner of the Braitenberg vehicles (Braitenberg 1986) it is possible to predict their movements based on external stimuli. Recent studies challenged this "deterministic" hypothesis. Researchers found evidence of selective attention within dragonfly visual systems (Wiederman and O'Carroll 2013; Lancer, Evans, J. M. Fabian, et al. 2019). The activity of individual neurons reflects the response to either of two simultaneously presented targets, but not a combinations of the responses to both. Other cases of non deterministic responses are found with internal modulation of neuronal processing (Maimon, Andrew D. Straw, and Dickinson 2010), via the release of neuromodulators during different locomotor, nutritional or arousal states, haltere activation, and sublethal toxicity of Neonicotinoid and sulfoximine pesticides (Suver, Huda, Iwasaki, et al. 2016; Longden, Muzzu, Cook, et al. 2014; Gorostiza, Colomb, and Brembs 2016; Andretic, Van Swinderen, and Greenspan 2005; Rosner, M. Egelhaaf, Grewe, et al. 2009; Parkinson, S. Zhang, and Gray 2020). These results bring a new dimension to the complexity of behavioural studies and may require additional experimental controls when the deterministic model is not sufficient

to explain the studied behaviour. In the work on aerial chasing behaviour presented here, we do not seek to deprive the animal of resources, nor compare different weather conditions during flight. Also, mating behaviour in male blowflies appears 4 days post-hatching and is fairly constant over the life time of the male. Thus, considering classical scheme of studies on insect flight, for which it is accepted that the behaviour can be considered largely deterministic (Censi, Andrew D. Straw, Sayaman, et al. 2013), other aspects may matter in this context: time-invariance and linearity.

1.2 Fly vision

Light influences behaviour in many ways. Locomotor activity is only one example of a biological process that shows a prominent circadian rhythm. A rudimentary eye with only a few photoreceptors can provide the organism with enough visual information to perform phototaxis behavior (Randel and Jékely 2016) and the best camera eyes feature a spatial acuity that can reach about 100 cycles/deg providing enough detail to recognize an individual, its distance and even infer a person's emotional state based on their facial expression.

Unlike mechanoreceptors which require contact force, vision is very convenient to identify threats and objects of interest over an extended distance range. Thus, vision provides obvious advantages among other senses in the context of survival, but also secondary effects, i.e. good vision enables accurate sensorimotor control, reducing the waste of energy due to inefficient locomotion.

The eyes receive the light information filtered and processed according to the ecological needs of the animal (principle of matched filters (Wehner 1987)). It is then pre-processed in the retina – extracting qualities such as light intensity, colour, angle of polarization, contrast movement – or later in the nervous system enabling pattern recognition, looming detection and self-motion estimation based on optic flow. In insects, the peripheral stage of the visual system is given by the compound eyes.

1.2.1 Compound eyes

General anatomy of the compound eyes: Most of the fly's head is covered by the compound eyes (Fig. 1.2***a***). With their 4,000 facets called ommatidia they provide the blowfly with a panoramic field of vision of nearly 4pi, except for a small patch in the rear, that is obstructed by the fly's body (Petrowitz, Dahmen, Martin Egelhaaf, et al. 2000). Each facet samples light within a small fraction of the visual environment. True flies spatial acuity depends on the species. *Drosophila* only has 400 ommatidia (review in Roger C Hardie 1985; Land 1997), but information coming from the compound eyes are essential for flight control and navigation (Land and D.-E. Nilsson 2012).

Ommatidia: Behind each facet there are 8 photoreceptors (storing the photosensitive molecule rhodopsin) arranged in a circular configuration numbered from 1 to 7

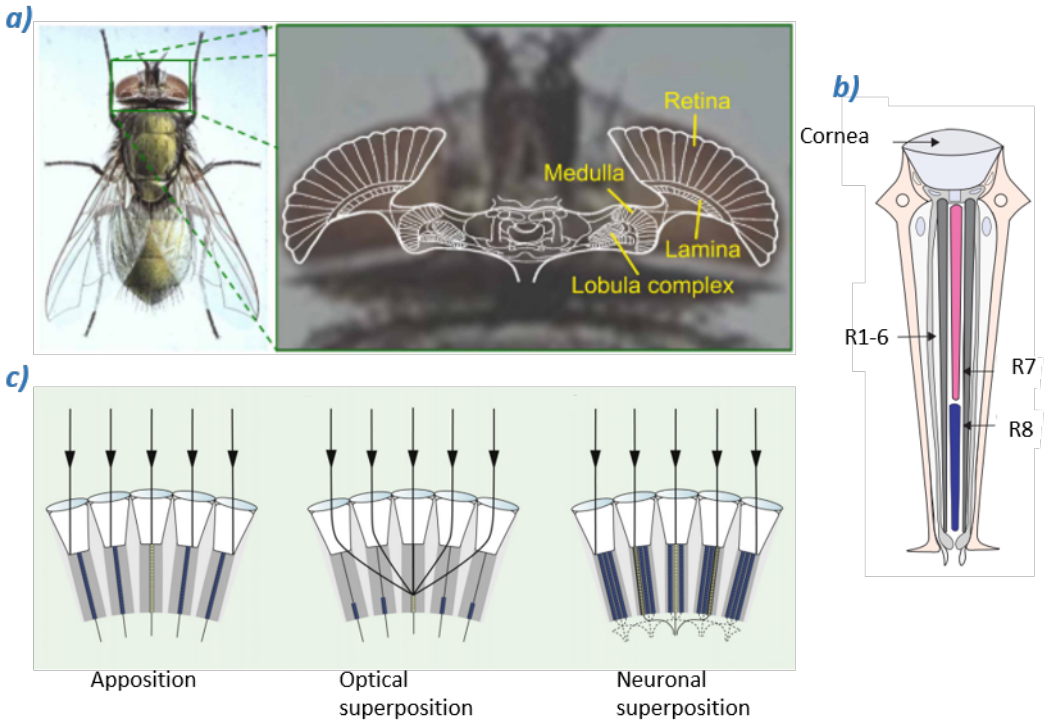

Figure 1.2 – **Fly's vision: compound eyes and optic lobes.** ***a)*** Schematic of a horizontal section of the fly's brain projected onto a photograph of its head, with the retina and the three main visual neuropiles labeled. Taken from Martin Egelhaaf, Boeddeker, Roland Kern, et al. 2012. ***b)*** Enlarged view of an ommatidium containing the cornea and photoreceptors R1–R8. The R1–R6 photoreceptors are located in the outer part of the ommatidia, while R7 and R8 are located in the middle, R7 being on top of R8. Light goes in through the lens (top) and enters the rhabdomeres of the different photoreceptors to stimulate rhodopsin. Taken from Andres-Bragado and Sprecher 2019. ***c)*** Compound eyes with apposition, optical superposition, and neural superposition structure, taken from Borst 2009.

with the number 7 in the center, and the 8 placed under the number 7 (Fig. 1.2***b***). The temporal response and spectral sensitivity of the photoreceptors is matched to the ecology of the animal. In *Drosophila*, photoreceptors R1–R6 have the same spectral sensitivity throughout the eye and are responsible for motion detection (see section 1.2.2). In contrast, photoreceptors R7 and R8 exhibit heterogeneity and are important for color vision (Yamaguchi, Desplan, and Martin Heisenberg 2010). Rapidly flying, manoeuvrable diurnal Diptera from several families have fast R1-6 photoreceptors with corner frequencies (the frequency at which signal power falls by a half) between 50 and 107 Hz (S B Laughlin and Weckström 1993).

Optical and Neuronal Superposition: The Diptera's eye is not a "classical" compound eye or apposition eye, in which each facet samples a distinct location in the visual field (Fig. 1.2***c***). The neural superposition eye present in the flies we are interested in – hoverflies, blowflies and houseflies– was first describes in the 70's (Fig. 1.2***c***). Kirschfeld and Franceschini (between 1967 and 1971) found that the angle between two adjacent facets, the interommatidial angle, is the same as the angle between two adjacent rhadomeres in two adjacent ommatidia. Franceschini illuminated the compound eye from behind to follow the light path. When the beam was very thin he observed that 7 adjacent facets were illuminated. This finding opens the way to neural and optical superposition structures.

The deep pseudopupil phenomenon, that comes from the neural superposition structure is often used to align the head of the animal in electrophysiology experiments with the coordinate frame of a given visual stimulation device. The presence of the neural superposition is consistent with Ramon y Cajal's drawings and Strausfield's numerous photographs of the connections coming out of the fly's retina show the same form of crossing and density (Strausfeld 1976).

1.2.2 Motion vision

Relative motions between the eyes and visual structured surroundings always result in retinal image shifts. Self-motion causes coherent wide-field motion patterns covering the entire visual field. In contrast, external object motions within the visual field of an otherwise motionless observer result in image shifts which are usually locally confined. Both kinds of image shifts can be described in terms of velocity vector fields, called 'optic flow fields', where the local vectors indicate the direction and magnitude of the respective relative motion (Gibson 1951; Koenderink and Van Doorn 1987). In general, the resulting optic flow contains information which may be used to control visually guided behavior. First, the global structure of the optic flow depends on the observer's self-motion – the overall appearance of a flow field induced by a translation differs from a flow field generated during rotation (Fig. 1.3 ***b-c***). And second, the magnitude of the translatory optic flow depends not just upon the respective translation speed but also on the distance between the observer and the visual structures of the surroundings (Fig. 1.3***d***). Objects close by result in higher image velocities than more

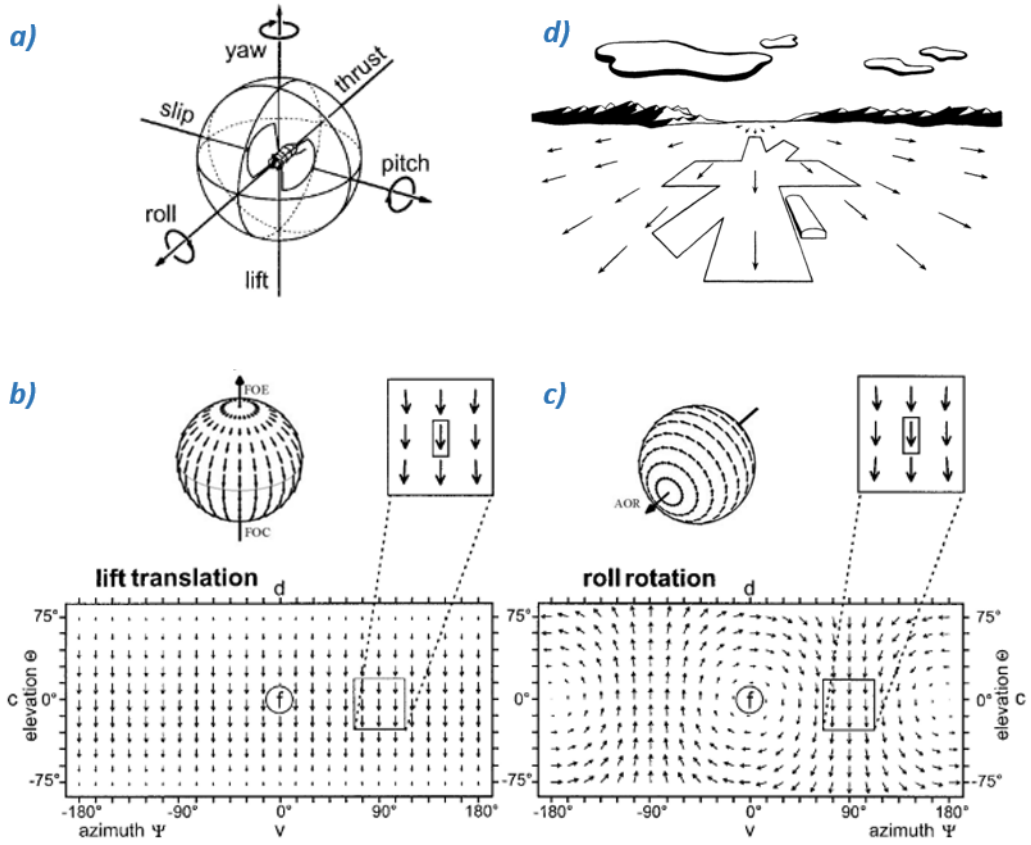

Figure 1.3 – **Global structure of translatory and rotatory optic flow fields, and local analysis of visual motion.** ***a)*** Motions of the fly can be described by their translatory (thrust, slip, lift) and rotatory components (roll, pitch, yaw) around the 3 body axes. The different motion components induce different optic flow fields over both eyes of the moving animal. ***b-c)*** Optic flow field caused by a lift translation (***b***), and a roll rotation (***c***). Optic flow patterns are transformed from the visual unit sphere into Mercator maps to show the entire visual space (f: frontal, c: caudal, d: dorsal, v: ventral). Globally the 2 optic flow fields can be distinguished from one another. In the visual system, however, motion is analyzed by sets of elementary motion detectors. Note that the vertical downward detector is equally excited by an upward lift translation or a roll rotation to the left (see magnified sections). ***a-c)*** Taken from (Krapp, B. Hengstenberg, Roland Hengstenberg, et al. 1998). ***d)*** Focus of expansion during landing. Each arrow represents the velocity and direction of flow of the surface-element. On the picture-plane there is a gradient of decreasing velocity from the bottom up to the horizon, and also a gradient of changing direction from the midline to either side. Taken from (Gibson 1951).

distant ones. Thus, by analyzing the relative velocity differences within translatory optic flow fields, an observer may get information about the distribution of relative distances within the environment presently encountered. Both information about the present self-motion and the 3D layout of the environment is essential for a mobile observer. To control its locomotion adequately (e.g., to stabilize its motion path or to avoid bumping into obstacles), it needs to sense his current self- motion and to estimate the distance to possible obstacles.

Specific pathways in the fly visual system are adapted to sense the direction of visual motion across the compound eyes. In the 50's, from a quantitative input output analysis in beetles Hassenstein and W. Reichardt 1956 were able to derive the functional structure of an elementary movement detector, *EMD*, underlying the analysis of visual motion. In a first approximation, neighboring facets, or ommatidia, in the hexagonal eye lattice of the compound eye feed signals into retinotopic arrays. The identification of the neural substrate responsible for the theoretical EMD in the fly brain has been a great challenge in the last 70 years, and despite the use of the most advanced neuroscience techniques, the whole picture is still incomplete today (Borst 2014b). *EMDs* model is competed by modern models (Torre and T. Poggio 1978; Gruntman, Romani, and Reiser 2018) that confirms the presence of ON-OFF pathway (Riehle and Nicolas Franceschini 1984; Joesch, Schnell, Raghu, et al. 2010). Most recent models include the local direction of retinal image shifts and their outputs are selectively integrated by individually identifiable interneurons in the posterior part of the third visual neuropil, the lobula plate (Krapp 2000). In flies, the response properties of most of these lobula plate tangential cells (LPTCs) have been studied in detail (Klaus Hausen 1993). Many of them have extended receptive fields with a distribution of local motion preferences, setting up matched filters for particular patterns of optic flow the animal encounters while moving (Krapp and Roland Hengstenberg 1996; Franz and Krapp 2000).

Optic flow and interommatidial angle: During forward translation, the optic flow is much faster on the sides. A nice solution observed in the configuration of most flies' compound eyes is to vary the interommatidial angle, $\Delta\phi$, along the medio-lateral axis of the compound eye with minimum $\Delta\phi$ at the vanishing point, and maximum $\Delta\phi$ on the side. The simple consequence of the different delta phi in the frontal and lateral eye is, that EMD analyzing motion in the frontal and lateral visual field are tuned to lower and higher temporal frequencies, respectively. This qualitatively matches the magnitude distribution of velocity vectors in an optic flow field generated during forward translation (thrust Fig. 1.3***d***)). Also, the EMD time constants are adjusted by motion adaptation. That is at least the common explanation for the fact that the temporal frequency tuning may be shifted to higher dynamic input range, e.g. when the animals are locomotor active (Jung, Borst, and Haag 2011; Longden and Krapp 2010).

1.3 Visually evoked behaviors, and experiments

As mentioned earlier, the aerial pursuit in flies is considered as exclusively visual guided behaviour. This is why I will introduce other visually guided behaviours that may interact with pursuit. Techniques and experiments developed to study these behaviours, and the visuomotor control models that scientists have built, were a great source of inspiration for my PhD project.

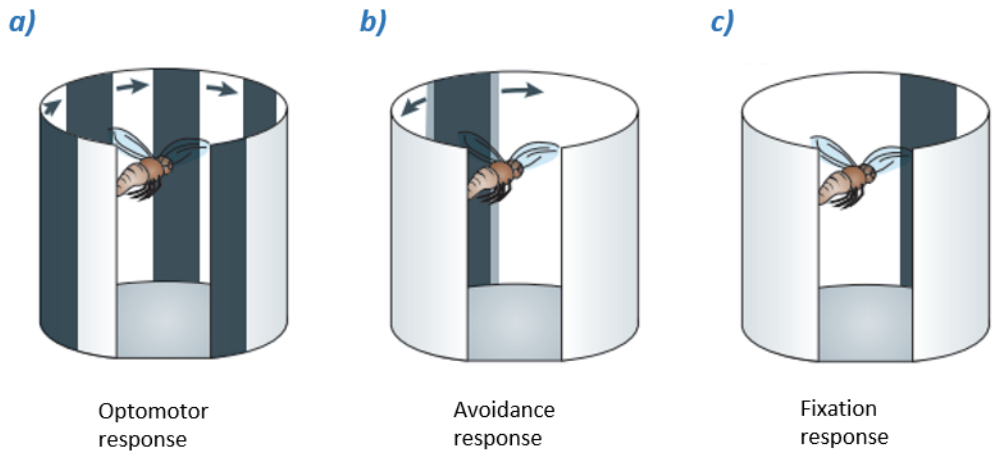

Figure 1.4 – **General principles of 3 visually driven behaviours in *Drosophila*.** ***a)*** Optomotor response: when a fly is suspended in the middle of a striped drum rotating around it, its turning tendency follows the direction of pattern movement. ***b)*** Avoidance response: when confronted with an object positioned laterally in the fly's visual field that all of a sudden starts expanding, flies consistently turn away from it. ***c)*** Fixation response: when the fly is given control over the position of a single bar, it tends to keep the stripe in front of it most of the time. Taken from (Borst 2014a).

1.3.1 Optomotor response

Like gaze stabilization in many different animals (Land 2019) including humans (Miles and Wallmab 1992), a fly subjected to panoramic wide-field motion (optic flow) due to external perturbations such as turbulent air, performs compensatory body and head rotations to minimize retinal image flow (Fig. 1.4***a***). This optomotor response is a stabilization reflex evoked by the visual wide-field motion and is common to stationary vertebrates and arthropods or during aquatic, terrestrial, and aerial locomotion (Fleisch and Neuhauss 2006; Abdeljalil, Hamid, Abdel-Mouttalib, et al. 2005; Karl Georg Götz 1968).

Optomotor response is a central feature of a fly's flight control system that has been thoroughly studied in tethered or freely flying animals allowing different levels of data

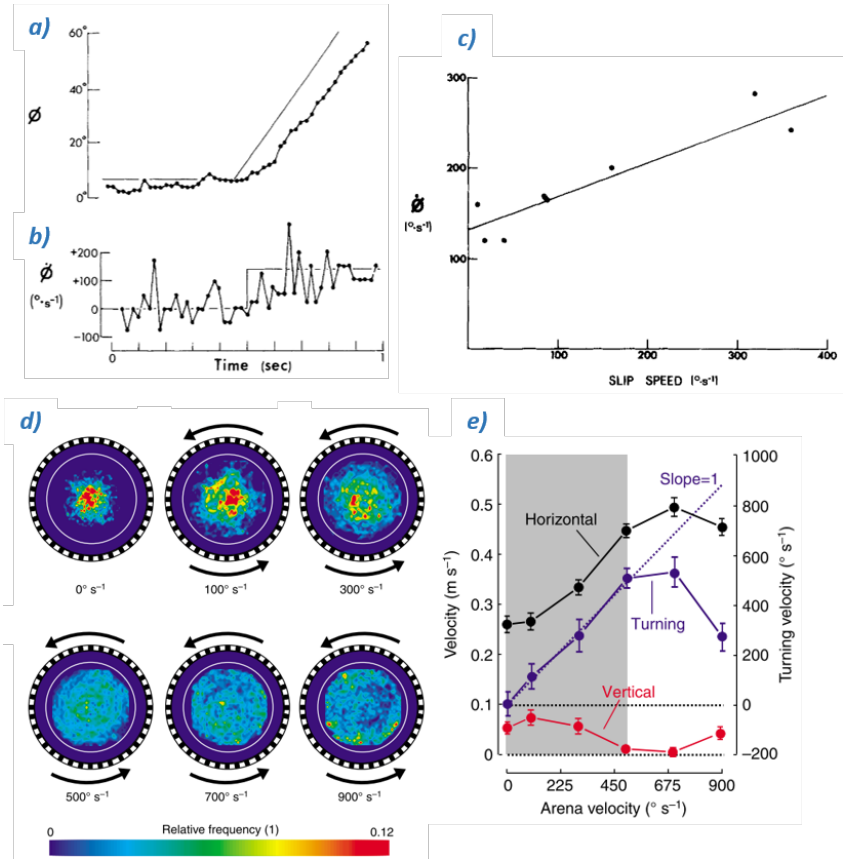

Figure 1.5 – **Optomotor response analysis in flies under free flight conditions.** ***a)*** Body orientation of a male hoverfly *Syritta pipiens* following a drum rotating at constant speed. ***b)*** The hoverfly's body angular velocity during the same experiment as ***a)***. ***c)*** The body-yaw velocity increased linearly with the retinal slip speed (difference between the angular velocity of the environment, and that of the fly). ***d)*** Top view of the mean position probability of freely flying *Drosophila* at various drum rotational velocities. The outer rings represent the random-square pattern. The white line marks the position of the immovable translucent inner cylinder used to prevent the flies to get in contact with the rotating drum. All position histograms are normalized to the same data sum and position probability is plotted in pseudo-colour. ***e)*** Mean flight velocities at various rotational velocities of the flight arena. Mean horizontal (black, left scale), turning (blue, right scale) and vertical (red, left scale) velocity of the animals in response to changes in stimulus conditions. The fly may fully achieve retinal slip compensation (grey area) when angular velocity, which is the rate of change in gaze, is equal to the angular speed of the rotating environment at a given horizontal velocity (slope=1, dotted blue). Positive turning and vertical values mean counter-clockwise turns and climbing flight, respectively. ***a-c)*** from T. S. Collett 1980 ***d-e)*** from Mronz and Lehmann 2008.

analysis (Martin Egelhaaf and Borst 1993).

Tethered flight experiments: First tethered flight experiments were performed with animals fixed in the centre of a rotating drum while measuring the torque produced around the vertical axis (Tomaso Poggio and W. Reichardt 1976). In other experiments, the fly was free to rotate around vertical-axis (T. S. Collett 1980). In both cases, when presented with visual wide-field motion, the fly followed the direction of the optic flow with systematic wing beat adjustments. The yaw velocity increased roughly linearly with the slip speed of the pattern across the fly's retina (Fig. 1.5***c***). Retinal slip speed is the difference between the angular velocity of the environment, and that of the fly. Response delays are in the range of 20 ms after the visual input has changed (Jamie C Theobald, Ringach, and Frye 2010).

With advanced high speed video cameras coupled with real time image processing it became easier to analyze wing beat amplitude of a fixed fly – based on the projected envelope of the wing beat trajectory when illuminated with infrared light. Also, direct evidence that the torque produced around z-axis is linearly related to the difference in wing beat amplitude (Dickinson and Lighton 1995; Lehmann and Dickinson 1997) facilitated the replacement of the torque-meter in modern studies (Haikala, Joesch, Borst, et al. 2013). Rotating drums with printed patters attached to their walls have been gradually replaced with LED panels, LCD screens or digital light projectors for stimulus generation in more recent experiments (Lindemann, R. Kern, Michaelis, et al. 2003).

However, despite the rich variety of experiments that can be performed in tethered flight, results can only partially capture the principles underlying optomotor responses, as they do not fully take into account the dynamic interactions between the animal and its physical environment (Dickinson and Florian T. Muijres 2016).

Free flight experiments: During free flight conditions the animal experiences a complex mixture of rotational and translational optic flow depending on self-motion but also the 3D structure of the environment (Section 1.2.2). When placed inside a circular arena surrounded by a random-square pattern, both the yaw-angular velocity and forward speed of the fly are increased with increasing angular velocity of the rotating drum (Fig. 1.5***d-e***). This has been observed for blowflies *Lucilia* (Trischler, Roland Kern, and Martin Egelhaaf 2010), *Drosophila* (Mronz and Lehmann 2008) and hoverfly *Syritta* (T. S. Collett 1980). As during tethered flight experiments, the yaw velocity increased linearly with the retinal slip speed, up to a turning velocity of 500 deg/sec.

1.3.2 Responses to looming stimuli

On tethered flies: To avoid collisions or predators, flies must quickly steer away, or take off, from a looming stimulus (Card and Dickinson 2008; Florian T. Muijres, Elzinga, Melis, et al. 2014)(Fig. 1.4***b***). This appears to be a common feature across

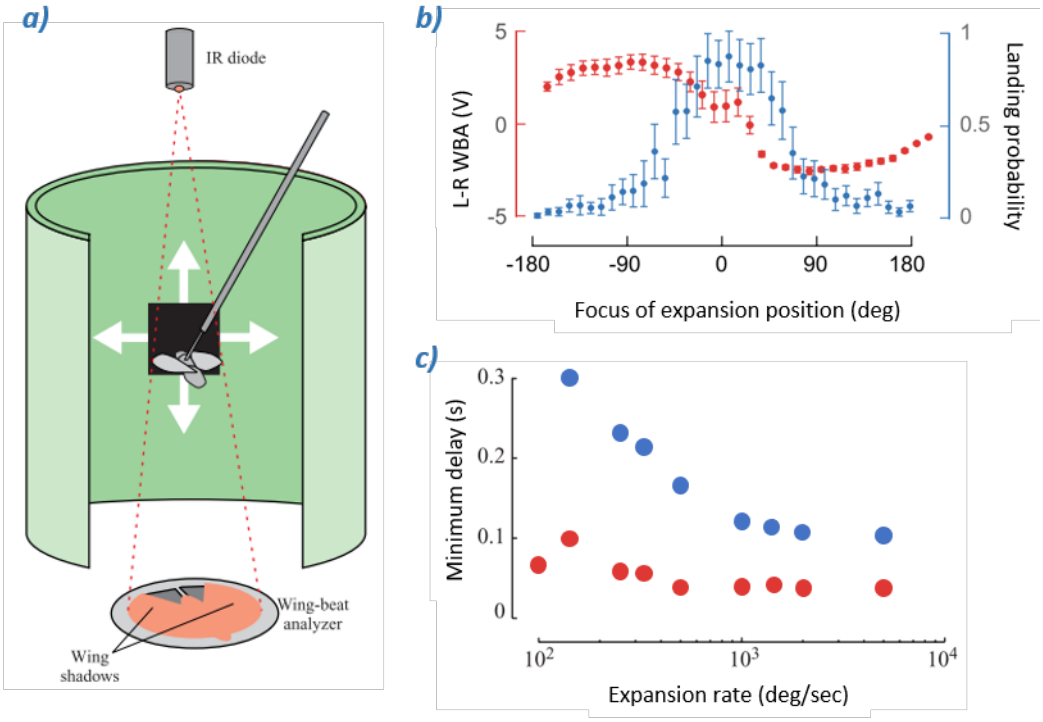

Figure 1.6 – **Fly's response to looming stimulus.** ***a)*** Schematized experimental setup for measuring a fly's response to image expansion. During tethered flight, the fly's wing-stroke amplitude and frequency are measured by an optical wing-beat analyzer (see tethered flight method in section 1.3.1). At periodic intervals, the square symmetrically expands, eliciting a behavioral response. Taken from Tammero and Dickinson 2002. ***b)*** Response to an expansion at a rate of 500 deg/sec. Response maps generated by systematically varying the horizontal position of a rapidly expanding square. Collision avoidance manoeuvres (red, left ordinate) are controlled independently from landing responses (blue, right ordinate). The probability of landing is maximum for a stimulus presented frontally. Taken from Frye and Dickinson 2004 (adapted from Tammero and Dickinson 2002). L-R WBA, left-right wing-beat amplitude. ***c)*** Response latencies plotted as a function of expansion rate. The minimum latency of the collision-avoidance response is 50 ms (red), and minimum landing response latency around 120 ms (blue). The landing response latency decreases with the rate of expansion, whereas for most expansion rates the delay of the collision-avoidance response is constant. Taken from Tammero and Dickinson 2002

Table 1.1 – This table sums up general optomotor properties in flies. See text for references.

	Optomotor response in flies
delay	20-30 ms
input	wide-field optic flow: angular velocity
type	smooth
limit	The yaw turns response plotted over stimulus velocity is linear up to 500 deg/sec

insect visual systems, often attributed to the response properties of an individually identified cell in fly (De Vries and Clandinin 2012; Klapoetke, Nern, Peek, et al. 2017; Ache, Polsky, Alghailani, et al. 2019), locust (Pinter 1979; Gabbiani, Krapp, Hatsopoulos, et al. 2004; Zhu, Dewell, H. Wang, et al. 2018) and moth (Wicklein and Strausfeld 2000). When presented to tethered flies (Fig. 1.6***a***), visual expansion elicits preprogrammed landing posture (Braitenberg and Ferretti 1966; Borst and Bahde 1986), or yaw torque to escape collision (Bender and Dickinson 2006).

Nonetheless collision-avoidance and landing responses are mediated by separate pathways in *Drosophila* as suggested by Tammero and Dickinson 2002. When positioned in frontal part of the fly's vision, the expanding stimulus is more likely to elicit a landing response, while an expending stimulus in the lateral vision field elicits a collision avoidance response. Differences in the latency of both the collision-avoidance reactions and the landing responses confirmed the hypothesis of two separate neural pathways (Fig. 1.6***c***). Most recent work by Ache, Namiki, Lee, et al. 2019 highlights how sensory and motor networks are coupled or decoupled according to the behavioral state of *Drosophila* in response to looming stimulus. Nonetheless, the two types of response to expansion flow-fields require the same local motion detectors (Schilling and Borst 2015).

The study from Tammero and Dickinson 2002 also allows me to introduce comparison between open and closed-loop behavioural experiments. During closed-loop experiments, the difference between the amplitude of each wing stroke controls the visual display, allowing the fly to orient actively toward the position of the 15 X 15 deg square. Authors show that fly's wing beat modulation varies between closed and open-loop conditions.

With free flies: During free flight, *Drosophila* presented with a looming object executes also the two types of responses: a rapid escape manoeuvre composed of a banked turn and forward speed acceleration (Florian T. Muijres, Elzinga, Melis, et al. 2014), or a landing course (Van Breugel and Dickinson 2012). The visual-motor delay during the escape response is on average 60 ms, which is consistent with previous measurements in *Drosophila* free flight (Card and Dickinson 2008) and tethered flight (Bender and Dickinson 2006). Landing honey bees control their speed by holding the rate of expansion of the image constant (Baird, Boeddeker, Ibbotson, et al. 2013). This

strategy guides smooth landings on surfaces of any orientation, without knowledge about the distance to the surface or the speed at which it is approached.

Experiments on landed flies showed that the take-off response is controlled by the approaching direction, angular size and angular expansion velocity, τ, of the looming stimulus Card and Dickinson 2008; Reyn, Nern, Williamson, et al. 2017; Ache, Polsky, Alghailani, et al. 2019.

Table 1.2 – This table sums up general collision avoidance properties in flies. See text for references.

	Collision avoidance in *Drosophila*
delay	60 ms
input	looming object, position, expansion rate
type	saccade
remarks	fastest response when object approaching laterally escape direction is +/- 90 deg away from the direction of approach

1.3.3 Following an object: object fixation or target pursuit?

We can distinguish super fast male hoverfly *Syritta* tracking females (T. S. Collett 1980) and female housefly *Musca* fixating flowers (W. R. Reichardt and Tomaso Poggio 1976). Despite some similarities, the function and underlying neural mechanisms of the two behaviours are different. The aerial pursuit by male Diptera species in the context of mating seems to be designed to following small, rapidly moving targets. Alternatively, in these species, both sexes are likely to be concerned with maintaining fixation of large stationary object (houseflies (Land and Thomas S Collett 1974; H. Wagner 1986), hoverflies (Thomas S Collett and Land 1975)). A target is any small moving object pursued for mating, defense or feeding purposes. A figure is defined as any other object, not necessarily in movement, but with motion relative to the background due to the animal translatory self-motion (J. W. Aptekar and Frye 2013). It is convenient to use separate terms for the two types of behaviour as object fixation and target pursuit (review in Gonzalez-Bellido, Samuel T Fabian, and Nordström 2016).

1.3.4 Object fixation

In addition to the optomotor responses that stabilize wide-field panoramic motion. Object fixation in flight can be evoked by multiple stimuli: from a simple high-contrast vertical bar (Karl Georg Götz 1975; W. R. Reichardt and Tomaso Poggio 1976) (Fig. 1.4***c***) to visual objects with higher order motion properties such as flicker, border or theta

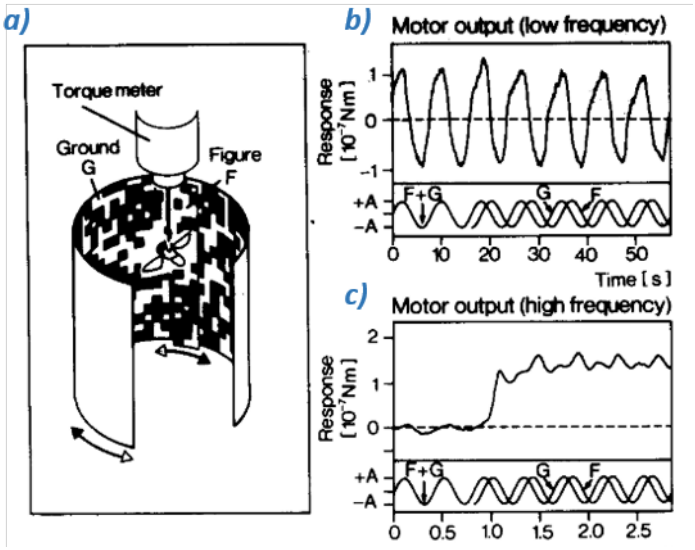

Figure 1.7 – **Optomotor response and figure (object) fixation from Martin Egelhaaf, Klaus Hausen, W. Reichardt, et al. 1988.** ***a)*** Experimental condition: the test fly is fixed to a torque meter. The fly is surrounded by a cylindrical panorama (ground, G) with a random texture. A vertically oriented textured stripe (figure, F) is placed in front of the ground. Its mean angular position was in front of the right eye 30 deg from the frontal mid-line of the cylinder. Its angular width was 12 deg. Both figure and ground could be moved horizontally either together or relative to each other. In ***b)*** the pattern was oscillated at a low frequency: 0.1 Hz. In ***c)*** the oscillation frequency was high 3 Hz. The oscillation amplitude, A, was +/- 6 deg. ***b-c)*** Show the visually induced yaw torque responses (upper trace) in experiments where figure and ground were initially oscillated synchronously and were then set to a relative phase of 90 deg. ***b)*** The responses to synchronous and relative motion do not differ significantly at the low oscillation frequency. The fly mainly tries to follow the ground motion with a large response amplitude. ***c)*** At high oscillation frequency, flies try to turn towards the figure, meaning that the figure is detected. Note that the torque responses to synchronous oscillation are much smaller at the high than at the low oscillation frequency. At low oscillation frequencies, the largest responses are elicited by synchronous motion of figure and ground. In contrast, at high oscillation frequencies the largest response amplitudes are elicited by small moving patterns.

motion (Chubb and Sperling 1988; Jamie Carroll Theobald, Duistermars, Ringach, et al. 2008; Ji, Yuan, Wei, et al. 2020; X. Zhang, H. Liu, Lei, et al. 2013). Orientation responses toward figures (fixation) and stabilizing responses to wide-field perturbations (optomotor response) differ in their sensitivity to stimulus size and their dynamics (Martin Egelhaaf 1987; Wagner 1986; Mongeau and Frye 2017). Object fixation is also found in walking and tethered flies (Schuster, Strauss, and Karl G. Götz 2002; Karl Georg Götz 1975). At low frequencies (30 deg/sec) the tethered housefly follows the background, and at high frequencies (1,000 deg/sec) the fly is more attracted by the object (Fig. 1.7). Thus, Martin Egelhaaf 1987 described: "*for equally textured stimuli relative motion is necessary, but not sufficient for figure-ground discrimination: the figure can only be discriminated at higher oscillation frequencies*". The authors proposed a model with two distinct pathways: one responding to *large-field* stimulus who mediates course stabilization. In contrast, the other system dominates at high oscillation frequencies and is sensitive to small patterns. The author wrote "*This small-field system mediates the detection, fixation and tracking of small moving objects*". The small moving objects the authors are referring to is a vertical bar 12 deg wide (Martin Egelhaaf 1987; Martin Egelhaaf, Klaus Hausen, W. Reichardt, et al. 1988).

Researchers found similar results with hoverflies (T. S. Collett 1980), *Drosophila* (M. Heisenberg and Wolf 1984; Mongeau, K. Y. Cheng, J. Aptekar, et al. 2019) and honeybees (S. W. Zhang, Xiang, Zili, et al. 1990).

In *Drosophila*, optomotor response and bar fixation are mediated by two distinct controllers (Mongeau and Frye 2017). A moving panorama elicited robust smooth movement interspersed with occasional optomotor saccades. These saccades were tuned to the dynamics of panoramic image motion and were triggered by a threshold in the integral of velocity over time. The bar-fixation saccades were finely tuned to the speed of bar motion and were triggered by a threshold in the temporal integral of the bar error angle rather than its absolute retinal position error. This is in line with prediction of the parallel processing by (Tomaso Poggio and W. Reichardt 1976).

During free flight, honeybees' *small-field* tracking control system tends to orient the bee such that the target – figure representing flower – is located frontally, at an angle of 35 deg below the bee's longitudinal body axis, which is considered by authors an optimum angle for landing.

Table 1.3 – This table gives general properties of object fixation in flies. See text for references.

	Object fixation in flies
feature detection	between 1 and 4Hz
input	intensity, colour, contrast, motion and non-Fourier motion cues
type	smooth and saccade
remarks	difficulty to identify visual features used as inputs

1.4 Target Pursuit

During courtship, territorial defence or even predation, an animal can be engaged in chasing behaviour towards another animal. In order to catch the target, the pursuer must successfully complete several tasks: target detection, tracking and capture. When blowflies engage in aerial pursuits, their flight behaviour markedly differs from cruising flight. During cruising flight, fly executes randomly yaw-body saccades and translates at speed slower than 1 m/s, whereas during pursuit, yaw-velocity presents rare body-saccades and mean forward speed is faster than 1 m/s (Trischler, Roland Kern, and Martin Egelhaaf 2010).

1.4.1 Target detection

The aim of the pursuit flight is to catch a prey, or a conspecific, of approximately known body-size, usually inferior or equal to that of the pursuer's. Stereovision is used by very few chaser insects: damselfly (Supple, Pinto-Benito, Khoo, et al. 2020), robber fly (Trevor J Wardill, Samuel T Fabian, Pettigrew, et al. 2017) and praying mantis (Nityananda, Tarawneh, Henriksen, et al. 2018). Monocular distance estimation was found in sun beetle larvae (Bland, Revetta, Stowasser, et al. 2014). The pursuer may estimate absolute prey size before take-off with the ratio between the prey's angular speed and angular size (Fig. 1.8***a***) as a loosely matched filter (Trevor J. Wardill, Knowles, Barlow, et al. 2015; RM M Olberg, Worthington, and Venator 2000). A sphere with a diameter of 1 cm located 15 cm away assumes approximately an angular size of 1 deg on the subject's eye (Fig. 1.8***b***). This is about the mean spatial resolution in, and above the frontal eye equator of the female blowfly.

To understand how the pursuer detects the target, we have to consider several parameters. For example, comparing the maximum distance if detection with the optical resolution of the compound eye can validate visual acuity. We will see in the upcoming section ***Hyperacuity*** that the animal can detect target smaller than its minimum interommadial angle. We will also see that the resolution can change along the surface of the compound eyes, thus the minimum angular size varies depending on the position of the target in the pursuer's field of view (Fig. 1.9***g***).

Sexual dimorphism of the compound eyes. In Dipteran aerial chasers, a sexual dimorphism is observed on the proportion of the head covered by the compound eyes. Males usually have eyes that almost join and cover the entire fronto-dorsal part of the head (Fig. 1.9***a***). This acute zone (Land and Eckert 1985) in the male's compound eyes is called *love spot* (Hornstein, O'Carroll, Anderson, et al. 2000). It benefits the male fly during pursuit in several ways. Most of the following points have been described for houseflies.

First, the type of photoreceptor in the love spot of male houseflies is slightly different from the rest of the compound eye. In this zone, R7 shares the same properties as its neighbours R1-6 (Nicolas Franceschini, R. Hardie, W. Ribi, et al. 1981; R.C. Hardie,

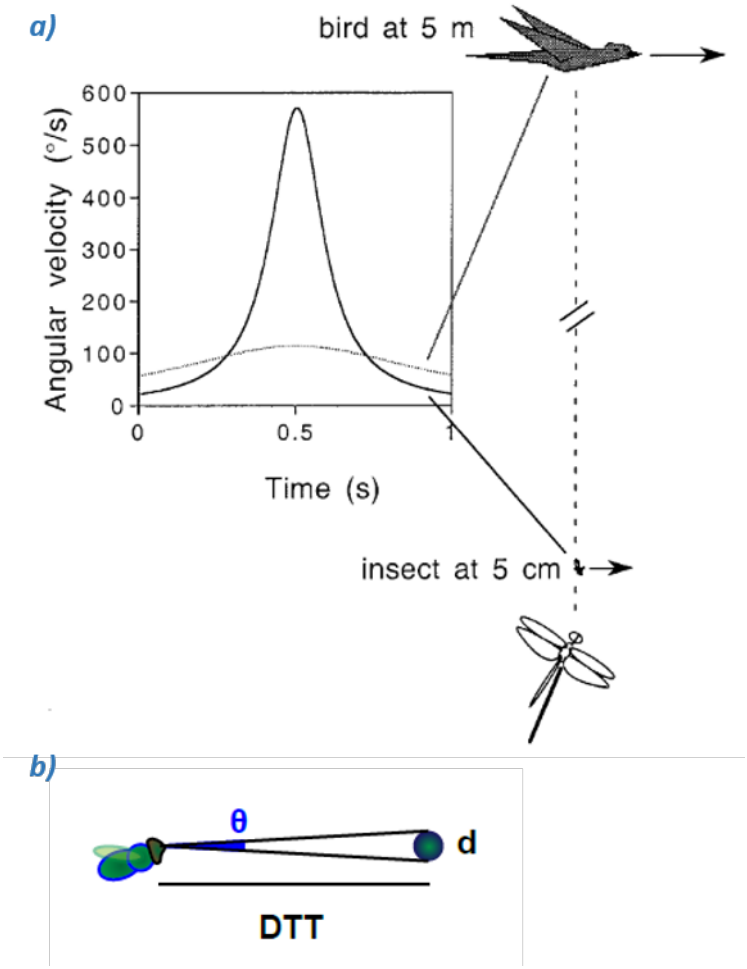

Figure 1.8 – **Retinal profile of the target.** ***a)*** A sharp rise and fall in angular velocity could be used as a cue to discriminate between nearby small objects (insects) and distant large objects (birds). Graph shows the angular velocity (deg/sec)for a 2.5 mm insect, 5 cm away, flying at 0.5 m/sec and for a 25 cm bird, 5 m away, flying at 10 m/sec. Each object makes a 3 deg visual angle on the retina of the dragonfly. ***b)*** Target's angular size. Angular diameter θ , Distance to target (DTT), diameter of the target d

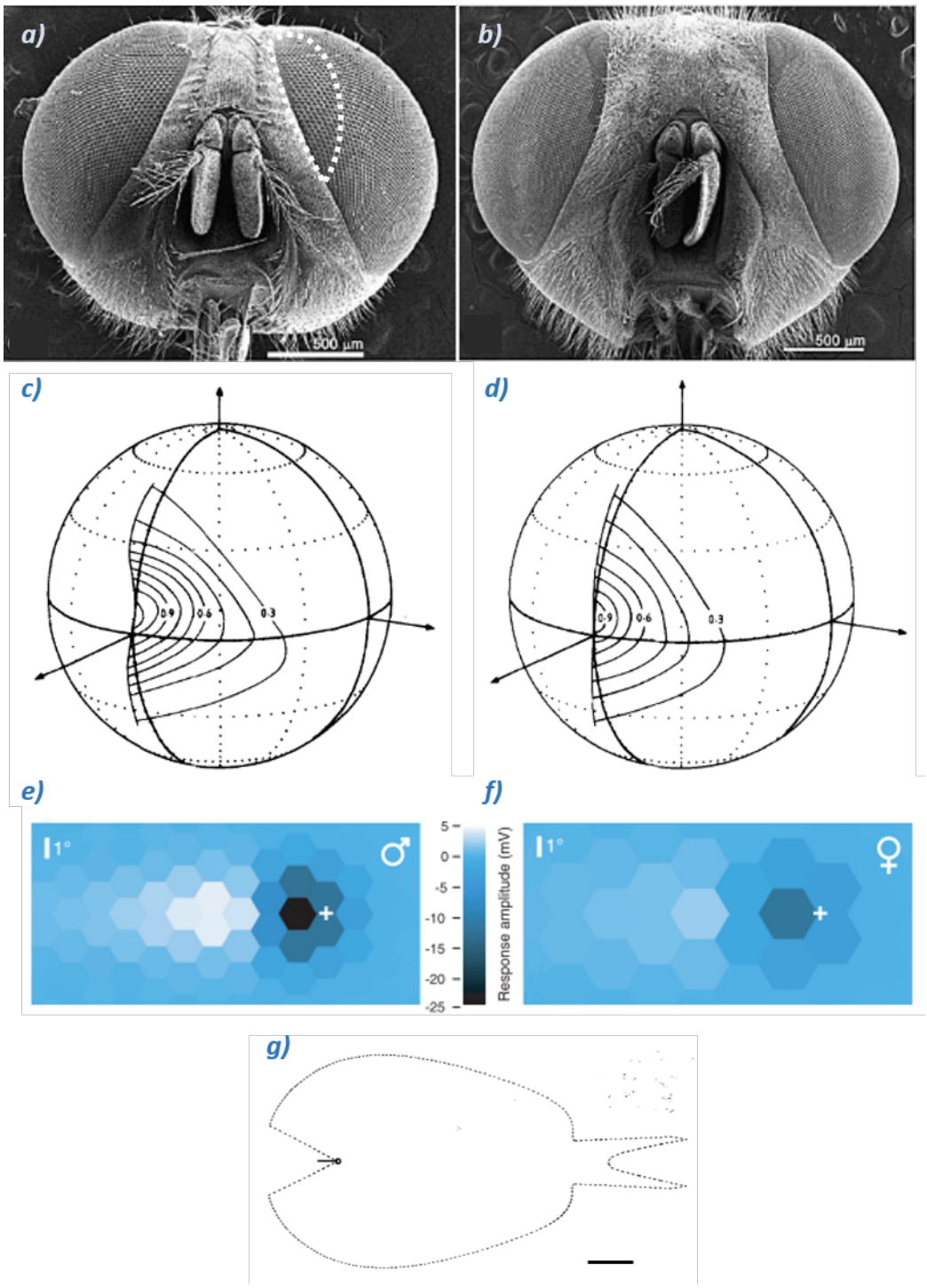

Figure 1.9 – (Caption on the following page.)

Figure 1.9 – **The 'love spots' of flies.** ***a-b)*** Male ***a)*** and female ***b)*** blowfly heads (*Lucilia cuprina*). Note how the eyes of males are closer, whereas those of females are quite separated. The extra eye surface — or 'love spot' — of males (dotted white line) provides the input to a sophisticated neural pathway for detecting and chasing females. Images from Sukontason, Chaiwong, Piangjai, et al. 2008. ***c-d)*** show plots of the densities of ommatidial axes in *Lucilia cuprina*, maximum density is 1.1 axes per degree^2 in males and 0.9 in females. Since the average interommatidial angle ($\Delta\phi$) is equal to $(2/(\sqrt{3}.\text{axis density}))^{1/2}$, these densities correspond to values of $\Delta\phi$ of 1.024 and 1.13 deg. Notice the greater axis density in the acute zone of the male ***c)*** and its more dorsal location in both sexes. Taken from Land and Eckert 1985. ***e-f)*** Neural images (from the frontal-dorsal eye region) in male ***e)*** and female ***f)*** houseflies reconstructed from photoreceptor responses to a dark 3.44 deg wide target moving at 180 degrees per second. The neural images show the instantaneous voltage responses of individual photoreceptors separated at angles appropriate for males ($\Delta\phi$ = 1.6 deg) and females ($\Delta\phi$ = 2.5 deg). The wider 'love spot' facets of males, and their superior 'love spot' photoreceptor performance, allow males to detect small moving targets with much greater spatial, temporal and voltage contrast. Crosses indicate the current position of the target. Pictures from Brian G. Burton and Simon B. Laughlin 2003. Figures inspired by Warrant 2016. ***g)*** Horizontal-plane sensory field for visual mate detection in male hoverfly *Syritta pipiens*. Females at approximately the same altitude as the male, which are within the sensory-field contour (broken line), may be detected; outside the contour, they are considered undetectable. Dorsal view: Male's head is shown as a circle, thorax and abdomen as a bar. The fly enlarged by a factor of 5 relative to the contour for clarity. To the rear, the male has a blind zone of approximately 60 deg. Scale bar: 10 cm. Taken from Cliff and Bullock 1993.

Nicolas Franceschini, W. Ribi, et al. 1981). We saw earlier that R1-6 are dedicated to motion vision, thus R7 will join this pathway. A male's lovespot photoreceptor detects a conspecific at twice the distance of a female photoreceptor, largely through better optics (Brian G. Burton and Simon B. Laughlin 2003). These photoreceptors in males offer better spatial resolution than females. Response amplitude is increased providing a better voltage contrast (Brian G. Burton and Simon B. Laughlin 2003). Photoreceptors also perform better temporal resolution, thereby allowing them to code higher velocities and smaller targets than other photoreceptors (Hornstein, O'Carroll, Anderson, et al. 2000). Consistent with this hypothesis, membrane-impedance measurements show that frontal photoreceptors have a higher specific conductance than other photoreceptors (Brian G Burton, Tatler, and Simon B Laughlin 2001). Finally this highly specialised region of the retina features neural connections feeding into sex specific pathways in males blowfly *Calliphora* (Strausfeld 1991) and flesh fly *Sarcophaga* (Gronenberg and Strausfeld 1991).

All these features provide a better temporal and spatial performance but they are metabolically expensive. This is why this photoreceptor cluster stays as small as possible and forms a specialized region of the eyes onto which the male stabilizes the image of the target during pursuit.

Hyperacuity: It is commonly accepted that the resolution of the eye is given by the interommatidial angle ($\Delta\phi$). The interommatidial angle depends primarily on two anatomical parameters, the facet diameter,D and the radius of the eye R, given by the formula $\Delta\phi = D/R$. But it has been observed that targets with angular size (Fig. 1.8***b***) smaller than the divergence angle between the optical axes of photoreceptors can be detected by, for example, killer flies and black flies (behavior Trevor J. Wardill, Knowles, Barlow, et al. 2015), hoverflies (neuronal Nordström, Barnett, and O'Carroll 2006), and robber flies (behavior Trevor J Wardill, Samuel T Fabian, Pettigrew, et al. 2017). It turns out that spatial resolution is rather related to the acceptance angle (function) of a single photoreceptor as suggested by Riehle and Nicolas Franceschini 1984; Brian G. Burton and Simon B. Laughlin 2003, and more recently by Rigosi, Wiederman, and O'Carroll 2017 in honeybees. Another phenomenon that allows the fly to detect an object smaller than its spatial resolution is a vibration of the retina relative to the facet array at a constant frequency (see reviews: Stéphane Viollet 2014; Juusola, Dau, Song, et al. 2017).

Design conservation: The design of the compound eyes is adapted to ecological requirements. The variations in facet diameter, arrangement of facet lenses, interommatidial angles, as well as in rhabdom diameter and length, all allow the eye to make the most of the information in the environment. This is in spite of the fact that the tiny lenses of compound eyes severely limit resolution. Nilsson has put it that way : "It is only a small exaggeration to say that evolution seems to be fighting a desperate battle to improve a basically disastrous design" (D.-E. Nilsson 1989).

1.4.2 Tracking

If the angular diameter and velocity profile of the target satisfies the detection system of the tracker, pursuit starts.

Pursuit strategies: Different pursuit strategies have been observed in flying animals (review in Pal 2015) and many of them are used in advanced technologies such as missile guidance (Shneydor 1998) as they are computationally inexpensive. When talking about pursuit strategies, we often oppose tracking and interception. Pursuit strategy is named tracking in the case when pursuer aligns its velocity vector towards the current position of the target. During an interception strategy, the pursuer aligns its velocity vector towards a future position of the target. The general idea of the control strategy is that the pursuer adjusts its flight trajectory according to target's flight direction, so that pursuer and target simultaneously arrive at one an the same place. The pursuer's angular velocity (or course change) is generally adjusted to stabilize one or more visual parameters such as the error angle, the bearing angle, and/or their derivatives, by smooth and/or saccadic control. In control theories, adjustment of a single variable may transform pursuer trajectory from tracking into interception. For instance, if error angle is stabilized at zero, pursuer will express a tracking attitude, if error angle is stabilized to a non-zero constant, pursuer will follow an interception path. This will be given in more details in Chapter 3.

Apart from controlling the steering, the chaser may also adapt its forward speed.

Identifying and quantifying the underlying control strategies constitutes one major objective in the research on aerial pursuit, and it is the main goal of this PhD work. I am interested to study strategies the flies apply to control their steering in the horizontal and the vertical planes.

Decision making: The pursuit control requires a combination of several matched filters (Wehner 1987) tuned to detect specific features including target colour, size and apparent movements (Trevor J. Wardill, Knowles, Barlow, et al. 2015; Eichorn, Hrabar, Van Ryn, et al. 2017). While the pursuer reacts to the movements of the target, it receives continuously feedback on the target's flight envelope. If the target moves in an abnormal way or shows suspicious visual characteristics, the pursuit is cancelled. This is what will prevent unwanted meetings, i.e the male fly catching a honeybee which is the same length as the female fly, but stings anyone who tries to catch it! As mentioned earlier the expansion rate τ, can be a decisive parameter to elicit collision avoidance reflex.

Thyselius, Gonzalez-Bellido, Trevor J. Wardill, et al. 2018 suggested that collision avoidance reflex can be amplified in hoverfly. Researchers observed that when a wasp approached the feeding occupant of a flower (female *Eristalis*), hoverfly reacted earlier and faster than for the other incomer species (male *Eristalis*, *Episyrphus*, *Apis*). Female *Eristalis* left the flower when the wasp was further away, at 110 cm compared with 26 cm for other insect, and its take-off speed was three times higher compared

with that when approached by other insect. The authors concluded that the feeding hoverfly might perceive the level of threat posed by a wasp, but none of the looming aspects of the wasp could justify these take-off differences. The authors suggested that other visual cues may be used to differentiate the wasp, but no further analysis was performed.

1.4.3 Final approach and capture

When the distance is small enough and the target profile is not repulsive, the pursuer must initiate the capture phase. Usually the target is caught with the legs. This is the last manoeuvre, during which the pursuer rears up to present its legs in the direction of the target. Long-legged flies simply stretch forward their legs to grab their target. But in case of species with shorter legs the body rotates almost 90 deg in pitch, which is more spectacular than the landing response presented earlier. When the fly rears up, the target may disappear from the pursuer's visual field. Without visual feedback, this last move may be an open loop phase. Landing on the ceiling may provide cues as this multi-steps aerobatic manoeuvre is triggered when crossing an expansion threshold (P. Liu, Sane, Mongeau, et al. 2019).

Perspectives: Between field experiments and controlled physiological experiments to characterize neuronal responses and cell identities, many types of approaches have been developed by scientists to study pursuit behaviour. This work aims to identify strategies flies apply to control their steering in the horizontal and the vertical planes. During this project I decided to let the pursuer fly without constraint, but with dummy targets moving on well-defined paths, a technique inspired by (Boeddeker, Roland Kern, and Martin Egelhaaf 2003).

In the next chapter I will present the experimental setup I have built to study aerial pursuit in *Lucilia*. This chapter will be composed of technical specifications followed by first results on the analysis of body movements of the blowfly while chasing the dummy, which will validate the method for further experiments.

2 A novel setup for the analysis of free flight chasing behavior.

Sommaire

2.1 Introduction . . . 47
2.2 System description . . . 49
2.2.1 Principle of operation: . . . 49
2.2.1.1 Moving the target . . . 49
2.2.1.2 Videography, object tracking and image analysis: . . . 53
2.2.2 Accuracy of generating and reconstructing target trajectories: . . . 54
2.2.3 Spatial resolution of the cameras . . . 56
2.3 Analysing 3D chasing flights . . . 59
2.3.1 Parameters describing strategies of catching targets . . . 59
2.3.2 Parameters describing the orientation of the fly during pursuit flights . . . 63
2.4 Discussion . . . 65
2.5 Latest system upgrades . . . 68

2.1 Introduction

Chapter outline: Previous studies on aerial pursuit focused on pursuit along circular paths or interception of translating targets. I designed an actuated dummy target to trigger chasing flights in male blowflies. This method allows me to generate more complex target trajectories. Measurements of body orientation in earlier accounts were limited to the flight direction while I extended the analysis to include the full body orientation during pursuit. This work has been published in Varennes, Krapp, and Stéphane Viollet 2019. This chapter follow the article template. In the introduction I will present several studies of aerial pursuits in neuroethology research. In a second part I will describe the design of an actuated dummy target and its performances, as well as a complete description of the recording and analysis of the pursuit. I will then propose a series of tests to estimate the system's accuracy in moving the target, and in measuring the fly's behaviour. In the third section I will present preliminary results on the reconstructed target and pursuer positions (temporal resolution: 5 ms, spatial resolution: maximum 3D error 5 mm). The pursuer's body pitch and yaw angles were resolved within an error range of 6 deg. An embedded observation point provides a close-up view of the pursuer's final approach and enables to estimate its body roll angle. The system has been continuously improved. I will present the latest implementations along with their limitations.

This setup offers an opportunity to investigate kinematics and governing visual parameters of chasing behaviour in species up to the size of blowflies. The chasing arena may accommodate a large variety of experimental conditions such as reaction to obstacles, or wind gust – not presented here.

Experiments on pursuit behaviour: In the late 1970's, Collett and Land observed that hoverflies pursued a cherry core after one of them spit one near a bush, inspiring the scientists to build a pea-gun for studying the flies' pursuit reflex (Thomas S Collett and Land 1978). Much later in early 2000's, to elicit prey capture R. M. Olberg, Seaman, Coats, et al. 2007 attached a bead to a fishing line and moved it by hand in the same plane as a perching dragonfly. In a recent study on dragonfly pursuit, Mischiati, Lin, Herold, et al. 2015 also used a bead fixed on a transparent fishing line. This time the bead moved in straight line, at a computer-controlled speed, with a height-adjustable pulley system. A similar study has been performed with robberflies by Trevor J Wardill, Samuel T Fabian, Pettigrew, et al. 2017 and a much smaller aerial predator, the killer fly (Trevor J. Wardill, Knowles, Barlow, et al. 2015). To summarize, targets triggering interception behavior were moved by hand, shot at a close proximity of pursuers or moved at various speeds along straight trajectories.

Boeddeker, Roland Kern, and Martin Egelhaaf 2003 reported the first study on chasing behavior where the speed of a dummy target was controlled more systematically. Male blowflies were pursuing a black sphere (dummy) moving at constant speed along a circular path of 10 cm radius. In a series of experiments, the speed (1, 1.25, or 1.5 m/s) and the size (5, 8, or 13 mm) of the target were varied, revealing the

parameter combination required for male flies to capturing the dummy. The scientists also provided a model describing the dynamics of the male blowfly's chasing flights in the horizontal plane. However, despite the excellent repeatability of the behaviour, the comparatively regular dummy trajectories used in those experiments are quite different from the complex trajectories observed under more realistic conditions. To overcome these limitations, I developed a method that enables me to study chasing behaviour in male flies confronted with complex target trajectories. In this chapter I describe (i) the system that controls target motion, including its mechatronics, (ii) a high speed camera-based 3D tracker used to reconstruct dummy and fly trajectories, as well as the orientation of the pursuer (yaw- and pitch-) and (iii) preliminary experimental results obtained with the blowfly *Lucilia sericata*. The setup can be upgraded with an embedded observation system that provides imagery of the pursuer's final approach offering valuable details of the capture phase, and estimation of the body roll.

2.2 System description

2.2.1 Principle of operation:

The custom-made flight arena is a rectangular volume of 70x50x50 cm. Flies have a spectral sensitivity slightly shifted to lower wavelengths compare with humans, excluding the red color spectrum above 650 nm (Menzel and Backhaus 1991; Harris, Stark, and J. A. Walker 1976). Thus I covered the walls with a 1D visual grating consisting of vertically oriented red and white stripes (Figs. 2.1***a***, and 2.2). Similar patterns have been used previously in experiments on honeybees passing through a long tunnel (Portelli, Ruffier, and Nicolas Franceschini 2010). They are creating visual information, needed by the flying insects to stabilize their flights. In my setup, the objectives of the two cameras were equipped with optical red filters to minimize the contrast between the red and white stripes so the background appears close to a uniform intensity distribution in the video footage. On top of the arena, I implemented an actuated pulley system controlling the movement of the target.

2.2.1.1 Moving the target

To accurately generate complex target trajectories, I implemented a 2D positioning system called CoreXY (Fig. 2.1***a***) developed by Ilan E. Mayer 2012, which is an upgrade of the H-frame XY positioning system (Sollmann, Jouaneh, and Lavender 2010). Those activated systems are widely used to position a part or a tool within a 2D area, often used in 3D printers. The smooth and fully controlled trajectories the CoreXY system generates when mounted on top of the arena (Fig. 2.1***aa***) are close to the dynamics of chasing flights (Boeddeker, Roland Kern, and Martin Egelhaaf 2003).

The mechanical assembly adapted from an H-frame positioning system enables high acceleration and therefore faster movement control than the traditional H-frame system. In this positioning system, there are two parallel tracks (linear extruded rails) along which another couple of rails called bridge can slide by using pulleys mounted like dolly wheels (Fig. 2.1***b***). A central cart slides on the bridge by using the same principle based on dolly wheels. At each end the two parallel tracks sit on a pulley. The ones at the lower end are directly connected to the motor shafts of stepper motors which drive toothed belt controlling the movements of the positioning system. The CoreXY system features two differences from an H-frame. Together these differences result in the major advantage regarding the power required to move the cart carrying a given amount of payload (see below). First, an extra couple of pulleys change the belt circuit, enabling the belt to cross outside of the working range (Fig. 2.1***b***). The second difference concerns the 4 attachment points establishing the link between the belt and the cart as opposed to only two in the H-frame design. Distributing the effort equally over 4 attachment points means that we can move an heavier payload on the cart for the same amount of power generated by the motors. The ceiling of the flight arena is made of white fabric that slides gently over the main structure when the cart moves. This prevents flies to escape during experiments. The moving cart (Fig. 2.1***c***)

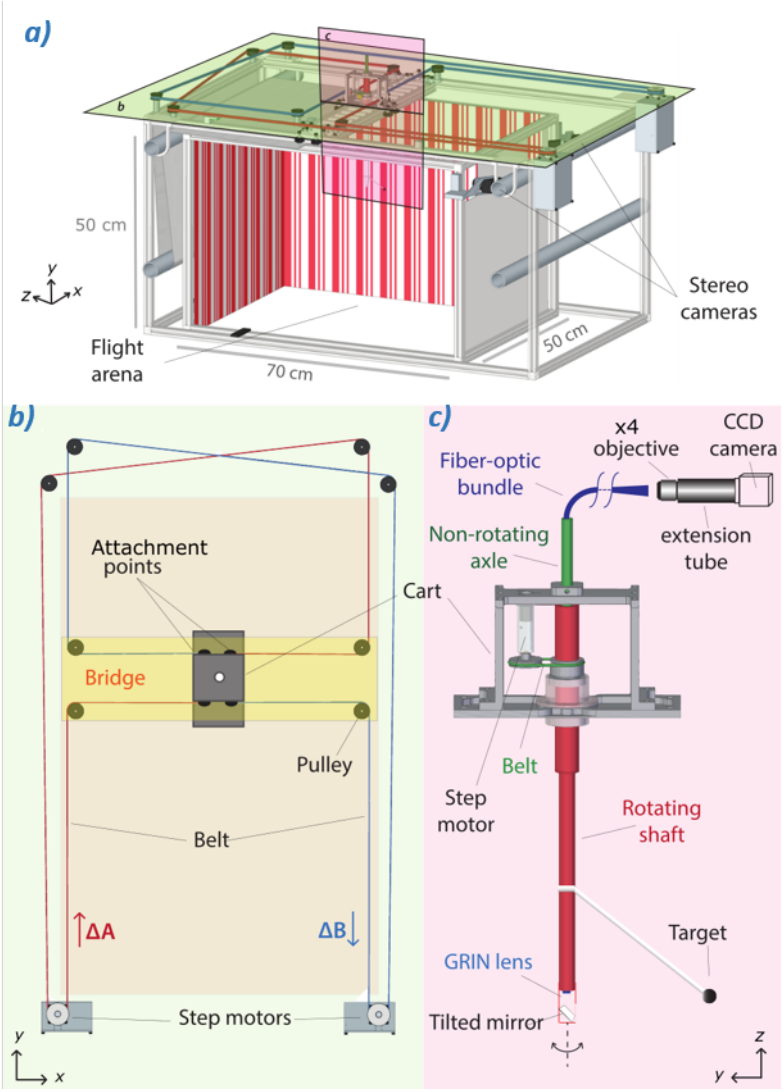

Figure 2.1 – **Schematic view of the chasing arena.** ***a)*** Global view of the setup. ***b)*** Top view of the setup presenting the CoreXY technique adapted from (Ilan E. Mayer 2012). The moving platform or cart (gray central rectangle) translates along the x-axis inside the yellow zone called bridge. The bridge moves along the y-axis. By controlling simultaneously the two translations, the cart can move within its working range shown by the pale orange zone. ***c)*** Side view of the cart equipped with a stepper motor that rotates the belt and thus the rotating shaft supporting the target. Other components are parts of an embedded micro-endoscope described in details in the ***Discussion***. For the sake of clarity, the rotating and non rotating shafts are colored (in red and green) on the schematics, but are white in the actual setup. Taken from Varennes, Krapp, and Stéphane Viollet 2019.

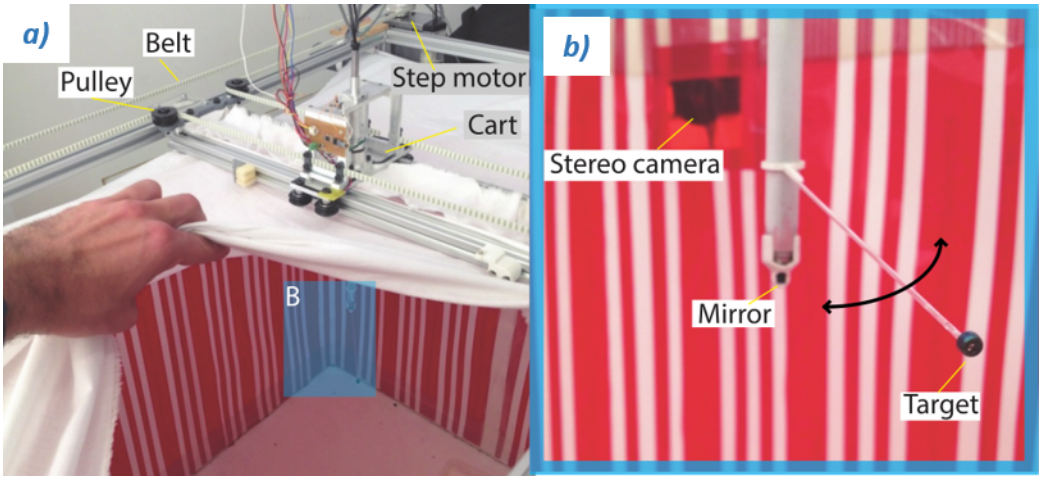

Figure 2.2 – **Chasing arena.** Picture of the chasing arena from outside ***a)*** and from inside ***b)*** with a close-up view on the target placed at the tip of a rod that is attached to an actuated rotating shaft. The latter supports both the rod and the small mirror enabling them to rotate simultaneously. Taken from Varennes, Krapp, and Stéphane Viollet 2019.

supporting the rotating target is composed of two co-axial shafts: i) a fixed inner shaft (diameter 6 mm) containing the light guide of an embedded camera and preventing connected wires to twist, as well as ii) a rotating outer shaft to which a rod holding the target and, at the end, a tilted mirror, are attached.

The outer shaft (in red in Fig. 2.1***c***) is actuated, through a belt, by a small stepper motor (Faulhaber, AM0820-V5-56, reduction gear ratio of 1). The latter is controlled at a resolution of 1200 steps per revolution allowing for a maximum rotational speed of 720 deg/s.

Target movements are thus controlled along the two translational degrees of freedom in the horizontal plane by the CoreXY system and one rotational degree of freedom by the mounted stepper motor. The CoreXY system alone reaches translations of up to 1 m/s, which can be combined with maximum angular velocities of two revolutions per second, enabling a large variety of target movements. The target is placed 15 cm below the ceiling and can reach any position within the floorplan of the arena.

Translation: In the following I give the equations of motion the CoreXY generates. The two actuators are the two stepper motors A and B and the moving object is the cart (Fig. 2.1***b***). Activating only one motor while keeping the other one still results in linear motion of the cart. Positive rotation (counter clockwise) of motor A while holding motor B still results in diagonal cart movement in the positive x- and positive y-direction, while a negative rotation of the same motor causes a movement in negative x- and negative y- direction. This can be written as:

$$\Delta A = \Delta X + \Delta Y \tag{2.1}$$

Activation of motor B, while keeping motor A stationary, moves the cart along the other diagonal. In this case positive rotation of motor B results in a movement of the cart in positive x- and negative y- direction.

$$\Delta B = \Delta X - \Delta Y \tag{2.2}$$

Combining Eq. 2.1 and 2.2, I obtain the movement of the cart along the x- and y- axis as a function of activation of motors A and B:

$$\begin{cases} \Delta X = 1/2(\Delta A + \Delta B) \\ \Delta Y = 1/2(\Delta A - \Delta B) \end{cases} \tag{2.3}$$

The description of the general relationship between the rotation of the motor pulley and the displacement of the belt moving the cart can be given by:

$$\Delta M = r\Delta\phi_M \tag{2.4}$$

Where r the radius of the motor pulley, $\Delta\phi_M$ is the number of angular steps (in radians) in the ϕ_M direction, and ΔM is the displacement of the belt. Thus, by substituting the activity of motors A and B in Eq. 2.3 and Eq. 2.4 I can obtain the movement of the cart along x- and y- axis as a function of the rotation of motors A and B.

$$\begin{cases} \Delta X = rR/2(\Delta\phi_A + \Delta\phi_B) \\ \Delta Y = rR/2(\Delta\phi_A - \Delta\phi_B) \end{cases} \tag{2.5}$$

I used a GT 5 mm timing belt mounted on step motor pulleys of 30 teeth. By adding micro-step drivers (with reduction ratio R), I can increase in precision the displacement of the cart. In the actual system $r = 23.85$ mm and $R = 1/4$.

Rotation: The rotation of the target around the center of the cart is presented as:

$$\theta(t + dt) = \theta(t) + \Delta\phi_{CAM}.res.dt \tag{2.6}$$

with θ is the angular position of the target with respect to the cart frame, dt is the time between two commands (10 ms), $\Delta\phi_{CAM}$ is the number of angular steps (in radians) in the ϕ_{CAM} direction and $res = 2\pi/1200$ is in steps per revolution.

Finally, the position of the target (ΔX_{Tar}, ΔY_{Tar}) is a combination of the CoreXY control of the cart (ΔX, ΔY) and the control of the rotation by the embedded system. It can be written as:

$$\begin{cases} \Delta X_{Tar} = \Delta X - cos(\theta).l \\ \Delta Y_{Tar} = \Delta Y - sin(\theta).l \end{cases} \tag{2.7}$$

with $l = distance(Mirror - Target)$ in millimetre.

Considering target movement at 1 m/s along the first diagonal as described above (positive x- and y- axis movement) at 1 m/s, all movement would be caused by motor A: $\Delta X = \Delta Y$ then $\Delta B = 0$. With a pulley radius, r of 23.85 mm a maximum angular rotation of 41.93 rad/s or 6.52 rev/s (see Eq.2.4) results, which is within the normal working range of the stepper motors.

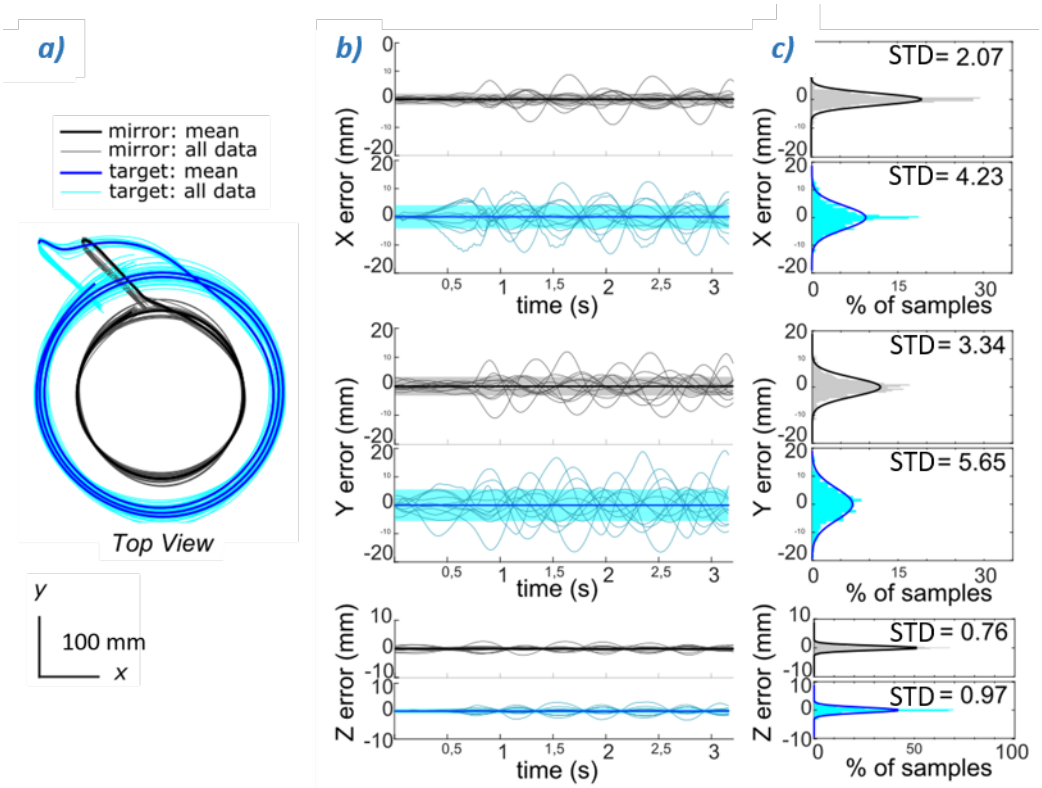

Figure 2.3 – **Precision of a circular target trajectory across 11 trials.** ***a)*** Superimposed circular trajectories reconstructed by the calibrated stereo vision system. Successive loops do not overlap perfectly: this is partly due to mechanical imprecision in moving the target, and party due to imprecision in the video tracking. ***b)*** Superimposed plots of the x-, y-, and z-components of the positional error observed for the target (blue) and the mirror (black) over time. The mirror positions are given in grey with the STD window, and the target positions in blue graphs. ***c)***: Distribution of errors + Gaussian fits for the mirror and the target positions along the x-, y- and z-axes. *(STD = standard deviation). Taken from Varennes, Krapp, and Stéphane Viollet 2019.*

2.2.1.2 Videography, object tracking and image analysis:

In the first version of the setup I implemented two CCD cameras CAM1 and CAM2 (PROSILICA GC640, spatial resolution of 640x480 pixels, temporal resolution of 200

frames per second), equipped with optics used at fixed focal depth (6 mm, F=1.4). Those synchronized cameras were arranged to set up a stereovision system that records the chasing sequences (see end of the chapter for description of the new recording system).

I used an open access tool (DLTdv5) which offers efficient calibration, tracking and 3D reconstruction functions (Hedrick 2008) using the Direct Linear Transformation (DLT) technique described by Aziz and Karara 1971. I followed the DLTdv5 calibration procedure applied to a custom built calibration cube with an edge length of 30 cm, the 64 individual markers spaced at 100 mm distances from each other along all three dimensions (Fig. 2.4). Then, I created a file containing the absolute position of each individual marker, and I determine their position in the two corresponding image frames obtained by CAM1 and CAM2. The toolbox generated a file (csv format) containing the 11 DLT coefficients, specific for my stereovision system, describing positions of the cameras and their orientation relative to each other (for more details see Hedrick 2008).

The DLTdv5 toolbox includes an integrated tracker module that computes the trajectories of multiple objects in a sequence of stereo images. In this project I track two objects: the target and the chasing fly. The tracker can be applied in different modes (automatic, semi-automatic, and manually) and runs a predictive algorithm based on Kalman-filtering to overcome missing matches of the tracked object due to temporary occlusions or excessive object accelerations. I successfully used the DLT method to reconstruct the centre of mass of the target and the fly in 3D based on consecutively tracked points (Fig. 2.6). The fly's centre of mass identified in the previous image frame of the sequences (2D) defines the Region Of Interest (ROI) for the subsequent tracking step. The application of an in-built 2D zoom to each frame allows me to identify and label the fly's head and abdomen to retrieve the animal's 3D body orientation. I validated the method by comparing the computed distance between the head and the tip of the abdomen with the actual length of the fly.

2.2.2 Accuracy of generating and reconstructing target trajectories:

To assess the accuracy of generating target movements and their 3D reconstructions using the CoreXY system, I studied the positioning error of a circular and an ellipsoid trajectory across eleven trials each. Both trajectories covered a large section in the horizontal plane of the experimental arena (Figs. 2.3***a*** and 2.4***a***). First, an initialization phase brought the cart to a reference point close to one of the walls defined by electromagnetic stops. Then the cart moved away from the wall and reached its cruising speed. Then the desired trajectory can start; here three successive circles on each of the 11 tries. The mirror (Fig. 2.2***b***) and target positions were measured every 10 ms, where the mirror is considered to be placed in the centre of the cart. For the circular trajectory, I measured the standard deviations (STD) of the mirror position along the x, y and z axis as small as 2.07, 3.34 and 0.76 mm, respectively (Fig. 2.3***c***),

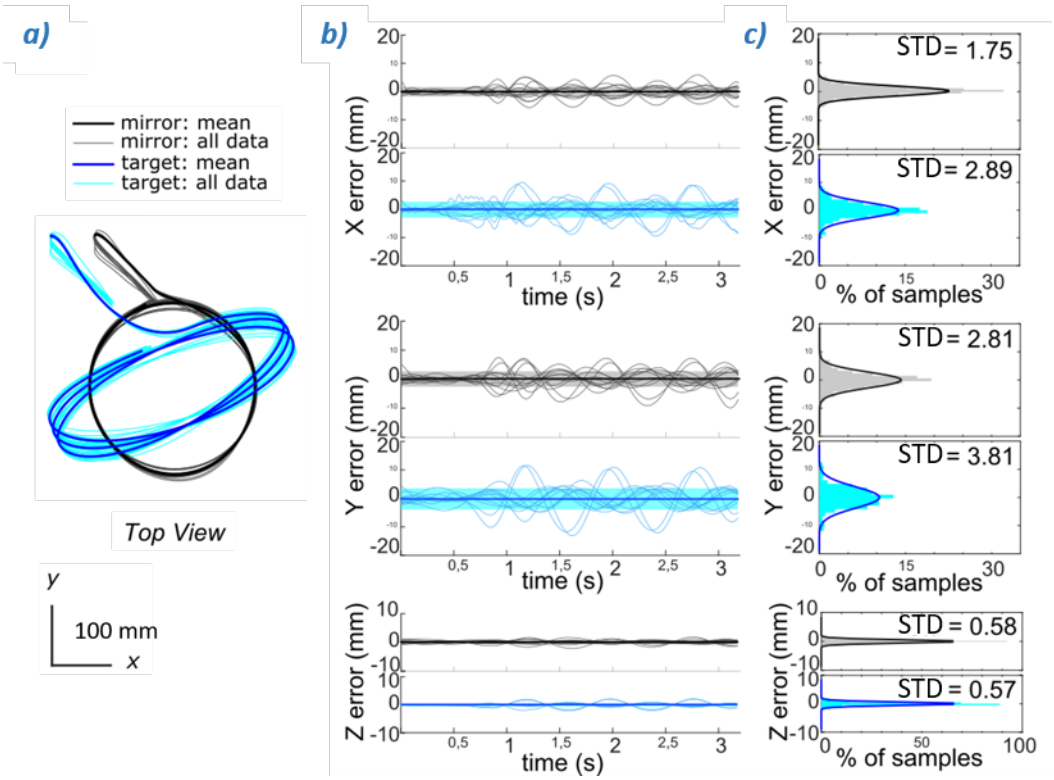

Figure 2.4 – **Precision of a ellipsoidal target trajectory across 11 trials** ***a)*** Superimposed circular trajectories reconstructed by the calibrated stereo vision system. ***b)*** Superimposed plots of the x, y, and z components of the positional error observed for the target and the mirror over time. ***c)*** Distribution of errors + Gaussian fits. *Fig. 2.3 for details.* Taken from Varennes, Krapp, and Stéphane Viollet 2019.

and STD = 4.23, 5.65 and 0.97 mm along the three axes for the target position. During this circular trajectory, the mirror and the target travelled 1.7 and 2.5 m, respectively. On the ellipsoid trajectory the mirror is still moving on a circular path, but the target generates an elliptical movement along which it changes its velocity profile. The standard deviations based on data across 11 trails were even smaller than those for the circular trajectory. The highest STD (for the y-axis) was below 3 mm for the mirror and below 4 mm for the target (Fig. 2.4).

2.2.3 Spatial resolution of the cameras

The spatial resolution of any object in the recorded video footage depends on the pixel resolution the cameras used in relation to the distance-dependant size of the objects. CAM1 and CAM2 recorded images at a resolution of 640x480 pixel (see section 2.1.2). The focus of the cameras was adjusted to the centre of the arena, about 50 cm away from the cameras. At this position 1 pixel on the cameras' CCD sensor corresponds to 0.73x0.97 mm along the spatial x- and y- dimension (assuming no image deformation). This means that the smallest silhouette of the fly with a diameter of 4mm, i.e when the fly is directly facing the camera (without considering wings or legs), will be mapped onto about 17 pixels of the CCD sensor. This number of pixel proved to be sufficient to extract the animal's body ellipse using custom-made image processing software.

To assess the performance of the system we designed a test module that was attached to the cart of our experimental setup. It consisted of a rotating shaft to which a rod was attached. At the end of the rod a dead specimen (male *Lucilia sericata*) was suspended (Fig. 2.5***a***).

The longitudinal body axis of the specimen was aligned with the centre (optical axis) of a mirror implemented at the lower end of the shaft. The distance between the mirror and the specimen (R_a) was 45 mm. Compared to life male flies which measure about 10 mm along their longitudinal body axis, the dead specimen was smaller with a length of about 7.5 mm – probably due to desiccation. The rotating shaft holding the mirror was moved on a circular path (Fig. 2.5***b*** black trajectory) while itself turning at 1000 deg/sec. As a result, the dead specimen did temporarily move at higher speeds than described for the mirror and target of the CoreXY system in section 1, more closely approximating the dynamics of natural chasing flights (Fig. 2.5***c***). These compound trajectory cover a large range of variations of fly and mirror orientations within a large part of the arena. The trajectories were recorded two times with both cameras at 190 frames per second (N=1191 frames). I assessed the spatial resolution of the method by comparing the known distance between the mirror and the fly (45 mm) and the fly length (7.5 mm) with the values produced by the 3D reconstruction system. The subscript A associated with LoS (θ_{AH}, θ_{AV}, R_A) denotes the bearing angle (A for absolute bearing angle), angle formed between the line which connects the center of mass of the fly P, and the center of mass of the target T, and external reference frame. The subscript B associated with LoB (θ_{BH}, θ_{BV}, R_B) denotes the pursuer heading angle,

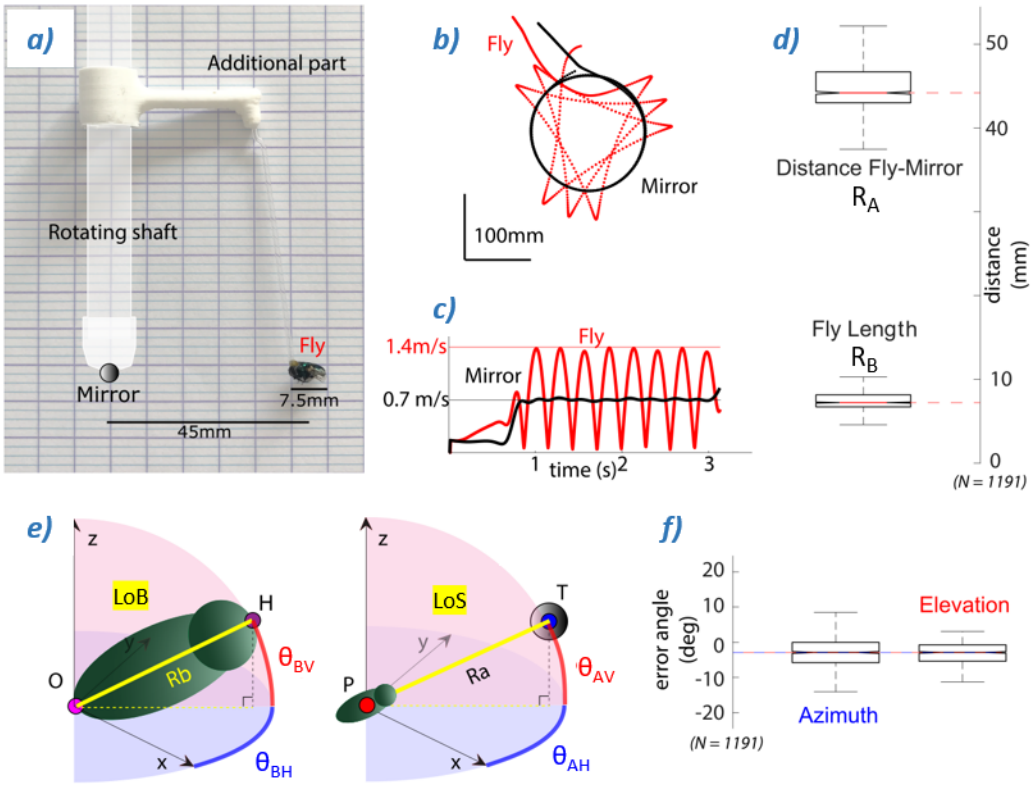

Figure 2.5 – **Validation of the 3D trajectory reconstruction method.** ***a)*** A dead specimen was attached to a transparent off-axis rod and aligned with a mirror at a distance of 45 mm. The fly's length along its longitudinal body axis was about 7.5 mm. ***b)*** top view of the measured trajectory of the mirror (black) and the specimen (red). Black scale bars refers to x- and y-axis of the arena. ***c)*** Mirror and specimen velocities of the trajectories presented in ***b)*** plotted as a function of time. The mirror moves at a constant speed of 0.7 m/s (black trace). The specimen is moved around the mirror with an angular velocity of almost 1000 deg/s and presents a linear velocity range between zero and 1.4 m/s (red trace). ***d)*** Measured distances. *Top.* Distance Fly-Mirror, R_A: mean=45.14 +/- 5.26 mm STD. *Bottom.* Fly length R_B: mean=7.53 +/- 1.24 mm STD. ***e)*** Tracked points of interest. *Left*: The line OH, or line of body, Line of body (LoB), describes the specimen's orientation defined by the tip of the abdomen O, and the front of the head H, given in spherical coordinates (θ_{BH},θ_{BV},R_B, B for body). *Right*: The line PT, or line of sight Line of sight (LoS), connects the center of mass P of the specimen (P for pursuer) with the center of mass T of the target, in spherical coordinates (θ_{AH},θ_{AV},R_A). ***f)*** Angular resolution. Errors were obtained by calculating the difference between the vectors **PT** and **OH** shown in ***e)*** (comp A - comp B).*Left.* Azimuth error (θ_{AH} -θ_{BH}) : median = -2.89 deg; mean = -3.07 +/- 5.88 deg. Elevation error (θ_{AV} -θ_{BV}): mean = 3.32 +/- 3.19 deg. Means and STDs based on N = 1191 frames. Taken from Varennes, Krapp, and Stéphane Viollet 2019.

or longitudinal body axis of the Pursuer (*B* for body), that connects the top of the head H to the tip of the abdomen O (Fig. 2.5***e***). The system returned a mean fly-mirror distance R_A of 45 +/- 5 mm STD and a mean fly length R_B of 7.5 +/- 1 mm STD (Fig. 2.5***d***).

As the longitudinal body axis of the fly was aligned with the specimen-mirror line, we could determine the azimuth and elevation error angles between those two axes. We found a mean azimuth error of -3 +/- 6 deg STD and a mean elevation error of -3 +/- 3 deg STD. Under the assumption that the head and body are fixed, when reconstructing the field of view of the pursuer, those errors of body orientation will represent an error of a couple of ommatidia for *Lucilia sericata*.

2.3 Analysing 3D chasing flights

I used the novel setup to record chasing flights in blowflies (*Lucilia sericata*). Pupae were purchased from an animal supplier (BioFlyTech) in Spain. For further work, I have established a colony in Marseille. Male flies aged between 5 and 12 days were placed in the arena. They were exposed to a 12:12 hours light:dark cycle with a luminance of about 2000 $cd.m^{-2}$ at a temperature between 20 and 25 degree centigrade. They stayed in the arena without engaging in an experiment for one day to get used to their new environment. Chasing flights were recorded around noon. I used a black sphere of 8 mm diameter as a target.

2.3.1 Parameters describing strategies of catching targets

Identification of pursuit strategies requires the analysis of relevant kinematic parameters. In this section I will describe some of the parameters I am able to extract from my behavioural experiments. I recorded free fight pursuits at a rate of 190 fps, corresponding to a time resolution of 5.3 ms. The 2-dimensionally tracked positions of the target and the pursuer were computed with direct linear transform (on how to get DLT coefficients see section 2.1.2 and Hedrick 2008) to reconstruct their 3D positions. When presenting the flies with a circular target trajectory I observed essentially the same behaviour as Boeddeker, Roland Kern, and Martin Egelhaaf 2003, who distinguished between 'capture-' and 'pursuit-chases'. In the former case, the pursuing fly soon captures the target while in the latter case the animal pursues the target moving on a circular trajectory for at least one circle (about 650 ms with a target moving at 1 m/sec). Examples of both flight type trajectories reported by Boeddeker, Roland Kern, and Martin Egelhaaf 2003 are shown in Fig. 2.6***b***. For comparison Fig. 2.6***c*** shows similar flight trajectories studied with my novel setup. In both pursuits the fly chases the target moving along a circular path at a constant speed of 1 m/s. The absolute velocity profiles of the target and the long pursuit flight are shown in figure 2.6***d***, where we can see that the fly velocity varies a lot, and it reaches a maximum of 2 m/s. The 3D reconstruction of the sequences provides valuable information about the fly's strategy to capture the target. In both types of chasing flights (fast capture or long pursuit, Fig. 2.6***c***), the flight path of the fly suggests that it is not guided by an interception strategy. Instead, the fly closely follows the circular trajectory of the target. To investigate the behaviour in more detail I presented the flies with more complex target trajectories.

Figure 2.7 shows a fast capture when the target follows a type of trajectory different from a circle. I called this specific trajectory 'spring-shaped'. It consists of a simple translation along the y-axis combined with a rotation of the target around the z-axis. The rod, the target is attached to, rotates at 600 deg/s, but is also subject to translation due to the movement of the cart. As a result, the angular rotation of the target varies between 380 and 1340 deg/s. Its linear speed component (in the horizontal plane) varies between 450 and 1060 mm/s with a mean of 700 mm/s. Along this trajectory,

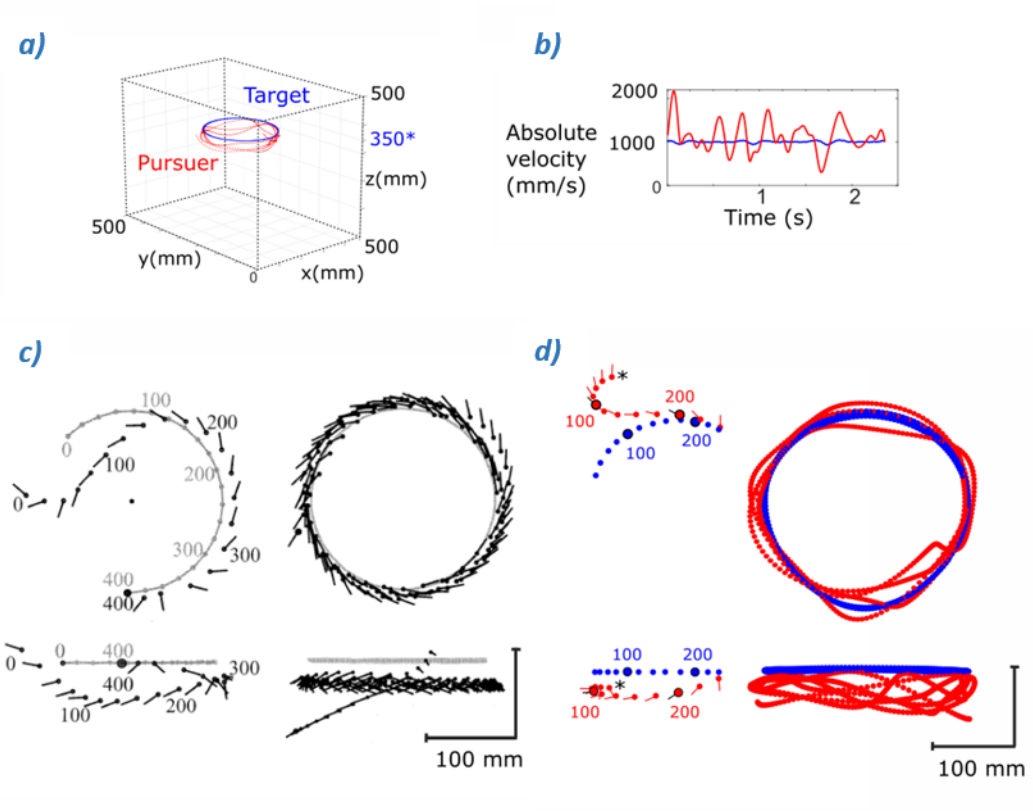

Figure 2.6 – **Preliminary results: Example of fast capture and long pursuit characterization** ***a)*** Reconstruction of a male blowfly chasing a dummy target. ***b)*** Absolute velocity of the target and the fly during pursuit seen in subfigure (***a,d*** *Right*). The target speed is centred around 1m/s whereas the pursuer's speed reached peak values of up to 2 m/s. ***c)*** *Left*: Reconstructed 3D trajectory of a fly (black markers) capturing the target (grey markers) viewed from on top and from the side. Filled circles and lines indicate the fly's centroid position and body orientation, respectively. The numbers denote time stamps during the chasing flight spaced at 100 ms. *Right* Chasing flight without target capture. Results shown in *left* and *right* subplot copied from Boeddeker and Martin Egelhaaf 2003. ***d)*** Pursuit of the target during a similar experiment as shown in ***c)***, performed in our chasing arena. *Left*: Reconstruction of a fly (red markers) capturing the target (blue markers) during a fast capture (250 ms). For sake of clarity the positions are placed every 20 ms, and except for colors, the caption is the same as in ***c)***. *Right*: Reconstruction of a long pursuit without target capture (data from subfigure ***a***). Each dot indicates the centre of mass of the target (blue) and the fly (red) plotted every 5 ms. For sake of clarity the body orientation and time stamps are not presented here. Taken from Varennes, Krapp, and Stéphane Viollet 2019.

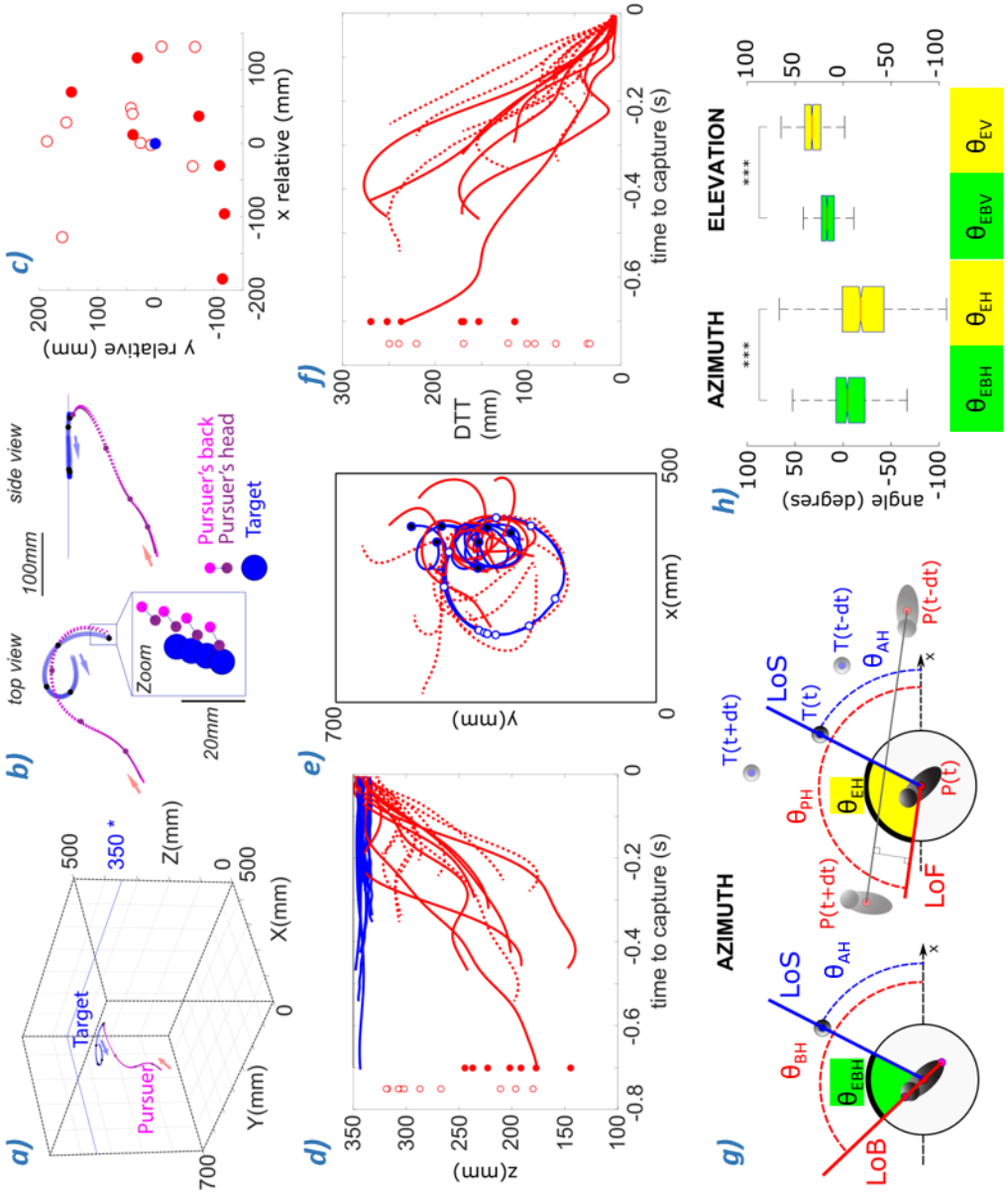

Figure 2.7 – (Caption on the following page.)

Figure 2.7 – **Preliminary results: Analysis of dynamics in a capture** ***a)*** Reconstruction of a chasing flight after a target moving along a 'spring-shaped trajectory'. Bigger points mark positions reached after 100 ms time intervals. The target is moving in the horizontal plane indicated by the blue lines (350*). Arrows show the direction of the target and the pursuer at the beginning of the sequence. ***b)*** Top and side view of the chasing flight shown in (A). Head and tip of the abdomen of the pursuer are represented by differently coloured markers. The high degree of overlap of the markers demonstrates the robustness of the method. ***c)*** Relative position of the pursuer when initiating the pursuit (top view).Two types of target trajectories are presented: open circles for the 10 circular trajectories, and filled circles for the 8 spring-shaped trajectories (target in blue). ***d)*** Altitude change of the pursuer before target capture. Dots on the left give the detection altitude (mm) of the pursuer for each chase. ***e)*** Top view of the chases. Note the distinct target trajectories, Central Circle, and spring-shaped on the right side of the circles. Positions where the fly initiates the pursuit are shown in white filled dots for Circle Trajectories, and black filled dots for spring-shaped trajectories. The black rectangle represents the experimental surface. ***f)*** Change of the DTT before the capture. Dots represent the detection DTT of each pursuit. Opened markers for circular trajectories, and filled markers for spinning trajectories. ***g)*** Definition of the measured angles θ_A, θ_P, θ_B and θ_E. From the top view only the azimuth component of the error angles is available. *Left*: The body error angle, θ_{EB}, or target-body angle is defined by the angle made between the LoS (azimuth: θ_{AH}, or bearing angle) and the longitudinal body axis LoB (azimuth:θ_{BH}, also Yaw of the fly). *Right*: Part of a pursuit sequence. Three consecutive horizontal positions of the Target (T) and of the Pursuer (P) are represented by their center of mass. The Line of flight (LoF) of the pursuer at time t is the line joining previous and next positions (azimuth: θ_{PH}). This line plotted on the point P(t) is similar to the tangent of the trajectory on this point. The flight error angle, θ_E, describes target heading angle. It is the angle made by the LoF of the pursuer and the LoS. ***h)*** Boxplot of the two components (horizontal θ_{EBH},θ_{EH}, and vertical θ_{EBV},θ_{EV}) of the two error angles for the 17 captures presented above. These two error angles are significantly different on both planes (Ttest, p_H=9E-17, p_V=2E-100, see ***, N= 1104). Adapted from Varennes, Krapp, and Stéphane Viollet 2019.

the target changes both direction and velocity, which brings it closer to the kinematics of the female flight. In this pilot study I focused only on capture chases, i.e. when the pursuer successfully catches the target in mid-air. Figure 2.7 shows some of the results, in addition to the 3D reconstruction of one chasing flight in the experimental arena together with a top and side view of the entire sequence. This capture sequence occurs in about half a second. The chaser was hovering close to a wall oriented opposite to the target when he detected it.

The start of a pursuit is initiated when the fly detects the target. It is manually identified in the recorded image sequences as the pursuer changes its body orientation in a saccade-like way followed by an acceleration phase. In Fig. 2.7***c*** the position of the fly at the point in time before the body saccade is plotted relative to the target position. The data suggests that pursuit flights are initiated independently of the current position of the fly .

An important parameter for the analysis of the pursuit flight trajectory is the DTT (Fig. 2.7***f***). The change of this parameter can give valuable information about the strategy if it is not linear (Trevor J Wardill, Samuel T Fabian, Pettigrew, et al. 2017; Kane, Fulton, and Rosenthal 2015). This change of this parameter along the z-axis (or altitude), which has rarely been taken into account in previous studies, is highly relevant when it comes to a 3D model of aerial pursuit strategies (Fig. 2.7***d,f***). It is also required for estimating forces (here lift) the fly produces when approaching the target.

2.3.2 Parameters describing the orientation of the fly during pursuit flights

The knowledge of the velocity vector during a flight trajectory alone does not necessarily allow me to reconstruct the region of the eyes onto which the image of a target is projected because its direction may not be aligned with body orientation of the animal in case of drift or side-slip (Wagner 1986). Thus, to characterize pursuit strategies, I will analyse three lines and the angles they form with the reference frame.

The longitudinal body axis of the fly, here called line of body (LoB), defines the body orientation (see **OH** in Fig. 2.5***e*** , θ_{BH}, θ_{BV} Fig. 2.5***e*** and Fig. 2.7***g***). Yaw and Pitch are the two angles that define this line. The line of sight (LoS), is the line connecting the centre of mass of the fly with the target (see **PT** in Fig. 2.5***e*** , θ_{AH}, θ_{AV} (A for absolute angle) Fig. 2.5***e*** and Fig. 2.7***g***), it is defined by the bearing angle. The direction of travel, or line of flight (LoF) is the tangential line of the flight trajectory, also referred to heading direction in literature.

It is important to note that in the context of aerial pursuit, the term "error angle" that is often found in the literature, may have different meanings. Here we propose the analysis of two error angles, defined by the three lines presented above. The body error angle (θ_{EB}), is the angle formed by the LoS and the LoB. This angle characterizes the alignment of the body with the target position, it is the reason why I call it target-body angle. In case the head is fixed to the body, it is directly linked to the position of the target on the fly's retina. The second parameter here called flight error angle (θ_E), is

the angle formed by the LoS and the LoF as defined by Land and Thomas S Collett 1974, **I may use the term target heading angle later in the manuscript.** This angle gives information about the kinematics of the pursuit's strategy (Fajen and Warren 2007; Gonzalez-Bellido, Samuel T Fabian, and Nordström 2016).

In this account I define the orientation of the fly by its yaw-, pitch- and roll- angles. This means that in an absolute coordinate system, angles which are relative to the orientation of the fly will have an azimuth and an elevation component. The method proposed here allows me to separately extract and analyze those components along the entire pursuit flight sequence. The comparison between the two types of trajectories used here (circle and spring-shaped) suggest that the target speed does not affect the azimuth of error angle 1 (two samples t-test: $p(\theta_{EB}) = 0.46$). The LoB stays aligned to the LoS, so the pursuer holds the target in the central part of its visual field: in the 'love spot' position.

As presented in more details in Section 1.4.1, in predatory species or in species where males catch female on the wing (Land and D.-E. Nilsson 2012), we observe a functional regionalization of the compound eye. In the former case, the animals are endowed with a small area in the frontal eye around the eye equator and above, called love spot (J. H. van Hateren, R. C. Hardie, Rudolph, et al. 1989; Trevor J Wardill, Samuel T Fabian, Pettigrew, et al. 2017; Sherk 1978; Thomas S Collett and Land 1975; Land and Eckert 1985; Brian G. Burton and Simon B. Laughlin 2003; Hornstein, O'Carroll, Anderson, et al. 2000). In either case, only a specialized high resolution area of the eye provides sufficiently fast and robust visual input to support tightly controlled pursuit flights. This requires, as presented above, an orientation of the visual system where the target is projected onto this specialized region of the eye.

I measured the two error angles when presenting to the males the two trajectories described above. Regardless of the trajectories (and so to the angular velocity tested), the two errors are significantly different (two samples t-test: $p(\theta_{EBH}, \theta_{EH}) = 9E^{-17}$, $p(\theta_{EBV}, \theta_{EV}) = 2E^{-97}$, Fig. 2.7***h***). This emphasizes the non alignment of LoS and LoB, causes are discussed below.

2.4 Discussion

A system adapted to blowfly and housefly speed. The setup presented in this chapter does not have the capability to generate dummy speeds equivalent to those of the hoverfly *Eristalis tenax* female, which, according to Thomas S Collett and Land 1978, was assumed to reach maximum speeds up to 8 m/s. But it can generate maximum dummy velocities of 3 m/s which is adequate to study slower fly species such as blowflies and houseflies, where females fly at mean speeds of 1.2 and 0.65 m/s, respectively (Ennos 1989; Land and Thomas S Collett 1974). A target velocity of 3 m/s was the maximum obtained when it was mounted on a 15 cm long rod (Fig. 2.8***b***). The flight trajectory acquisition system allows me to detect changes both in LoF and body orientation (LoB) with a temporal resolution limited by the 5.3 ms time interval between two consecutive frames. This sampling rate is enough to compare our results with the values of the model created by Boeddeker and Martin Egelhaaf 2003 which will be presented in the next chapter.

Kinematic models of the chasing fly. Building a kinematic model allows me the analysis of capture strategies (Pal 2015) as a balance between speed and manoeuvrability (Howland 1974). It also helps to characterize the pursuer's flight envelope. Once I designed the pursuer's object, here an ellipsoid defined by its centre of mass and its yaw- and pitch-angles, its envelope can be defined as the possible combination of translational and rotational movement components. The method presented here enables me to measure 3D target and pursuer positions with a maximum error of 5 mm. This position error is due to distortions caused by the camera optics, increased with increasing eccentricity and distance from the cameras, but less than 2 mm when the fly in the center of the arena. The chasing fly's yaw- and pitch- body orientation are measured with a maximum error of 6 deg, and were sampled every 5.3 ms. This makes the method suitable for building acceptable kinematic model of the pursuit. In comparison, the latest kinematic model of the blowfly pursuer (Boeddeker and Martin Egelhaaf 2003) was based on pursuits recorded in a cubic flight arena with 30 cm size, where the target moved along a circular path at constant speed. In this study, 3D-reconstruction system offered a spatial resolution of +/- 1.5 mm and a temporal resolution of 20 ms. Sampling rate was too close to the 15 ms time delay estimated to change the heading angle. In addition, body pitch- and roll- of the fly could not be extracted.

Close-up approach visualization module. In addition to recording the positions and orientations of the male fly during the chase, I also decided to integrate an onboard observation point as close as possible to the target. The images obtained will provide investigative support for two major studies. *i)* I have presented in chapter 1 the different phases of the pursuit: detection, tracking and capture. The capture phase is crucial and yet it has been insufficiently evaluated. I would like to investigate the manoeuvre in which the pursuer rears up to catch the target with its legs. *ii)*

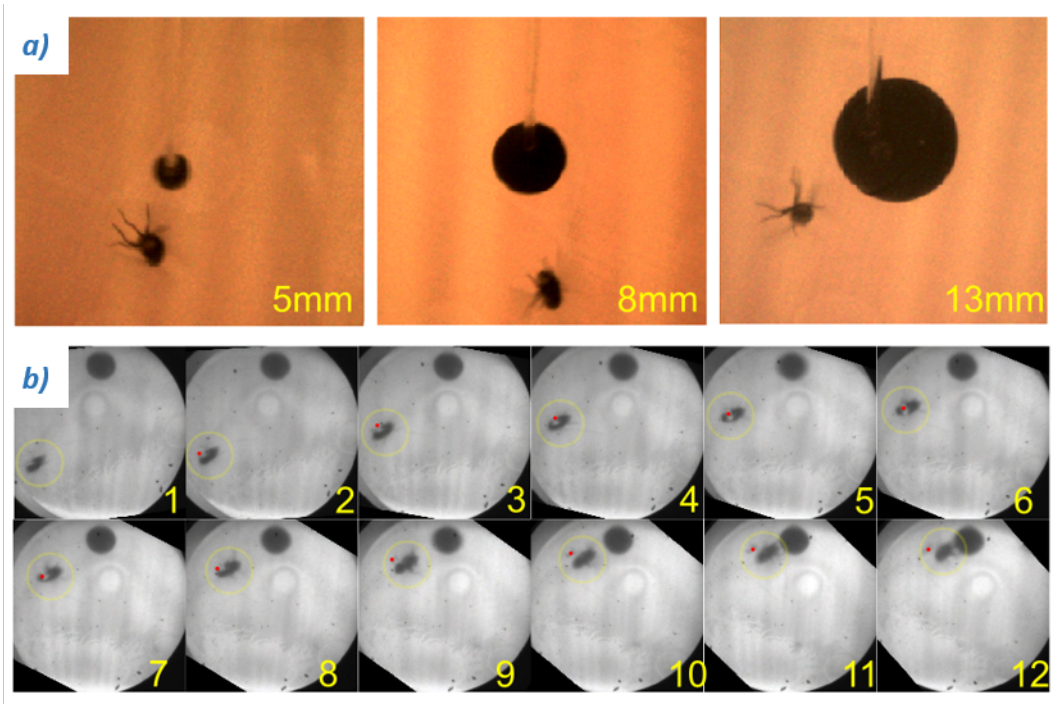

Figure 2.8 – **Embedded pictures of the target and the pursuer *a)*** Three pictures taken from the MicroCamera placed originally in the vertical tube of the moving cart (Fig. 2.1***c***). Three sizes of targets have been tested to evaluate the field of view of the rotating mirror. The video footage recorded with micro-endoscope module (MEM) allows us to detect the pursuer's legs, wings and eyes when approaching the target. ***b)*** Last 63 ms of the target capture (same chase as in Fig. 2.7***a***), monitored with the MEM. The pursuer approaches the target before the final catch. A small flag was waxed onto the pursuer's dorsal thorax indicating its dorso-ventral body axis. Tracking the tip of the flag (red dot) enables the reconstruction of the external body roll- coordinate. Reconstruction of the full body attitude (yaw-, pitch- and roll-) is possible at high temporal resolution (5.3 ms). Taken from Varennes, Krapp, and Stéphane Viollet 2019.

Even more advanced real time video tracking systems such as the one developed by Andrew D Straw, Branson, Neumann, et al. 2011 did not capture the body-roll of the animal. To achieve the sufficient spatial resolution, smaller areas can be an option, because of smaller distances and therefore higher spatial resolution in combination with extended focal depth of the cameras such as in Florian T. Muijres, Elzinga, Melis, et al. 2014, but it would be inadequate to study pursuit strategies in bigger species which require more space to perform chasing flights. Other techniques have been developed to estimate body-roll during free cruising flight (Ristroph, Berman, Bergou, et al. 2009), in tethered flies (Tammero and Dickinson 2002), or in semi-tethered flies (Schilstra and Van Hateren 1998) but never during aerial pursuits in free flight. The additional module will allow me to monitor the body orientation of the fly while chasing the target.

The micro-camera and its low temporal resolution. Video footage from embedded camera offers nice pictures of the pursuer. I could identify leg orientation, as well as head-roll. The first version of this module consisted of a micro-camera (NanEye from Awaiba) facing a rotating mirror that keeps the target in the camera's field of view (Fig. 2.8***a***). First results have validated the functional design of the module which enabled me to stabilize a frontal view of the chasing fly even during a curved trajectory of the dummy. They also confirmed qualitative observation of banked turns during those pursuits, where the body roll- angle can assume values above 90 deg. The initial test version of the module, however, did not have sufficient temporal resolution to support a meaningful quantitative analysis of the video footage.

The Micro-Endoscope Method (*MEM*). The second version of the module was based on a microendoscope technique, proposed by Pierce, Yu, and Richards-Kortum 2011 (Fig. 2.1***c***). This technique offers a high temporal resolution configuration that can be used to monitor the pursuer's body orientation until when the pursuer catches the dummy. I performed first tests using a 50.000 pixels optical fibre bundle (MyriadFiber) combined with a 1 mm Grin lens (infinity focal depth, and visual field of 60 deg, GrinTech). Images were transmitted via the optical fibre bundle to a CCD camera, which was equipped with a microscope objective focused on the end of the fibre bundle. The CCD camera was synchronized with the other 2 high speed cameras which monitored the position of the dummy and chasing fly at 190 fps. Figure 2.8***b*** shows the frames obtained during the final phase of a capture flight. A flag attached to the dorsal part of the thorax of the fly was tracked relative to the position of the legs to compute the roll angle of the fly. The spatial resolution with the 50.000 pixels fibre bundle was not high enough to extract confidently the body angle in all pursuits. In the latest version I implemented a 100.000 pixels fibre bundle which unfortunately still not provide sufficient spatial resolution.

2.5 Latest system upgrades

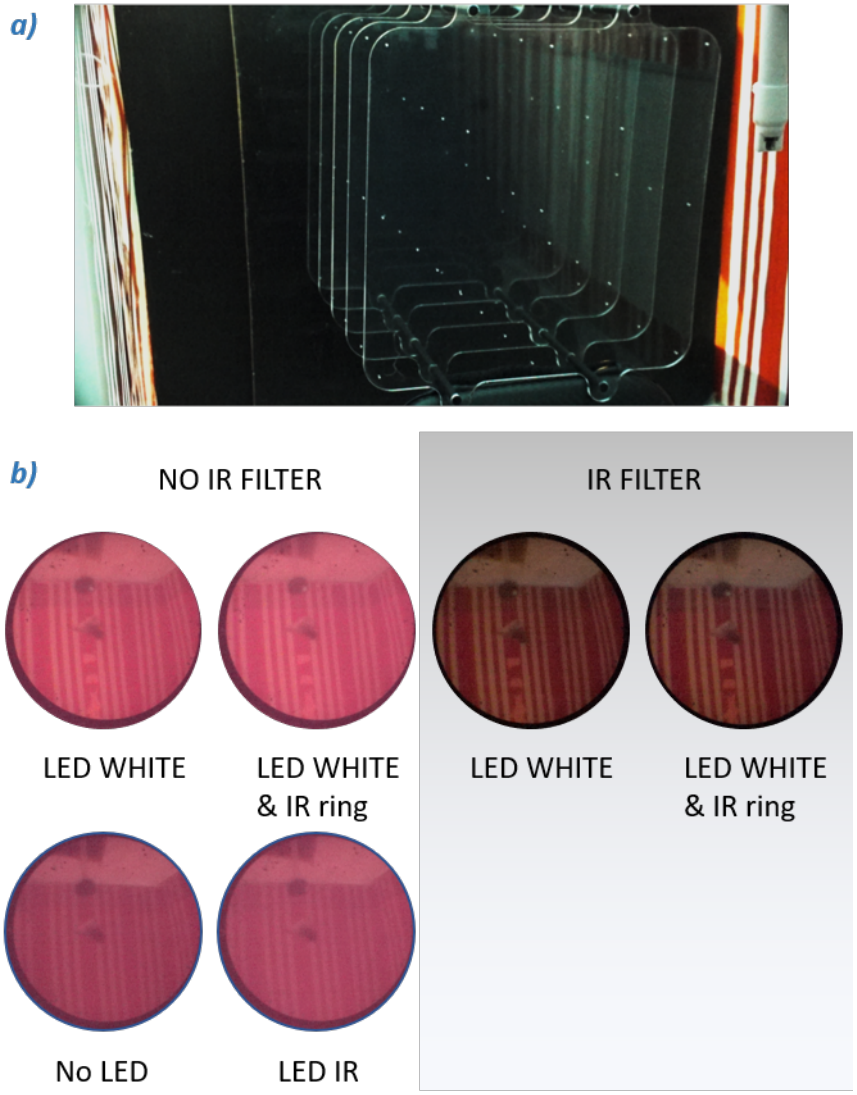

Figure 2.9 – **Improvements of the videography and calibration.** ***a)*** Picture taken from one of the stereocameras during calibration. Presentation of the calibration cube (with 65 space markers) in front of a black background to enphasize the markers contrast, and presence of the rotating shaft plus mirror on the upper right part of the picture. ***b)*** Images of the target and a fixed fly taken from the new MEM, under light variation. None of the exposures tested would allow to extract the orientation of the fly. The best combination was the double exposure: white led wall panel, and IR shower. Taken from Varennes, Krapp, and Stéphane Viollet 2019.

Several materials and techniques were improved during the course of the study.

Cameras: The three Prosilica cameras have been replaced by a set of Sony RXO cameras, equipped with synchronization boxes. They offer much better spatial and temporal performance (I used the following configuration: 1676x566 pixels , 240 fps).

Calibration technique: I have improved the 3d calibration with the design of a new calibration cube - presenting more and smaller markers than previous cube (Fig. 2.9***a*** compared to SupFig. S2.4 *Top*), and I also improved the calibration method. Efforts to improve the calibration and better performance of the recording system will certainly result in better accuracy in the 3d reconstruction of the tracking. I have not measured this improvement yet.

MEM, version 2: I replaced most of the components of the MicroEndoscope Module. These modifications were a big challenge and should lead to a considerable improvement of the embedded vision. Replacement of the old fiber optic bundle by a new offering a better image quality (50 to 100k fibers). The new fibre is also much longer (3m). This length reduces the risk of breakage when the target's movements are too abrupt. Fibre's diameter is also larger, a new grin lens was fixed at the scene extremity, and mountage close to the mirror was adapted. On the other end of the fiber (image side) I designed a new microscope with equipment from Thorlabs (Fig. 2.10). This module was equipped with a beamsplitter, which allows me to project a light on the surface of the target (and eventually to the pursuer). Unfortunately, the resolution of the fiber is still too low to extract quantitative head-body orientation.

Changing the light conditions: The Sony cameras are equipped with an Infra-Red filter. As flies are blind to infrared light, I illuminated the scene with IR LED projectors and remove the IR filter from the cameras. I installed a ring-illumination around the rotation axis of the target (inside the arena) of IR light which lights the pursuer from above when approaching the target. I also fixed white led panels on the flight arena walls to increase the overall light level, and I tested the conditions offering the best contrasts (Fig. 2.9***b***). Outcomes were not as good as expected, I even tried phosphorescent powders reacting to IR light. The amount of visible light emitted by the phosphorescent powder exposed to IR light was too small under the lighting conditions. Increasing the IR power would present risks of overheating and consequences on the tracking behaviour.

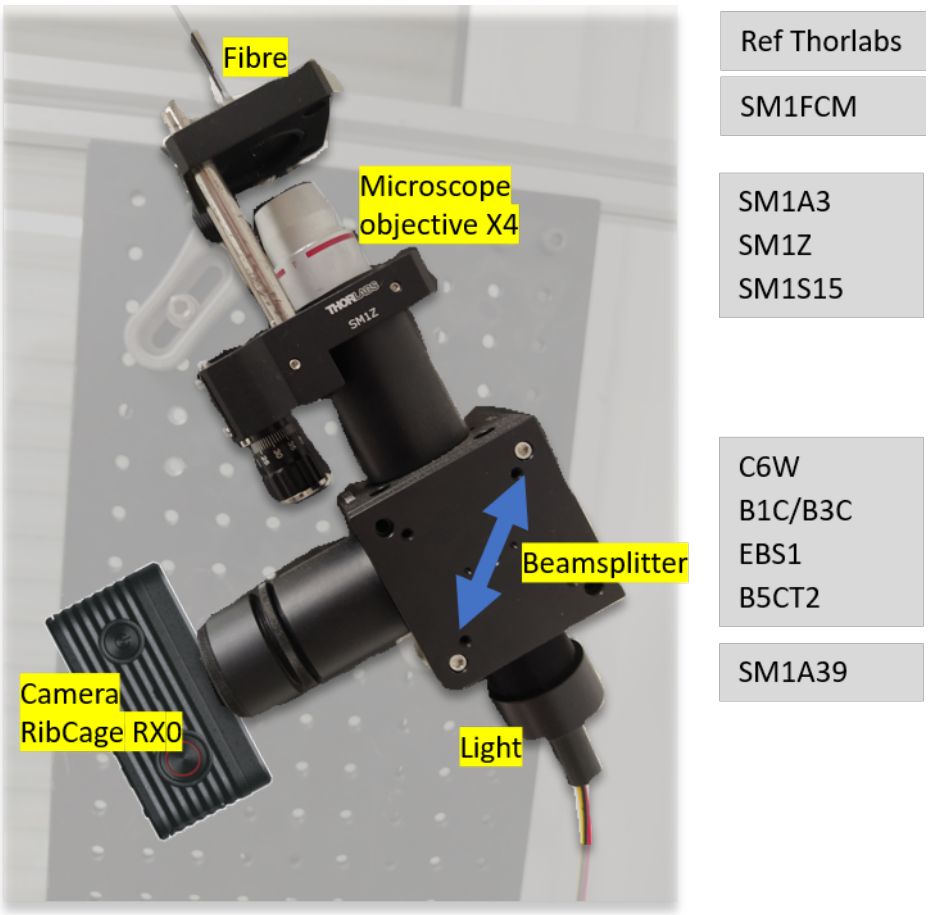

Figure 2.10 – **Latest version of the microendoscope.** Image on the surface of the fiber is enlarged by the x4 objective, then projected on the surface of the beamsplitter finally dispatched on the Camera sensor. Translation mount offers fine adjustment along the optical axis to compensate focusing errors in fiber alignment. The beamsplitter is also used to guide an external light (bottom right) to the surface of the fiber through the x4 objective.

Conclusion

I have developed a novel experimental setup that enables me to monitor the 3-dimensional movements of a freely flying fly chasing a dummy target along an arbitrary 2-dimensional trajectory. The quantitative analysis of the dummy movements shows that this method is suited to generate highly reproducible trajectories across tries. Both target position and the position of a pursuing fly are monitored and reconstructed at high spatial as well as temporal resolution, including the pursuer's body orientation. Those data are instrumental to retrieve the kinematics of the pursuing fly and to study the visual parameters the animal controls during chases.

Supplementary figures

Name of Material/ Equipment	Company	Catalog Number	Comments/Description
ARENA			
			4x100cm 4 x70 cm 4x60cm
Aluminium Strut 20x20mm	RS	466-7219	8x50cm 4x46cm
Corner Cube Kit (x16)	RS	466-7433	
Angle Bracket (x4)	RS	466-7354	used for stops and fixations on the arena
Strut Profile T-Slot Nut, M4 (x20)	RS	466-7281	used in the text as ***Nuts***
OpenBuilds Dual V Wheel Kit - Delrin (x12)	OPENBUILDS	SKU 500	
Tee Nuts (/25 Pcs)	OPENBUILDS	SKU 50	
Aluminium spacers (M5 6mm /10pcs)	OPENBUILDS	SKU 90	
Aluminium spacers (M5 9mm /10pcs)	OPENBUILDS	SKU 225	
Aluminium spacers (M5 20mm /10pcs)	OPENBUILDS	SKU 65	
ACTUATION			
Teensy 3,1			Electronic card from ARDUINO familly
Dual port ethernet card	INTEL	EXPI9402PTBLK - PRO/1000 PT DUAL PORT SERVER ADAPTER RJ45 PCIE	used to connect the stereovision cameras
Stepper motors (x2)			200 steps per rev
Microstepper drivers (x2)		CW-215	mode microstep 4
aluminium toothed pulleys	HPC europe	30T5-11	
timing belt T5 (8m)	HPC europe	T5M/1000/6	
all effect sensors (x3)			with custom made electronic card and magnets
Stepper Faulhauber		AM0820 -V5-56	gear reducer 51,2:1

Sup Figure S2.1 – **List of equipment: arena and actuation**

Name of Material/ Equipment	Company	Catalog Number	Comments/Description
OBSERVATION	Version 1		
CCD Cameras (x2)	Prof Krapp's lab	PROSILICA GC640	640 x 480 200 fps
Objectives 6mm F1.4			C-mount
mirror 45°	EDMUND	#49-405	
AWAIBA NANEYE OPTIC FIBER	AWAIBA MyriadFiber	FIGH-50-1100N	50K fibers
GRIN lense	GRINTECH		1mm f:infinite
UV glue	NORLAND	NAO61	
CCD Cameras (x2)		MAKO G G030	644 x 484 300fps
OBJECTIVE MICRO 4X DIN	EDMUND	67706	
C-MOUNT TO DIN OBJECTIVE	EDMUND	54868	
SMA Fiber Adapter Plate with External SM1 (1.035"-40) Thread	THORLABS	SM1SMA	
Multimode Connector, Ø1275 µm Bore, SS Ferrule	THORLABS	11275A	
SMA Polishing Disc	THORLABS	D50-SMA	
SMA 905 Connector: MM , 1250um, Stainless	THORLABS	11275A	
Ruby DualScribe Fiber	THORLABS	S90R	
Threaded Cage Plate	THORLABS	CP02/M	
SM1 Series Fiber Adaptor	THORLABS	SM1SMA	SMA fiber adapter plate with external SM
SMA 905 Connector: MM 1250um, Stainless	THORLABS	11275A	SMA905 Multimode Connector
Cage rods and plates	THORLABS		

Sup Figure S2.2 – **List of equipment: Observation, first version**

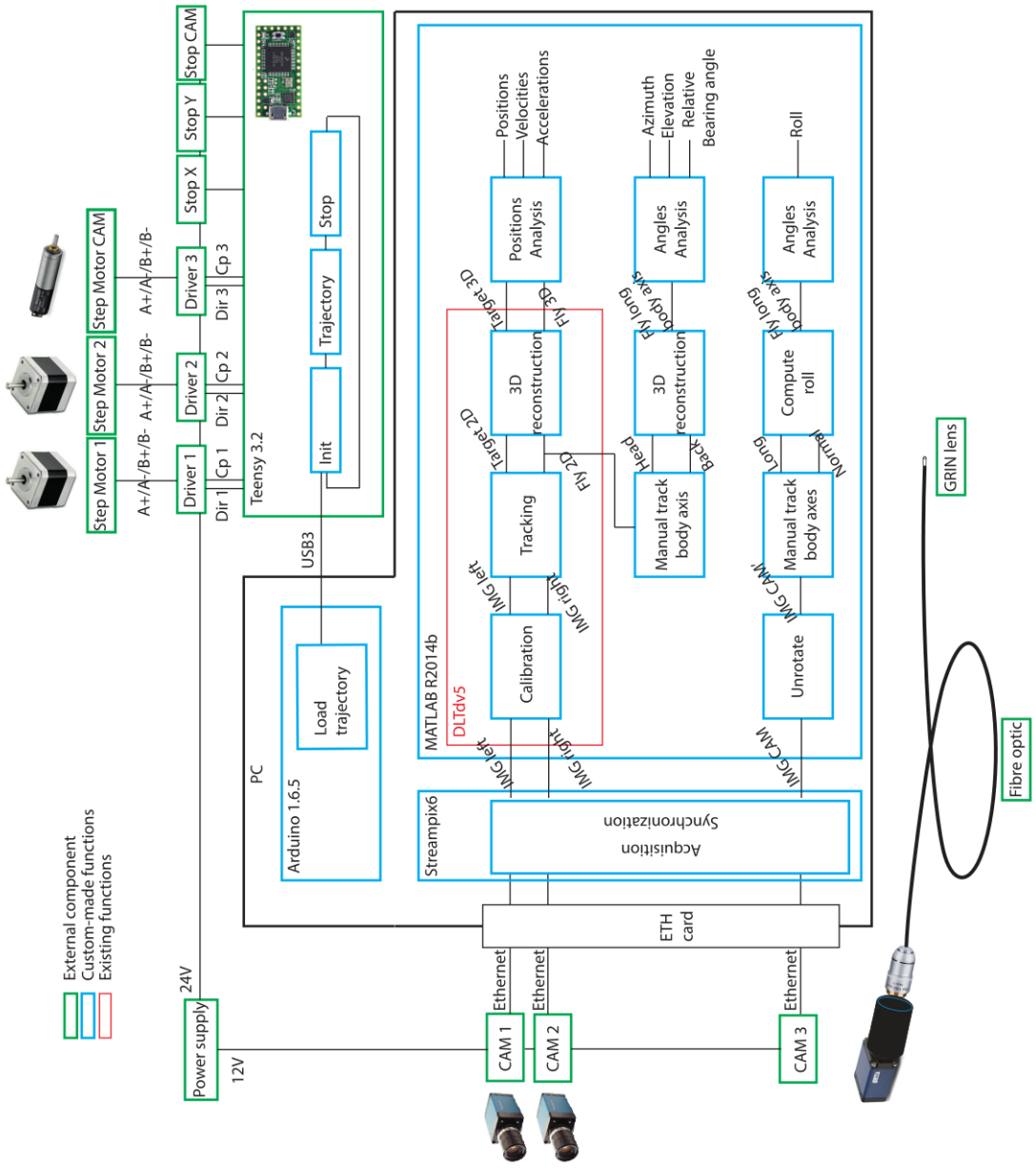

Sup Figure S2.3 – **System representation as functional schematics**

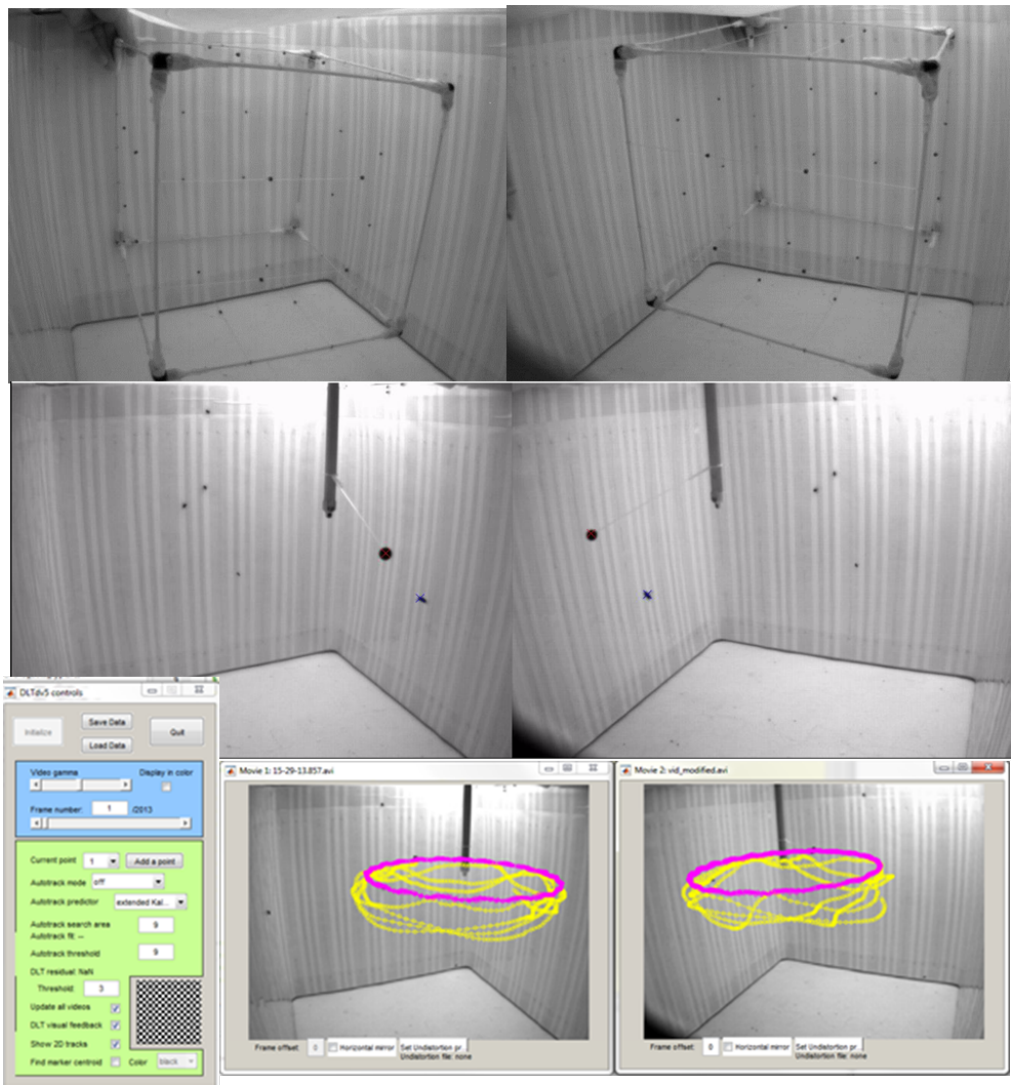

Sup Figure S2.4 – **Stereovision, record and track** *Top* Calibration cube with the 64 markers, view from the two stereo cameras. *Middle* Example of the picture analyzed during a chasing sequence with the target and the pursuer. Left and Right are synchronized pictures. *Bottom* Pointed target and pursuer, with DLT dv5 toolbox presented on the left. Taken from Varennes, Krapp, and Stéphane Viollet 2019.

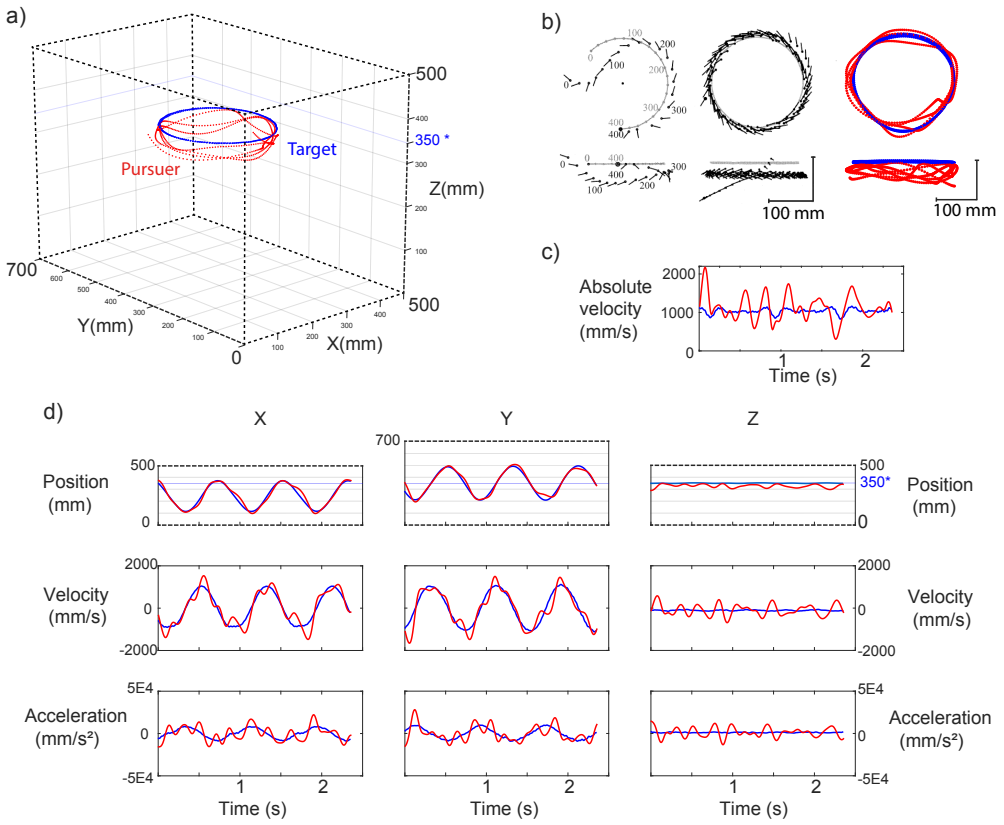

Sup Figure S2.5 – **3D reconstruction and positions analysis. Example of a very long pursuit characterization** a) Reconstruction of a male blowfly chasing a target as point particles. b) *Left* Example of a reconstructed flight trajectory of a fly (black markers) capturing the target (grey markers) from top view (*Upper*) and side view (*Lower*). The fly is indicated by the position of its centroid (circle) and the orientation of its body axis (line). The numbers denote corresponding positions of the fly and the target every 100 ms. *Middle* Pursuit of the target without capture, plotting as in *Left*. b)*Left* and *Middle* are from [Boeddeker et al. 2003]. b)*Right*: Pursuit of the target during a similar experiment in the chasing arena (same pursuit as a)). Each dot is the center of mass of the target (blue) and fly (red) plotted every 5ms. d) Analysis of position, speed and acceleration *upper, middle, lower* row respectively, along three axis x, y and z axes. Taken from Varennes, Krapp, and Stéphane Viollet 2019.

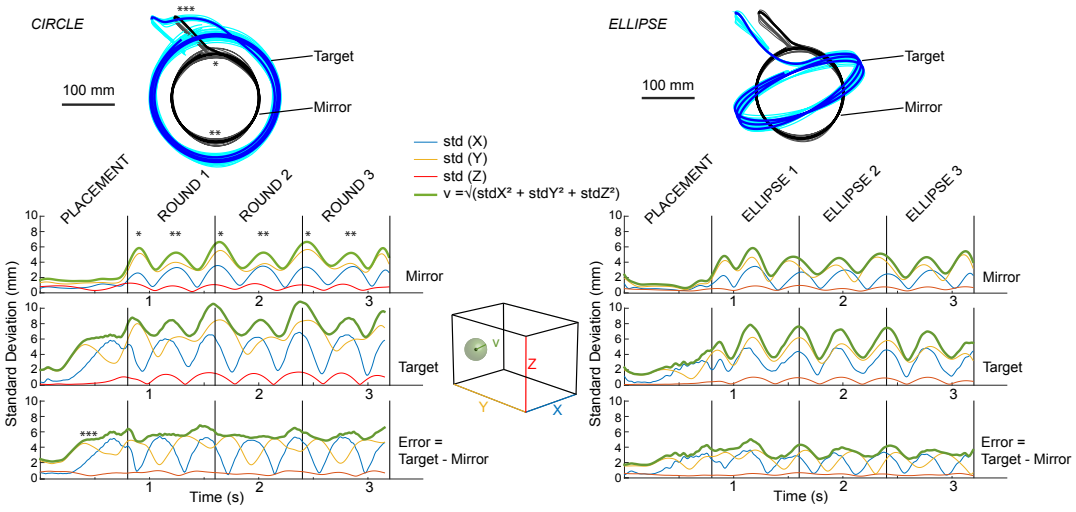

Sup Figure S2.6 – **Analysis of the mechanical repeatability** Standard deviations *STD(X,Y,Z)* along the three axes and the error volume around each point of the trajectory plotted in green (parameter v). *Left*: Circular trajectory and its STD analysis, *Right*: Ellipse trajectory and its STD analysis. Taken from Varennes, Krapp, and Stéphane Viollet 2019.

3 Two pursuit strategies for a single sensorimotor control task in blowfly.

Sommaire

3.1 Introduction . . . 80
3.2 Pursuit strategies in flying animals . . . 82
3.2.1 Constant target heading angle . . . 82
3.2.2 Constant bearing angle . . . 84
3.2.3 Mixed pursuit . . . 84
3.3 Analysis of blowfly's pursuit . . . 85
3.3.1 Experimental conditions . . . 85
3.3.2 Distribution of invariant parameters . . . 86
3.3.3 Kinematics: control of steering . . . 88
3.3.3.1 Horizontal plane: hybrid control for tracking . . . 88
3.3.3.2 Vertical plane: hybrid control for interception . . . 88
3.3.3.3 Similarities in the two planes of approach . . . 90
3.3.4 Limits of the constant target altitude . . . 90
3.4 Developing kinematic models . . . 91
3.5 Developing dynamic models . . . 95
3.6 Conclusion . . . 97

3.1 Introduction

Chapter outline: This chapter focuses on the kinematics of aerial pursuit in the male blowfly *Lucilia sericata* using the actuated dummy method presented in Chapter 2. Most of the results have been presented in an article currently under revision, entitled "Two pursuit strategies for a single sensorimotor control task in blowfly". This chapter roughly follows the outline of the article. First I will introduce kinematic strategies in aerial pursuit, and variables used to control steering. In the second part I will present the analysis of blowfly kinematics and how the flies perform target tracking in the horizontal plane and target interception in the vertical plane. Behavioural data suggest that the flies' trajectory changes are a controlled combination of target heading angle and bearing angular rate. Then I will describe kinematic models implemented based on behavioural measures, and that the contributions of a proportional navigation strategy are negligible. I concluded that the difference between horizontal and vertical control relates to the difference in target heading angle the fly keeps constant: 0 deg in azimuth and 23 deg in elevation. The offset, or 'bias angle' in elevation corresponds to the position of the 'love spot', an extended region of the male compound eye that features physiological and anatomical specializations thought to support aerial pursuit. My work suggests that male *Luciliae* control both horizontal and vertical steering by employing proportional controllers operating at time delays as small as 10 ms in the horizontal plane, the fastest steering response observed in any flying animal, so far.

Background: During a chasing flight the pursuer continuously follows the manoeuvres of its target. This is the sensorimotor control task. The underlying controller takes as visual input angular parameters between pursuer and target, and by a sequence of basic neuronal operations and muscular action it adjusts the steering – *i.e* changing heading – to stabilize the input parameters. In kinematics, two angles link the pursuer to the target: one in the pursuer reference frame, the target heading angle, θ_E, between LoF and LoS, and one relative to an external frame of reference, the bearing angle, θ_A, between LoS and an arbitrary axis. The relationship between pursuer's heading angle, θ_P, and the target's relative angles, θ_E and θ_A, are presented in Figure 3.1***a***. In this chapter I will concentrate on kinematics, thus when I mention steering it will concern the change of the direction of the speed vector. Angular definitions in pursuit literature may differ between research groups, however here I will follow notation used in human ecology, where bearing is defined with respect to an exocentric (allocentric) frame of reference (Klatzky 1998; Fajen and Warren 2007; Bootsma, Ledouit, Remy Casanova, et al. 2016). In the next section I will present pursuit strategies that rely on stabilizing θ_E, θ_A, or a combination of both (Eqs. in Table 3.1).

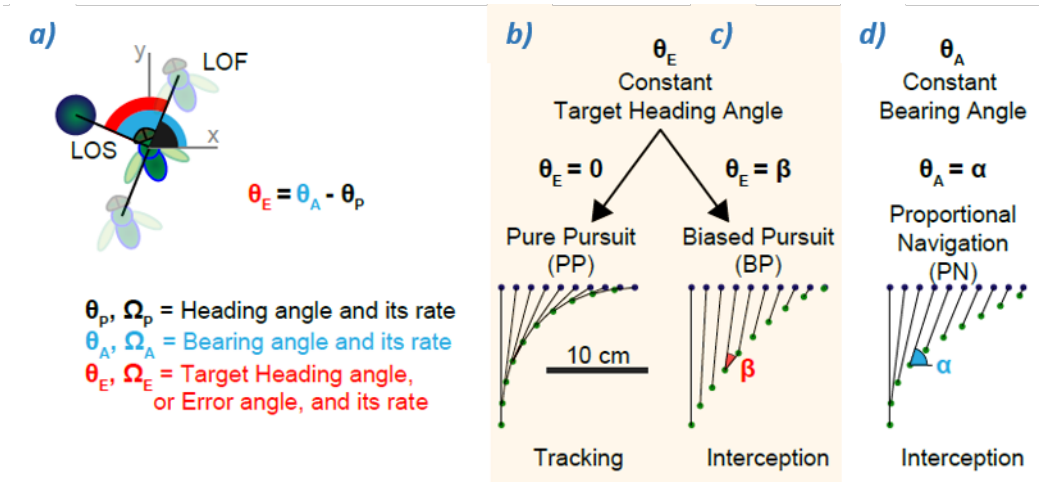

Figure 3.1 – **Definition of angular parameters during pursuit, and planar pursuer's trajectories with different control strategies.** ***a)*** View of angular parameters during pursuit. x and y-axes form an external frame of reference, Line of flight, LoF, connects successive positions of the pursuer, and line of sight, LoS, connects the pursuer to the target. The pursuer's heading angle, θ_P, is formed between LoF and x-axis, bearing angle, θ_A, between LoS and x-xis, and target heading angle, θ_E, is the difference between θ_A and θ_P. ***b-d)*** Simulation of different pursuit strategies. Steering controllers are divided in two categories. The first category aims to maintain a constant target heading angle θ_E equal to zero in the case of pure pursuit, Pure pursuit (PP) in ***b)***, or equal to a non-zero angle, β, in the case of biased pursuit, Biased pursuit (BP) in ***c)***. The other control category maintains the bearing angle θ_A equal to a constant angle other than zero, α, such as in proportional navigation, Proportional navigation (PN), presented in ***d)***. For pursuit simulations, the target linear speed is 1 m/s and the pursuer's speed is 1.5 m/s. The positions of target and pursuer (dark blue and green, respectively) are shown every 20 ms. LoS is shown in black. ***b)*** PP with kp = 1 s^{-1} and Δt= 0 s leading to a tracking strategy. ***c)*** BP with kp = 1 s^{-1} , Δt = 0 s and 'bias angle' β = -30 deg, leading to an interception. ***d)*** PN with N = 3 and Δt = 0 s, leading also to an interception.

3.2 Pursuit strategies in flying animals

3.2.1 Constant target heading angle

Pure pursuit: The mathematical tools used to study chases and escapes date back to antiquity. They advanced during the Renaissance with the boom in maritime trade and the problems of piracy. A famous pursuit problem, 'dog tail' or classical pursuit, was described by Pierre Bouguer, a French mathematician and hydrographer in a paper published in the French Academy's *Memoires de l'academie royale des sciences* in 1735 (from (Nahin 2012)). It presents the trajectory of a pursuer in the case where the pursuer aligns its velocity vector towards the current position of the target, this way the pursuer stays in the wake of the target. This strategy was later observed in tiger beetles (Haselsteiner, Gilbert, and Z. J. Wang 2014), houseflies (Land and Thomas S Collett 1974), blow flies (Boeddeker and Martin Egelhaaf 2003), and honey bees (S. W. Zhang, Xiang, Zili, et al. 1990) (Fig. 3.1***b***), and is now referred to pure pursuit, PP. The PP control can be described by a simple gain – proportional term – as described in Equation (3.1.1), or a proportional and a derivative term, applied to the target heading angle, θ_E. This controller aims at stabilizing θ_E at zero degrees.

Biased pursuit: While during tracking the chaser is heading towards the target's position, during interception it aims at a point in front of the target. Classical interception, also called deviated pursuit strategy in the interception literature, aims to maintain a constant (but non-zero) target heading angle, which I call here bias angle β (Eq. (3.1.2) and Fig. 3.1***c***). The term 'deviated' describes a temporary event, whereas in the technical literature 'non-zero error' mostly refers to an offset angle. I therefore introduce the term 'biased' when referring to a pursuit strategy that keeps the target at a constant, non-zero angle, and BP referring to the biased pursuit. In hoverflies *Eristalis* and *Volucella*, males use their innate knowledge of female's size to compute the optimum interception angle based on the combination of position and angular speed of the target (T. S. Collett 1978). Other species maintain the bias angle constant throughout the pursuits such as Bluefish *Pomatomus saltatrix*, who keeps a 10 deg horizontal bias angle (McHenry, Johansen, Soto, et al. 2019). Dragonflies use a biased pursuit strategy in the vertical plane to hold the target image in the dorsal acute zone, a crescent of a particularly high resolution about 55 deg above the eye equator. Behavioural experiments in dragonfly have shown that the pursuer keeps the target in this region when hunting flying-insect prey (R. M. Olberg, Seaman, Coats, et al. 2007). The dorsal acute zone in the dragonfly *Sympetrum* is exclusively sensitive to short wavelengths of light (blue and UV) (Labhart and D. E. Nilsson 1995), a regional specialization for foraging against the blue sky. In their acute zones some dragonfly species feature a remarkably high spatial resolution in the range of about 0.1 deg, which is - apart from some robberflies (Trevor J Wardill, Samuel T Fabian, Pettigrew, et al. 2017) - probably the best found in any insect/arthropod species.

Steering commands that aim to maintain the target heading angle constant can

Control law for steering		**Equation**	
Constant Target Heading Angle (Constant target heading angle (CTHA))	$\Omega_P(t) =$	$f(\theta_E(t))$	
Pure pursuit (PP)	$\Omega_P(t) =$	$kp.[\theta_E(t-\Delta t)+\beta]$, with $\beta = 0$	(3.1.1)
Biased pursuit (BP)	$\Omega_P(t) =$	$kp.[\theta_E(t-\Delta t)+\beta]$, with $\beta = constant$	(3.1.2)
Constant bearing angle (CBA)	$\Omega_P(t) =$	$g(\theta_A(t))$	
Proportional Navigation (PN)	$\Omega_P(t) =$	$N.\Omega_A(t-\Delta t)$	(3.1.3)
Hybrid control (CTHA + CBA)	$\Omega_P(t) =$	$f(\theta_E(t)) + g(\theta_A(t))$	
Mixed pursuit (MP)	$\Omega_P(t) =$	$kp.[\theta_E(t-\Delta t_1)+\beta] + N.\Omega_A(t-\Delta t_2)$	(3.1.4)

Table 3.1 – Equations governing steering for different pursuit strategies. The controller can use two angles as input: target heading angle (θ_E) or bearing angle (θ_A), and will stabilize it while changing the pursuer heading by mean of functions f in CTHA, and g in CBA. For pure pursuit and biased pursuit, f is a first order function, with gain, kp and time delay Δt. Proportional navigation is a first order function (g) with gain N, and time delay Δt, applied on first temporal derivative of the bearing angle. Mixed pursuit is addition of the two controllers BP and PN.

thus lead to different pursuit strategies. When the system stabilizes the target heading angle to zero the pursuer presents a tracking strategy, and when it stabilizes to a non zero constant, the pursuer follows an interception path.

3.2.2 Constant bearing angle

Proportional navigation: The other control category maintains a constant bearing angle θ_A (Fig. 3.1***d***). Proportional navigation, PN, is often used in the aerospace industry for missile guidance (Loannis Peppas 1992) as it was considered as a control strategy with energy saving optimum (Shneydor 1998). The change of course is governed by changes of the bearing angle multiplied by a factor, N, between 1 and 5, see Equation (3.1.3). This control strategy has been found in an insectivorous echolocating bat (Ghose 2006), killer fly and robber fly (Trevor J Wardill, Samuel T Fabian, Pettigrew, et al. 2017; Samuel T. Fabian, Sumner, Trevor J. Wardill, et al. 2018). The latest comparative study (Brighton and Taylor 2019) suggests that a small N is more effective in cluttered environments and with highly-manoeuvrable targets (see killer fly with $N = 1.5$ (Samuel T. Fabian, Sumner, Trevor J. Wardill, et al. 2018)). If $N = 1$, PN is similar to PP, and assures a capture in any case, if the pursuer's speed is higher than that of the target. If N gets higher (3-5), the pursuer will perform a parallel navigation path, also called *Constant Absolute Target Direction* strategy (Ghose 2006), which is optimal for low-manoeuvrable target, or for high-speed chasers operating in open field such as peregrine falcon (Brighton, Thomas, Taylor, et al. 2017) and some robber flies (Samuel T. Fabian, Sumner, Trevor J. Wardill, et al. 2018). In practice, it is not very clear how the animal measures this absolute bearing angle to keep it constant. One possibility could be the addition of θ_E and θ_P (Fig. 3.1***a***), but it supposes the animal can estimate it's own orientation. The fly could also use first temporal derivatives, since changes in body orientation may be sensed by the fly's gyroscopic halteres which measure body rotation rates (Nalbach and Roland Hengstenberg 1994), and changes in error angle encoded in male specific visual neuron MLG1 (Trischler, Boeddeker, and Martin Egelhaaf 2007), discussed in the next chapter.

3.2.3 Mixed pursuit

Brighton and Taylor (Brighton and Taylor 2019) first showed the possibility of a mixed orientation law in hawk adding PP and PN (Eq. (3.1.4)), that would give an advantage when the target moves fast or in a cluttered environment. This strategy has been used in missile guidance (Shneydor 1998).

My work aims to identify the control strategies underlying aerial pursuit in the male blowfly *Lucilia sericata*. To this end, I carried out a series of experiments in which male flies were chasing dummy females moving on a computer-controlled 2d trajectory. The resulting 3-dimensional free flight data enabled me to study strategies the flies apply to control their steering in the horizontal and the vertical planes.

3.3 Analysis of blowfly's pursuit

3.3.1 Experimental conditions

Target trajectories: Males were presented with two types of target trajectories. In the first case, the target was moved on a circular path at a speed of 1 m/s. The second trajectory combined a translation along the y-axis with a rotation around the vertical axis, which created a spring-shaped movement of the target. The forward speed of the target varied between 0 and 1.5 m/s , and its angular velocity ranged between 360 and 1300 deg/sec (while the rotation around the z-axis was kept constant). With these two trajectories, I presented to the pursuers a variety of dummy kinematics, varied enough to study the sensorimotor control of the animal during its pursuit flight.

Data analysis: A fly was considered to engage on a pursuit flight when abruptly changing its speed and orienting towards the dummy. Pursuit flights normally ended by the fly catching the target. Flight trajectories vary in shape, and are distributed throughout the volume of the flight arena. I observed a broad range of flight speeds, in line with data reported for the slightly bigger blowfly species *Calliphora* (Schilstra and J. Hateren 1999; Bomphrey, S. M. Walker, and Taylor 2009). General features of the chasing behaviour were comparable with results obtained in a previous study on *Lucilia* (Boeddeker, Roland Kern, and Martin Egelhaaf 2003). In this analysis, I only included flights with a final capture. Indeed, in 30% of the chases, pursuer abandoned tracking before capture. This figure is roughly aligned with abandoned pursuits ratio of 43% in the muscoid fly *Coenosia* and 36% in the asilid fly *Holcocephala* (Samuel T. Fabian, Sumner, Trevor J. Wardill, et al. 2018). I was unable to identify the reason for the animals to abandon their chasing flights, but this point will be discussed in 4.2.2, *Looming type neurons*.

Variables of interest: To quantify the pursuit strategies observed in *Lucilia* I use the parameters introduced in the last chapter: line of sight, LoS, and line of flight, LoF. Position of the centre of mass of the pursuer is given by (x_P, y_P, z_P), and centre of mass of the target by (x_T, y_T, z_T). The Cartesian coordinates of the positions were transformed into spherical coordinates. For the sake of clarity, spherical coordinates about LoF will be noted (θ_{PH}, θ_{PV}, R_P), with P referring to the *pursuer*. Spherical coordinates relative to the LoS will be noted (θ_{AH}, θ_{AV}, R_A) with A referring to *absolute bearing angle*. The spherical radii R represent the distance to the target for the LoS, noted R_A, and the distance travelled by the fly per time unit for the LoF, noted R_P.

The absolute reference frame form with LoF and LoS azimuth angles θ_{PH}, θ_{AH} ϵ $[-180:180]$ deg and an elevation angle θ_{PV}, θ_{AV} ϵ $[-90:90]$ deg. Finally the target heading angle or *error angle* noted θ_E is also composed of a horizontal and a vertical component θ_{EH} and θ_{EV}. They are formed between LoS and LoF, in other words the difference between θ_A and θ_P.

$$\begin{pmatrix}\theta_{EH}\\ \theta_{EV}\end{pmatrix} = \begin{pmatrix}\theta_{AH}\\ \theta_{AV}\end{pmatrix} - \begin{pmatrix}\theta_{PH}\\ \theta_{PV}\end{pmatrix} \tag{3.2}$$

When I present the vertical plan of the pursuit (Fig. 3.2 *right*) I plotted the elevation on the *y*-axis against the absolute horizontal displacement, *x'*, on the *x*-axis.

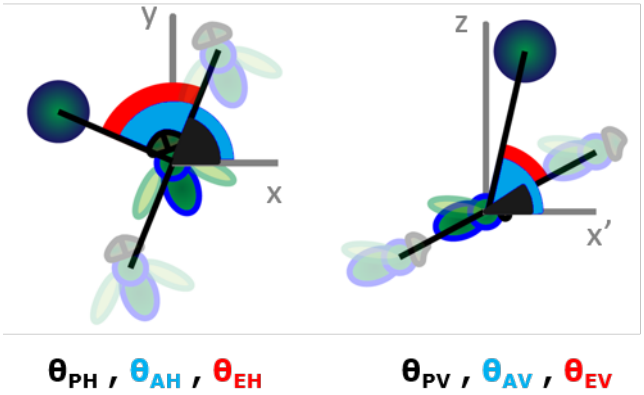

Figure 3.2 – **Graphical definition of the angular parameters in the horizontal and the vertical plane.** Heading angle, bearing angle, and error angle, θ_P, θ_A and θ_E, respectively, as defined in Equation (3.2). I distinguished values in the horizontal plane (noted *H*) and in the vertical plane (noted *V*), where angles are measured relative to *x'*-axis, the horizontal displacement defined in Equation (3.3).

$$x'_{P(n)} = \sum_{k=1}^{n} |\sqrt{(\hat{x}_{P(n+1)} - x_{P(n+1)})^2 + (\hat{y}_{P(n+1)} - y_{P(n+1)})^2} - \sqrt{(\hat{x}_{P(n)} - x_{P(n)})^2 + (\hat{y}_{P(n)} - y_{P(n)})^2}| \tag{3.3}$$

Where $(\hat{x}_P, \hat{y}_P, \hat{z}_P)$ are the measured and (x_P, y_P, z_P) are the simulated positions of the pursuer at each time step *n*.

3.3.2 Distribution of invariant parameters

RM M Olberg, Worthington, and Venator 2000 proposed a static approach to define the pursuit strategy of the dragonfly. The authors compared the variations of θ_E and θ_A during pursuits. They discovered an average variation of 2.8 deg for the bearing angle θ_A, and 8 deg for the error angle θ_E. As the variation is smaller for the bearing angle, the authors proposed that the dragonfly changes course in order to keep θ_A constant. Based on our experimental data I argue that the study of the distribution

of θ_E, θ_A and θ_P gives important information but it will be necessary to perform a thorough temporal analysis of the trajectories to derive a robust control system.

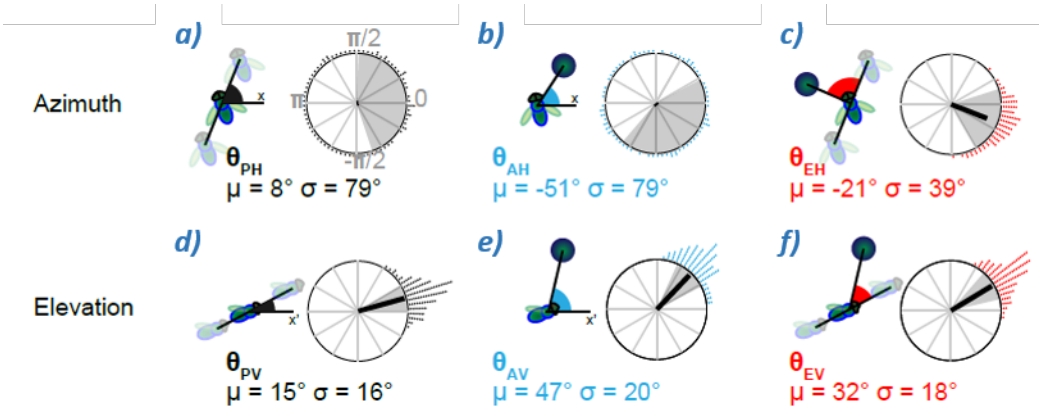

Figure 3.3 – **Distribution of the angular parameters: mean vector and standard deviation.** ***a-c)*** in the horizontal plane, and ***d-f)*** in the vertical plane. The mean vector, thick black line, points to the direction of the mean angle, and its length is linked to the data distribution: 0 if uniformly distributed, or 1 (radius) if all data are centred on a single value. In ***a-b)*** the horizontal heading angle θ_{PH} and the horizontal absolute bearing angle θ_{AH} are uniformly distributed, and the mean vector is barely visible. In ***c-f)*** the horizontal bearing angle θ_{EH} and all vertical angles θ_{PV}, θ_{AV} and θ_{EV} are centred on specific values with small variation. μ is the angular mean and σ the angular deviation. Data were gathered by 5 deg steps, each dot represents 10 measures (N = 1100). Shaded areas indicate $\mu + / - \sigma$.

In azimuth: The pursuer heading angle θ_{PH} and the bearing angle θ_{AH} (P for pursuer, A for absolute bearing angle, and H for horizontal plane) are uniformly distributed, resulting in the mean vectors' length of nearly zero degrees (Figs. 3.3***a, b***). In other words, the pursuer flies and chases in any direction. The mean vector of the bearing angle, θ_{EH} (E for error angle) was centred on -21 deg (Fig. 3.3***c***). The preferred direction angle -21 deg is an offset due to the definition of the direction of rotation of the target (see chapter 2). The length of it's mean vector suggests that in the horizontal plane, the fly is using a constant target heading angle controller. On the other hand, because of the large variance of θ_{AH} this angle is unlikely to be used for the controls within the horizontal plane, which excludes the constant bearing angle controller and thus the proportional navigation strategy, PN.

In the vertical plane: θ_{PV} and θ_{AV} differ in their mean value, 15 and 47 deg, respectively, but they both show small standard deviation, 16 and 19 deg, respectively (Fig. 3.3***d,e***). The vertical error angle θ_{EV} is centred around 32 +/- 18 deg (Fig. 3.3***f***). In contrast to the horizontal plane, it does not matter whether the fly turns left or right,

the mean θ_{EV} always stays at 32 deg elevation. At first glance, it is impossible to know which parameter θ_A, or θ_{EV} the fly is trying to keep constant. Thus, the fly may use in elevation a constant target heading angle controller (Eq. (3.1.2) with $\beta = 32deg$), or a constant bearing angle controller (Eq. (3.1.3)), or an hybrid controller (Eq. (3.1.4)). I will address this question in the next section.

3.3.3 Kinematics: control of steering

I began by looking at the relationship between θ_P, θ_A and θ_E. In the horizontal plane, $\theta_P = \theta_A$ (Fig. 3.4***a***), whereas θ_E is maintained around 0 deg (Fig. 3.4***b***). It confirms the hypothesis that the fly tries to stabilize θ_E. In vertical plane, the values of θ_P, θ_A and θ_E are grouped together (Fig. 3.4***c,d***). For further investigations I need to introduce the angular velocities Ω_P, Ω_A and Ω_E, which correspond to the first temporal derivatives of θ_P, θ_A and θ_E, respectively.

3.3.3.1 Horizontal plane: hybrid control for tracking

Essentially, the change of steering, Ω_P, should be strongly correlated with θ_E and Ω_E if the pursuer follows a PP or a BP strategy (Eqs. (3.1.1, 3.1.2)). Alternatively, Ω_P would be correlated with Ω_A if it follows a PN strategy (Eq. (3.1.3)). The analysis of the data reveals that Ω_P has a strong linear correlation with θ_E ($R = 0.75$) and with Ω_A ($R = 0.7$). The maximum correlation ($R = 0.75$) is for $\Omega_P = kp.\theta_E(t + \Delta t)$ with $kp = 17.4$ s^{-1} and $\Delta t = 10$ ms (Fig. 3.4***f***). I found a very low correlation between Ω_P and Ω_E (Fig. 3.4***j***). Most aerial chasing insects which employ a PP use a proportional-derivative controller to stabilise Ω_P. This includes *Fania* (Land and Thomas S Collett 1974) as well as the honeybee when tracking small moving platforms (S. W. Zhang, Xiang, Zili, et al. 1990). Dilochopodid flies, on the other hand, use a simple proportional controller (Land 1993).

Indicating a PN strategy, I found a good correlation ($R = 0.7$) between the variation of the bearing angle and the horizontal steering $\Omega_P = N.\Omega_A(t + \Delta t)$, with $N = 0.43$ and $\Delta t = 26$ ms (Fig. 3.4***i***).

This analysis suggests that *Lucilia sericata* uses a hybrid steering control (Eq. (3.1.4)), similar to what has been observed in hawks (Brighton and Taylor 2019).

3.3.3.2 Vertical plane: hybrid control for interception

For steering in the vertical plane I found that the change of course, Ω_P, is linked to the same parameters as for the horizontal plane. Ω_P is linearly related to θ_E ($R = 0.75$) with $kp = 15.6$ s^{-1} and $\Delta t = 21$ ms (Fig. 3.4***h***). Ω_P is also linearly related to Ω_A ($R = 0.7$) with $N = 0.62$ and $\Delta t = 32$ ms (Fig. 3.4***k***). The other similarity with the results found for the horizontal plane is that Ω_P in not linearly correlated with Ω_E (Fig. 3.4***l***). On the other hand, the curve $\Omega_P = k.\theta_A$ in Figure 3.4***g*** has a non-negligible R of 0.5 that was not observed in horizontal plane (Fig. 3.4***e***). Because the maximum correlation was found for a zero delay between Ω_P and θ_A, I have not included θ_A in the formulation

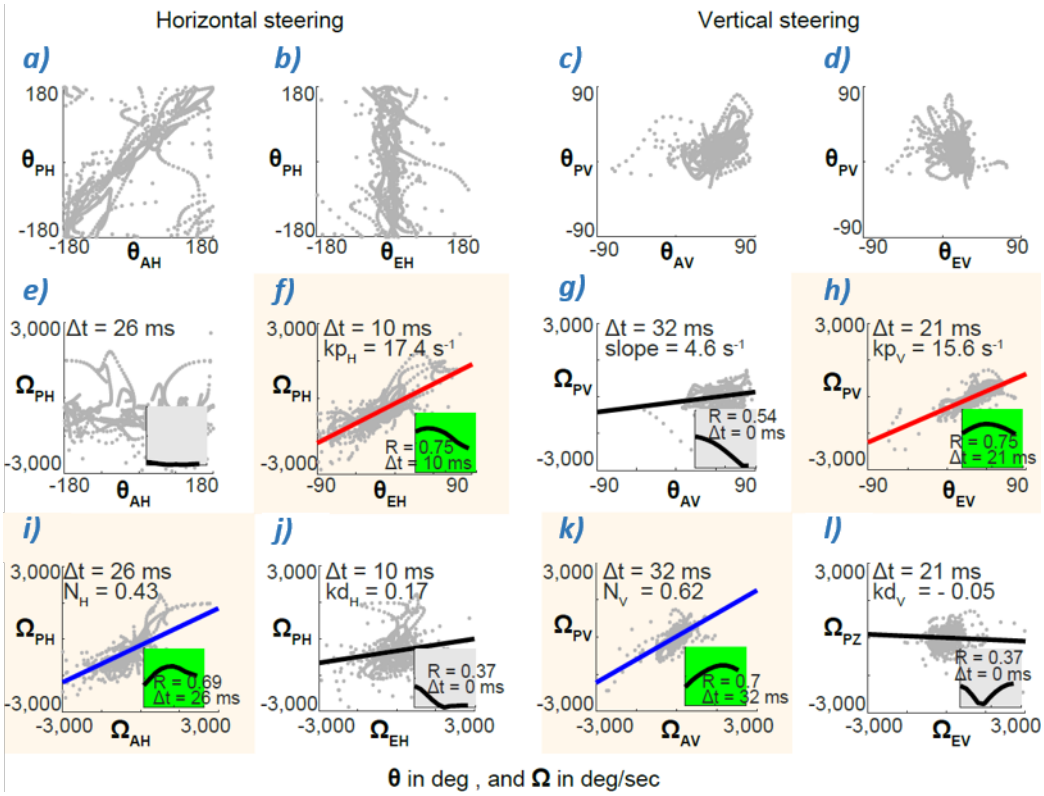

$$\Omega_{PH}(t) = \quad 17.4.[\theta_{EH}(t-10ms)] + 0.43.\Omega_{AH}(t-26ms) \tag{3.4.1}$$

$$\Omega_{PV}(t) = \quad 15.6.[\theta_{EV}(t-21ms) - 32deg] + 0.62.\Omega_{AV}(t-32ms) \tag{3.4.2}$$

Figure 3.4 – **Impact of angular and angular rate parameters on the heading.** ***a-d)*** Heading angle θ_P as a function of bearing angle θ_A and error angle θ_E. While in azimuth, the angular range covers +/- 180 deg, in elevation the angular range is +/- 90 deg. ***e-h)*** Change of heading rate Ω_P as a function of angles θ_A and θ_E. ***i-l)*** Change of heading rate Ω_P as a function of angular velocity Ω_A and Ω_E. Maximum correlation R and its delay Δt are displayed in green insets if $R \geq 0.7$. Scale X = [0:50ms], Y = [0:1]. Red lines show linear fits between θ_E and Ω_P suggesting a biased pursuit strategy. Blue lines show the linear fits between Ω_A and Ω_P indicative of a proportional navigation strategy. Gains (kp and N) and delays (Δt), from coloured graphs were used in the two control Equations (3.4.1) and (3.4.2). To facilitate comparison of linear fits between θ_E and Ω_P in horizontal and vertical planes in ***f)*** and ***h)*** , respectively, the same angular range of +/- 90 deg is applied for θ_{EH} and θ_{EV}. 93% of all θ_{EH} values were in this angular range.

of the control laws. Indeed, the correlation is unlikely to be smaller than the sampling rate (5 ms) and > 0 ms. In the next chapter I will discuss the possibility that the fly may use a forward model or predictive controller.

3.3.3.3 Similarities in the two planes of approach

There are conspicuous similarities between the coefficients I obtained for the equations describing the horizontal and vertical control: the data shown in Figures 3.4***f,h*** have the same profile which is also true for Figures 3.4***i,k***: $kp_H = 17.4s^{-1}$, $kp_V = 15.6s^{-1}$, $N_H = 0.43$, and $N_V = 0.62$. However the differences are notable on the sensorimotor delays. For vertical corrections between θ_E and Ω_P, the delay is twice as long as the one for horizontal corrections ($\Delta t_H = 10$ ms and $\Delta t_V = 21$ ms). The delay is also longer for vertical corrections between Ω_A and Ω_P ($\Delta t_H = 26$ ms and $\Delta t_V = 32$ ms). We have already shown that in the vertical dimension variances of angular parameters are smaller than for the horizontal dimension.

3.3.4 Limits of the constant target altitude

As the z-position (altitude) of the target was not varied in our experiments, the dynamic input range I used to identify the vertical control strategy is somewhat limited. Further experiments where the z-position is systematically varied would help to overcome the current limitation. Although the vertical input range is limited due to the constant z-position of the dummy, different initial conditions regarding the start positions for the flies' chasing flights introduce a certain degree of variability in altitude-related parameters. To my knowledge, the rare studies on vertical approach have been realised with targets moving in the horizontal plane for dragonfly (Mischiati, Lin, Herold, et al. 2015), robberfly (Trevor J Wardill, Samuel T Fabian, Pettigrew, et al. 2017) and killerfly (Samuel T. Fabian, Sumner, Trevor J. Wardill, et al. 2018). In another experiment with drone bees pursuing a suspended queen, Praagh, Ribi, Wehrhahn, et al. 1980 measured the elevation angle between body axis and line of sight. The distribution of this angle (noted α) is similar to the measures of θ_{EV} and θ_{AV}. It is reassuring that the flies keep the target projected onto a vertical angular range which corresponds well with the position of the love spot, described for the drone bee. Indeed blowfly males and drone bees (also males) share several morphological properties such as body size, restricted movements of the head during flight, and the presence of a dorsal acute zone.

3.4 Developing kinematic models

The correlations between Ω_P and kinematic-related parameters (θ_E, θ_A, Ω_E and Ω_A) give rise to useful observational relationships. It becomes important to consider building a model to understand the contribution of each relationship to the global steering strategy.

In a first step, I simulated the responses of a virtual fly by implementing the steering control Equations (3.4.1, 3.4.2) in Matlab/Simulink 2019. I used the experimental data to specify the initial conditions and forward speed used in my simulations.

The trajectories of the simulated fly were evaluated based on their deviation from the trajectory of the experimental animal by the error, ε, defined as the mean absolute distance between the measured $(\hat{x}_P, \hat{y}_P, \hat{z}_P)$ and simulated (x_P, y_P, z_P) positions of the pursuer at each time point:

$$\varepsilon_H = \frac{1}{n}\sum_{k=1}^{(n)} \sqrt{(\hat{x}_{P(n)} - x_{P(n)})^2 + (\hat{y}_{P(n)} - y_{P(n)})^2} \tag{3.5}$$

$$\varepsilon_V = \frac{1}{n}\sum_{k=1}^{(n)} \sqrt{(\hat{x'}_{P(n)} - x'_{P(n)})^2 + (\hat{z}_{P(n)} - z_{P(n)})^2} \tag{3.6}$$

where x' corresponds to the horizontal displacement, (Eq. 3.3).

Based on the model derived from behavioural parameters, I created three virtual fly models, and tested them both for the horizontal and the vertical plane. The models simulated: (*i*) biased pursuit, BP, (*ii*) proportional navigation, PN and (*iii*) a mixed pursuit strategy, MP, which combines biased pursuit and proportional navigation. The gains implemented in each model were estimated using the smallest error, ε, as a performance measure (Fig. 3.5).

We then compared the performance of the different models to real pursuits. The MP and BP models performed best and second best, respectively, with the PN model coming third. I did not find a significant performance difference between the MP and the BP model, neither in the horizontal nor in the vertical plane (Fig. 3.6).

The comparison of the model performances may suggest that PN has no sizable impact on the fly's control strategy. On the other hand, if PN is not necessary, but I observed a linear relationship between Ω_P and Ω_A, how can I exclude PN? One answer can come from the small value of the coefficient N. When PN strategies are applied in nature, N is always greater than or equal to one (see section 3.2.2). Here I found $N_H = 0.43$ and $N_V = 0.62$ for the behavioural data (Figs. 3.4***i,k***), and $N_H = 0.15$ and $N_V = 0.05$ for the MP model (Figs. 3.5***c,g***). The advantages of such a small N coefficient are rather unclear even if the PN and BP strategies are combined. Overall, our results suggest that the control strategy offering the best performance is the biased pursuit with a proportional controller in both azimuth and elevation heading control. Finally, I varied the bias angle values in our BP model for elevation, and found that $\beta = 23$ deg gave the best performances.

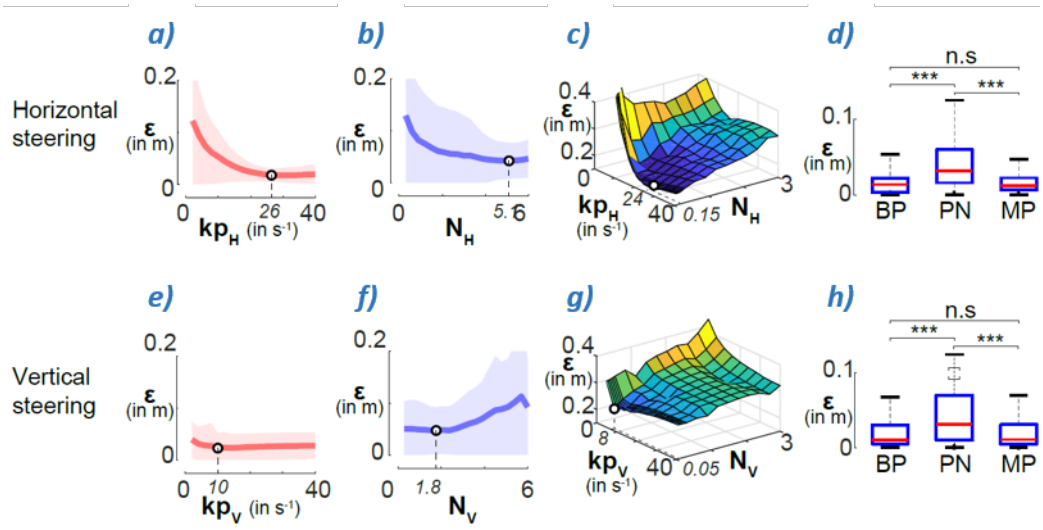

Figure 3.5 – **Optimization of gains for the three steering control models.** The reduction of the error between model and real trajectories, was quantified by the error ε according to Equations (3.5,3.6). ***a,e)*** Biased pursuit, BP, minimum ε for $kp_H = 28\ s^{-1}$ and $kp_V = 10\ s^{-1}$. ***b,f)*** Proportional navigation, PN, minimum error ε obtained for $N_H = 5.1$ and $N_V = 1.8$. ***c,g)*** Mixed pursuit, MP, minimum ε obtained by varying kp and N. Horizontally $kp_H = 24\ s^{-1}$ and $N_H = 0.15$, and vertically $kp_V = 8\ s^{-1}$ and $N_V = 0.05$. The thick lines in ***a, b, e, f)*** represent the average ε obtained over all 17 captures. Shaded areas indicate standard deviations. ***d,h)*** Box plot of all errors ε when using models with parameters values from ***a-c, e-g)***, and *ANOVA* tests. There is no significant difference between the BP and MP strategies in horizontal and vertical direction (n.s : $p > 0.05$). Note that the PN strategy induces bigger error compared to the two others. (*** : $p < 0.001$)

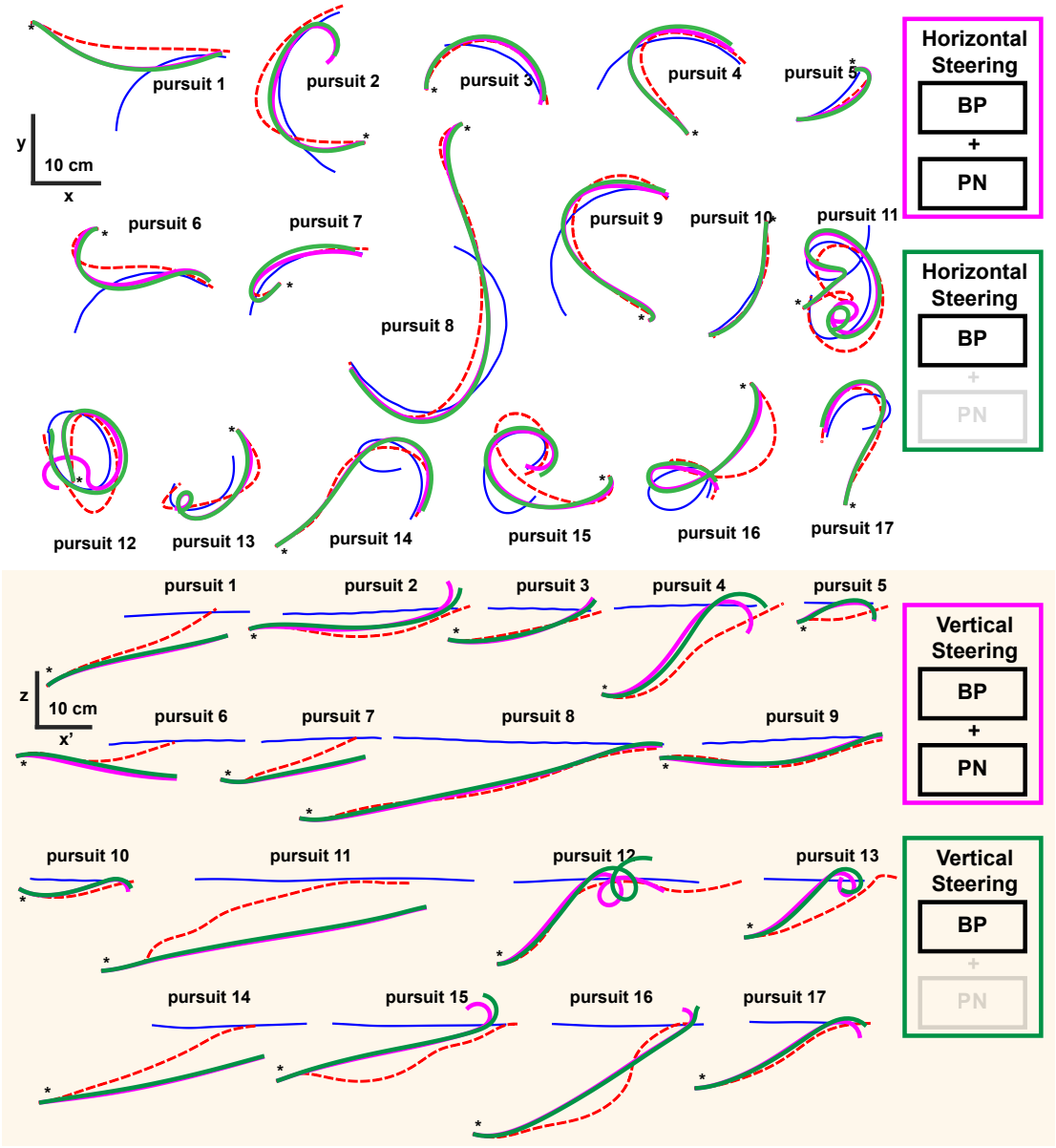

Figure 3.6 – **Experimental and model trajectories.** The 17 studied chases are plotted and compared to the trajectories of a model fly whose steering control is governed by mixed pursuit strategy, MP: Equation (3.1.4) with parameters from Figures 3.5***c,g***, and biased pursuit strategy, BP: Equation (3.1.2) with *kp* from Figures 3.5***a,e*** . Trajectories on white background are horizontal projections of the pursuits, and trajectories on yellow background are vertical projections. Asterisks indicate the starting point of the chases. The speed of the model fly is equal to the speed of the real fly. For the vertical plane: x' is the displacement along horizontal plane (see Equation (3.3)). Note that the MP and BP models produce highly similar results which come close to the trajectories of the real fly. To quantify the differences between experimental and model trajectories I used a point-to-point error, ε (Eqs. (3.5, 3.6))

$$\Omega_{PH}(t) = 26.[\theta_{EH}(t - 10ms)] \tag{3.7}$$

$$\Omega_{PV}(t) = 10.[\theta_{EV}(t - 21ms) - 23deg] \tag{3.8}$$

The difference in strategy between the two planes lies essentially in the values of the bias angle, β, gain, kp, and the time delay Δt. In the horizontal plane $\beta_H = 0$ deg, which leads to a tracking strategy. In the vertical plane $\beta_V = 23$ deg leads to an interception strategy. The position of the love spot in the fly's retina may be linked somehow to this bias angle. I will discuss this point in the next chapter. Also, in the vertical plane the body axis is hardly aligned with the speed vector, nor with the LoS (Varennes, Krapp, and Stéphane Viollet 2019). The role that the orientation of the body plays for the interception strategy (kinematic) and in the dynamics of the pursuit will also be discussed in the next chapter.

Finally, about energy concerns, interception is more efficient than pure pursuit (Strydom, Singh, and Srinivasan 2015). If the fly employs a pure pursuit strategy in the vertical plane, it takes the risk of overshooting - i.e. be on top of the target. In this case the pursuer would orient its thrust force in the same direction as gravity, causing considerable energy losses. After all, chasing is energy-intense and may be used as fitness selection criterion. We have to keep in mind that only the fittest (in terms of sensory processing/accuracy and flight performance) males get to mate and produce offspring.

3.5 Developing dynamic models

In kinematic models we consider that inputs of the system are directly transformed into motion (Fig. 3.7***b***). In reality, fly's actions are controlled by the production of torques and forces that subsequently affect angular and translational velocities. Taking the example of a car driver: it is the action upon the accelerator that allows speed adjustments. The driver acts on the propulsion force, which will affect vehicle speed. He or she does not directly acts on the speed. It is the same for the fly, whose wing movements produces torques and forces to adjust self-motion. I have started to develop a dynamic model of the pursuer but found some unexpected outcomes. This work would certainly require further investigation. I will present here only part of the results that will be useful for the general discussion.

Steering control: The kinematic study showed strong linear correlation between the retinal error and the angular velocity (Fig. 3.4***f***). During the development of a dynamic model I could not find such a strong correlation between any retinal variable and angular acceleration. Indeed, in angular dynamics, torque around an axis is linked to angular acceleration: $\tau = I.\alpha$ with τ describing torque, I is the moment of inertia (*Lucilia* : $I_{yaw} = 8.8E^{-10}$ kg.m^2) and α is the angular acceleration. In the horizontal plane, the linear relationship between θ_E and ω_P suggests that the fly may control directly its angular velocity – not the torque. I think there may be a feedback loop with implication of halteres in steering control (Fig. 3.7***d***). Unfortunately, I have not found a dynamic steering model giving results close enough to behavioural measures.

Velocity control: Forward velocity control is quite different. When I developed the kinematic model I could not find satisfactory forward velocity control in the horizontal plane. It is the reason why I implemented measured velocities into kinematic simulations (Fig. 3.6). The dynamic model offers more satisfactory results. Linear dynamics give the following relationship: $F = m.a$ with F force, m mass (for *Lucilia* I used m = 0.0001 kg), and a linear acceleration.

I found linear correlation between the thrust and the absolute value of the error angle $\theta_E = k.m.a$ with k = -7.8E^{-4} N^{-1}, R = -0.6 and a delay time equal to zero. Thus, the fly stabilizes its thrust to a constant as long as the target is projected onto the centre of the retina. When the retinal position of the target deviates from the center, the thrust decreases until it becomes negative when $|\theta_E| > 45$ deg.

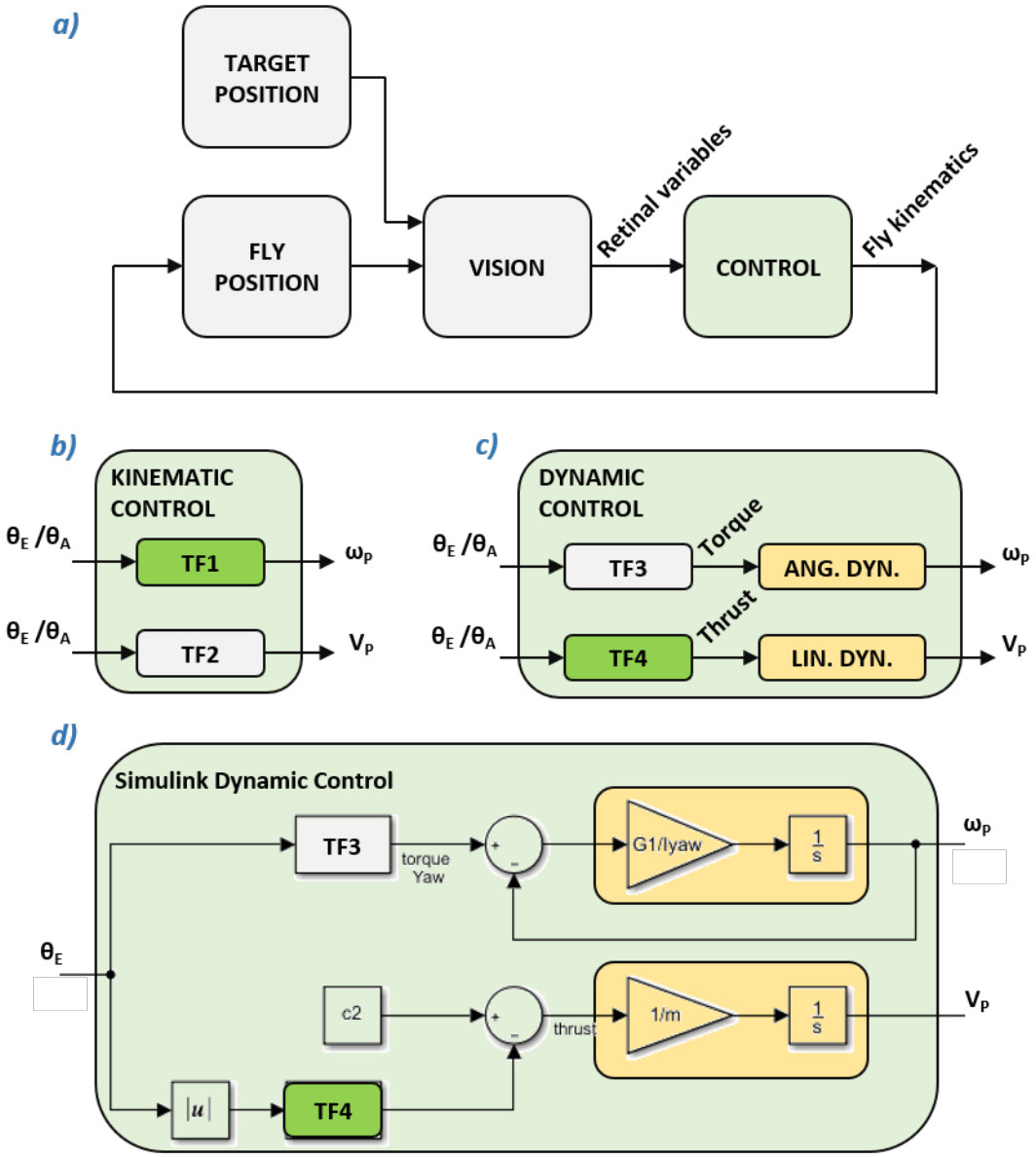

Figure 3.7 – **Models of chasing behaviour.** ***a)*** Block diagram of the general structure of pursuit. ***b-c)*** Theoretical kinematic and dynamic models. Transfer functions are applied to retinal variables (θ_E/θ_A) to produce the fly's kinematics (ω_P/V_P). In case of dynamic control, this process goes through production of torques subjects to angular dynamics, and forces subjected to linear dynamics (see text for details). ***d)*** Dynamic model created with Simulink. For steering control (top path), TF3 is applied to θ_E to generate yaw-torque. This yaw-torque is transformed into ω_P through rotational dynamics. My hypothesis is that there is a feedback loop which implies halteres. For velocity control (bottom path), the thrust is reduced when θ_E moves away from zero. Thrust is transformed into forward speed through linear dynamics. TF: Transfer Function. **TF1** and **TF4** gave satisfactory results.

3.6 Conclusion

In summary, I have analyzed a series of 17 chasing flights where a male blowfly was pursuing a moving dummy. The behavioural analysis suggests that the pursuit strategy is not the same along the horizontal and the vertical plane. A comparative modelling study suggests that a constant target heading angle controller best captures the kinematics of the chasing flights I have analyzed. This controller leads to tracking if driven by the target heading angle in the horizontal plane, and it leads to interception if driven by a biased elevation angle in the vertical plane. Thus I can assume that a constant target heading angle shapes the general strategy and both *tracking* and *interception* are just consequences of the presence of a bias angle. It is both beautiful and remarkable that the combination of two simple proportional controllers are capable of reproducing behaviour as complex as fly chasing flights at ultra-fast time scales.

The fly adjusts its trajectory by producing torques and forces. This preliminary study suggests that steering control is directly related to angular velocity, potentially with the involvement of halteres (Chan, Prete, and Dickinson 1998) (**TF1** in Fig. 3.7***b***). Whereas the fly's forward speed results in the control of the error angle based on the adjustment of thrust (**TF4** in Fig. 3.7***d***).

The difference between tracking in the horizontal plane and interception in the vertical plane may be explained by a trade off between evolutionary fitness and energy efficiency. I will discuss these aspects in the next chapter.

Additional information

High-speed videos of the pursuits will be uploaded in supplementary data. Reconstructed trajectory data analysed during this study, and the matlab/ simulink models of the steering controllers are available in the following GitHub: https://github.com/veandre/blowfly-pursuit.

Caption from Video Folder: Additional movies are edited videos presenting the pursuit sequences recorded from the two high speed stereo cameras. Movies are annotated with the chase number (to refer to Figure 3.6). Fly's and target's positions are tracked with blue and red markers, respectively. Sequences lasted less than a second at normal speed, so I decided to present them at a speed ten times slower than original.

4 Discussion

Sommaire

4.1 Introduction 101
4.2 Neuroanatomical structures of the pursuit 102
4.2.1 Love spot in *Lucilia* 102
4.2.2 Neurons implicated in pursuit 102
4.2.3 Body shape and horizontal side-slip 108
4.3 Coordinated flight 110
4.3.1 Banked turns 110
4.3.2 Forward speed 112
4.3.3 Horizontal steering influences vertical steering 113
4.4 Head-body movements while chasing 115
4.4.1 Gaze stabilization 115
4.4.2 The head is not locked to horizon 117

4.1 Introduction

Chapter outline: During my project I accumulated a rich data base of observations on aerial pursuit of blowfly. In this final chapter I will present some qualitative results which could unfortunately not all be treated in a quantitative way. I will take the liberty to develop my personal ideas about the neuroanatomical, or algorithmic structures involved in certain characteristic movements during the pursuit.

The first part of this chapter is a presentation of neuroanatomy that may explain the kinematics of the pursuer presented in previous chapter. I believe that the difference in pursuit strategies in horizontal and vertical plane are linked to the dorsal position of the love spot in male *Lucilia* compound eyes. The steering control emerges from activation of biological substrates that I will present here, in particular male specific neurons. Other visually evoked behaviour (presented in section 1.3) may also be involved in the pursuit. The interaction between the animals' motion vision pathway and pursuit will be discussed: implication of the looming pathway, and inhibition of the optomotor response. I will also discuss the possibility that the misalignment observed between LoB and LoS, may be caused by the fly's body shape.

Then I will focus on maneuvering aspects of acrobatic flight. During pursuit my behavioural study suggests that the fly performs coordinated flight manoeuvres. Combining banked turns and forward velocity adjustments, the fly maintains energy efficiency during flight. But this control is not perfect, as my data suggest the presence of side slips in horizontal plane, observed by occasional misalignment between LoB and LoF during sharp turns such as during cruising flight (Lindemann, Roland Kern, J H van Hateren, et al. 2005).

Head body movements play an important role in insect flight. In cruising flight gaze stabilization serves a number of functions, which include: reducing motion blur in the retina, simplifying the estimation of translational self-motion, and aligning the head-based sensory systems with the inertial vector. The pursuer's control system takes as input the projection of the target on fly's retina. To model precisely the pursuit, we need to reconstruct the fly's vision, by mean of head orientation estimation. Implication of gaze stabilization is essential on the this point and will be subject of my discussion.

Finally, I will conclude this chapter with a brief description of the accomplished work and future directions.

4.2 Neuroanatomical structures of the pursuit

4.2.1 Love spot in *Lucilia*

In Chapter 1, I mentioned the love spot or acute zone in the compound eyes of male dipteran flies. We know that this area features larger lenses that capture more light, increasing light sensitivity, faster photoreceptor responses, and neural connections feeding into sex specific pathways. During the pursuit, the male stabilizes the image of the target onto this specialized region of its compound eyes.

In *Lucilia cuprina* the male acute zone has a higher central density of ommatidia (1.1 per deg^2) than that of the female (0.9), and it is also more extended when the 0.3 per deg ^{2} contours are compared (Fig. 1.9). The centre of the male acute zone in *Lucilia* is only about 5 deg above the equator, as in the female. It has a less dorsal position than the male *Caliphora* with love spot centered at 15 deg elevation (Land and Eckert 1985). The dorsal position of the love spot may explain the misalignment between speed vector and LOS, or biased angle presented in Chapter 3.

4.2.2 Neurons implicated in pursuit

During pursuit, the chaser needs to extract from global optic flow relevant motion features. Previous behavioural and modelling analyses of flies' aerial pursuit have indicated that angular target size, expansion rate, retinal target position and retinal target velocity can be variables for the pursuit control system (see Chapter 3). These variables of interest may be analysed by dedicated neuronal circuits. At least four motion-sensitive systems demonstrate that motion information is sent to motor neurons: 1) sex specific neurons in the lobula serving the male's retinal love spot, 2) small field neurons that detect small target motion, and 3) flow-field neurons in the lobula plate of both sexes. 4) Looming detectors also suggest another type of motion detection that may have evolved early in arthropods to escape predators (Strausfeld 2012).

Male specific neurons: Male specific neurons in blowfly and housefly have been identified anatomically (Strausfeld 1980; K. Hausen and Strausfeld 1980), but as far as I know the functional organization of male-specific visual neurons was performed only in fleshfly *Sarcophaga bullata* by Gilbert and Strausfeld 1991. Researchers identified the neuron's response properties upon various type of visual stimuli from male lobula giants, *MLG* 1-5, and male-specific columnar neurons, *MCols* C-E. All these neurons are male specific, and most of them take their input from the love spot.

These neurons have the same properties as those postulated by Land and Thomas S Collett 1974 in their model of the sensorimotor control of the pursuit in housefly (Fig. 4.1). Most recent studies found evidence of these neurons also Trischler, Boeddeker, and Martin Egelhaaf 2007 studied the male lobula giant neuron number 1 (*MLG1*) in the blowfly *Calliphora*. Intracellular recordings were performed while replaying optic

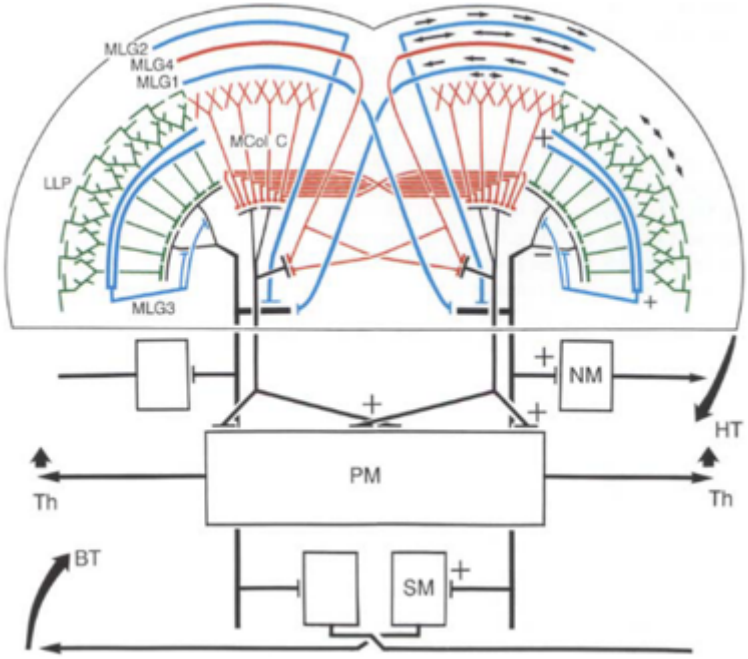

Figure 4.1 – **Organization of the male specific neuronal pathway.** Taken from Gronenberg and Strausfeld 1991 which is revised from Land and Thomas S Collett 1974. The locations and projections of elements in Land and Collett's velocity system correspond to *MLG* 1 and 2 (blue). *MLG* 1 and 2 of the right eye respond, respectively, to anti- and clockwise movement of targets. Land and Collett's position system is suggested to comprise small field sex-unspecific neurons (*LLP*, green) which provide peripheral excitatory inputs to the dendritic tree of *MLG* 3 (blue) and proximal excitatory inputs to the descending neurons *DN* (black) receiving terminals from *MLG* 1 and 2. The strength of inputs to *MLG* 3 depend on the *LLP* location. The ipsilateral *MLG* 2 converges with *LLPs* and the contralateral *MLG* 1 onto unilateral DNs (one shown black) driving the ipsilateral neck muscle and flight steering muscle motor neurons (*NM*, *SM*). These innervate ipsilateral neck muscles and contralateral basalar flight muscles driving head yaw (*HT*) and body yaw (*BT*), respectively, in the directions indicated. A parallel system has been identified (red). *MLG* 4 (*MLG* 4) is sensitive to movement of small objects, without direction selectivity. A local assembly of object detectors (*MCol C*) are restricted to inputs from the acute zone. In this context it is important to make the point that the visual system is retinotopically organized. Both *MLG* 4 and *MCol C* neurons terminate bilaterally on *DNs* that supply the bilateral power motor neurons (*PM*) controlling thrust (Th).

flow reconstruction of a real chase. The results suggested that blowfly *MLG1* responds in the same directional-selective way as those in fleshfly, preferentially if the target motion contains an upward component.

Circuits that compute elementary motion (in the medulla) are conserved across Diptera (Buschbeck and Strausfeld 1996). Neuroanatomical comparisons between closely related species having different behaviours suggest that such differences may be related to differences of giant tangential cell architecture in the lobula plate (Buschbeck and Strausfeld 1997; O'Carroll, Bidwell, S. B. Laughlin, et al. 1996). Conversely, similar behaviour traits may suggest similar motion-sensitive systems, which justifies the comparison between male blowfly, housefly and fleshfly.

Wide-field motion: Local motion signaled by ON and OFF channels and processed by means of a spatio-temporal correlation (Hassenstein and W. Reichardt 1953; Riehle and Nicolas Franceschini 1984) is transformed through series of electrical and chemical synapses into wide-field motion at the level of the lobula plate tangential cells (Fig. 4.2), *LPTC* (Klaus Hausen 1982; Hengstenberg 1982). *LPTCs* are preferably activated by optic flows resulting from the animal's self-movements (Krapp and Roland Hengstenberg 1996), what is known as the idea of "neuronal matched filters" for optic flow (Franz and Krapp 2000). This inspired the mode-sensing hypothesis (Taylor and Krapp 2007; Krapp, Taylor, and Humbert 2012). Thus, basic rotations are encoded by specific horizontal or vertical neurons (*HS* or *VS* cells, respectively): roll rotation encoded by *VS6*-cell, pitch rotation by *VS1*-cell and yaw rotation by the *HSN*- and *HSE*-cells. Neurogenetic and lesion studies applied to *HS* cells, confirm the implication of these neuron in the control of the fly optomotor responses (Klaus Hausen 1982; Haikala, Joesch, Borst, et al. 2013).

Hoverfly and blowfly, present a few differences in flight behaviour, such as the capacity to hover, the forward speed and the body orientation while flying. Studies have shown that the "same" neuron *vCH*, in these two Dipteran species are sensitive to different visual stimuli, adapted to the flying behaviour of the animal (Geurten, Roland Kern, and Martin Egelhaaf 2012).

Lobula-plate tangential cells (*LPTCs*) take motion information from specific points covering a large part of the visual field. Most of the known *LPTCs* are horizontal and vertical cells, but their characteristic response is not a straight horizontal and vertical movement in the fly's field of view as an object moving up and down, but rather a characteristic movement of the fly during flight, e.g. specific combinations of body rotations depending on the flight dynamics of the given species. The best example of a mode of motion is a lateral periodic mode called "dutch roll". It consists of a 90 deg phase shifted combination of yaw and roll rotation components. That is the mode that was used to explain the idea in Taylor and Krapp 2007. It would activate different *VS*-cells during different phases of the mode, the output of which could be used to control the (potentially unstable) Dutch roll mode.

It is important to mention that during pursuit, the chaser's own motion generates displacement of the visual surroundings, inducing wide-field optic flow across the

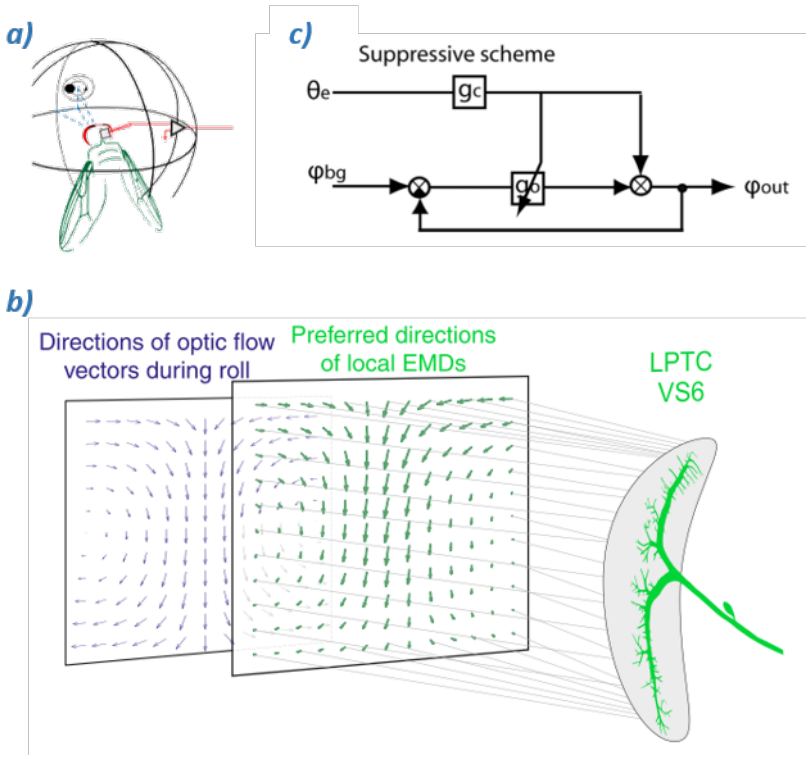

Figure 4.2 – **Wide-field motion-sensitive neurons, optomotor response and pursuit.** ***a)*** Sequence of local motion stimuli, applied to different azimuths and elevations within the animal's visual field: a black disk moving on a circular path to probe the cell's local preferred direction. Method modified from Krapp and Roland Hengstenberg 1997. ***b)*** To estimate self-motion, the visual system sets up 'matched filters' for optic flow, whereby the distribution of local preferred (reconstructed in experiments using method in ***a)***) directions are aligned with the directions of the velocity vectors throughout the visual field. A neuron, here *VS6*, integrating wide-field motion (outputs of all local elementary movement detectors, EMDs), would be highly activated when the visual system is presented with the optic flow field generated during a roll rotation. Optic flow-based estimation of body rotations is a key mechanism required for efficient gaze stabilization. Figure taken from Hardcastle and Krapp 2016. ***c)*** φ_{out} is the final turning response of the animal which is the sum of the turning responses mediated by the optomotor system and the chasing system. The chasing system takes as input θ_e, g_c and g_o are the internal gains of the chasing system and the optomotor system, respectively. The input to the optomotor system is provided by φ_{bg}, the angular velocity of the background. Suppressive scheme: A copy of the chasing control signal reduces the internal optomotor gain or even suppresses the optomotor signal completely. Taken from Trischler, Roland Kern, and Martin Egelhaaf 2010.

retina. We have already seen that this wide-field optic flow is used to sense unwanted deviations from a given flight course which are corrected by the optomotor response. When turning left to follow a target that moves to the left, the background will turn to the right, which should activate an optomotor response to the right. This conflict would prevent any attempt to track a salient object. This problem - i.e. the integration of inner-loop reflexes (optomotor) and outer-loop goal-directed behaviours has been addressed by Von Holst and Mittelstaedt 1950 and was reviewed for instance by Hardcastle and Krapp 2016. A potential neuronal basis for resolving this problem is the use of efference copies which cancel the response of wide-field motion sensitive neurons to self-induced (goal directed) manoeuvres and thus prevent the inner-loop control to kick in (Kim, Fitzgerald, and Maimon 2015). Researchers performed behavioral experiments on male blowflies and examined the characteristics of the two flight control systems in isolation and in combination. They found that the optomotor following response is largely suppressed by the chasing system (Trischler, Roland Kern, and Martin Egelhaaf 2010). Indeed when the background is moved artificially with various velocities in either direction, it did not much deteriorate the performance of catching the moving target. Under these conditions, the fly could maintain a reasonable error angle under which the target is fixated in the frontal visual field (the love spot), with the time course of chasing flights not showing any significant difference compared to the situation where a stationary background was used.

Small target motion detectors: These neurons have been described only in hoverfly and dragonfly, and in both sexes. *STMD* are excited by moving dark targets and not by leading or trailing edges or by bright targets (O'Carroll 1993; T. S. Collett 1971; Nordström, Barnett, and O'Carroll 2006) see review: Nordström 2012. In hoverflies *Eristalis tenax*, columnar neurons, identical with the one described in male housefly (see Fig 4.1 *MCols* C-E), have been recorded intracellularly: SF-STMDs (small-field small-target-motion detectors) in both sexes (Barnett, Nordström, and O'Carroll 2007). These neurons connect to descending neurons (*TSDNs*), 8 pairs of which code directional retinal target motion in dragonflies (Gonzalez-Bellido, Peng, Yang, et al. 2013). Wiederman, Shoemaker, and O'Carroll 2008 have built a model of the detection of small moving target capturing the response properties of neurons identified in the dragonfly brain. *STMD* exhibit localized enhanced sensitivity for targets displaced to new locations just ahead of the prior path, with suppression elsewhere in the surround. This focused region of gain modulation is driven by predictive mechanisms and demonstrates anticipation of the object's path (Wiederman, J. M. Fabian, Dunbier, et al. 2017). The presence of this type of neurons in blowfly has not been demonstrated yet. If they were present, their properties could justify the very small time delays observed in steering command (see chapter 3).

Looming type neurons: Looming-type motion-detectors may play a role in target tracking, as suggested in a recent study on praying mantis (Rind, Jones, Tarawneh,

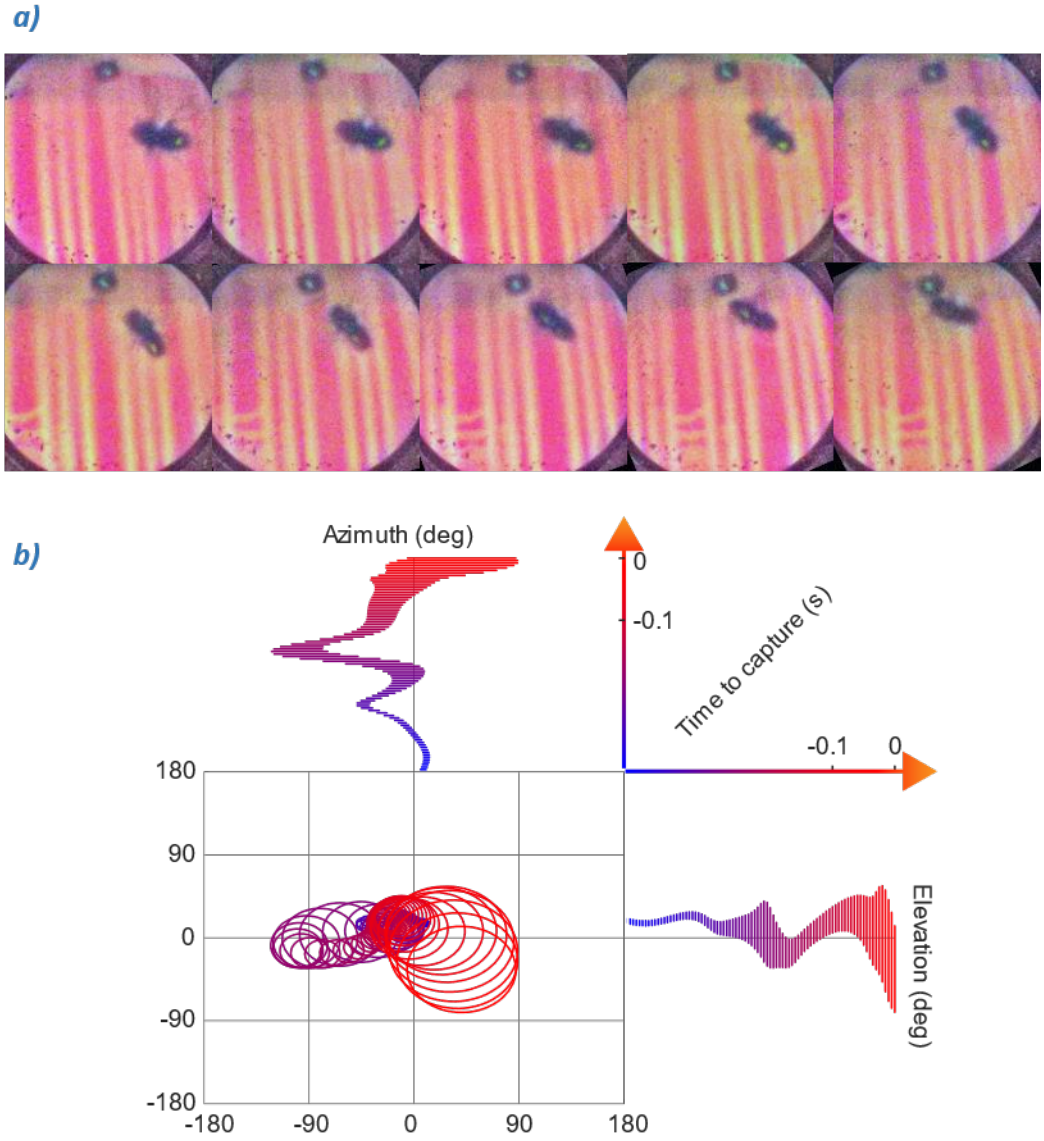

Figure 4.3 – **Final approach and target's projection on fly's retina.** ***a)*** Final approach and target capture recorded with the second version of the Microendoscope module. The pursuer approaches the target before the final catch. Time laps 5ms, and same chronological presentation as Fig 2.8. ***b)*** Projection of the target on the pursuer's retina. I assumed a fixed body-head pursuer, body (and so head) orientation were defined only with longitudinal angles yaw-angle and pitch-angle, but no roll-angle. Colours refer to the time to capture. All the retinal target features (size, expansion rate, positions and velocities) can be extracted, but I was not able to measure when the capture initiates (pulls up and legs extensions) with precision.

et al. 2020). There is no direct evidence of the same implication of the looming motion pathway in pursuit in flies yet, but the following may suggest its possible existence.

We know looming stimuli may elicit collision-avoidance manoeuvres or landing response as I have outlined in Chapter 1 (with relevant references given there). When an object approaches frontally, the choice between escape and landing depends on the expansion rate of the object, *tau*, (Tammero and Dickinson 2002). Thus, thresholds on *tau* are used by the animal to switch between attraction and avoidance. In the model of a male blowfly engaged in pursuit, developed by Boeddeker and Martin Egelhaaf 2003, the output of the virtual fly's speed controller was assumed to depend on retinal target size. Although I did not find the same relation in my behavioural data, it is very interesting to imagine the situation from the perspective of capture success. In Boeddeker, Roland Kern, and Martin Egelhaaf 2003 the authors presented a percentage of chance of success – i.e pursuit ends with capture – as a function of target's diameter and speed. The maximum chance for success was found for a target 5 mm large, moving at 1m/s. When increasing the target's diameter and/or speed, this percentage of success decreased. The chaser somehow adapts its behaviour to the target's morphology and motion. Because they are all black spheres, I will only consider that if the pursuer does not terminate the chase, it is because of the retinal target profile. Multiple visual features define this retinal profile, position, size and their first derivatives: velocity and expansion rate, respectively (Fig. 1.8). If the retinal target profile does not satisfy the pursuer's matched filters, the chase is cancelled – or the pursuer can be blocked at a constant distance from the target without capture, a phenomenon Boeddeker, Roland Kern, and Martin Egelhaaf 2003 called pursuit chases, a behaviour I did not observe in my experiments. A recent study in *Drosophila* suggests that a giant fiber escape pathway encodes position, angular size and expansion rate (Ache, Polsky, Alghailani, et al. 2019). This recent discovery is in line with the reflection developed above.

We have seen that another important behaviour when the fly is confronted with looming stimuli is its landing response (Borst and Bahde 1986). I described in Chapter 1 that in the final phase of the pursuit just before capture, the fly pulls up and extends its legs to catch the target. This behaviour looks very similar to landing reflex. When engaged in aerial pursuit, during final approach the expansion rate – which is maximum due to the proximity with the target – may trigger the capture in a similar way as it triggers the landing response.

Potentially, the looming motion pathway may play two important roles during pursuit: avoiding pursuit of a wrong target and initiating the capture.

4.2.3 Body shape and horizontal side-slip

Different pursuit strategies in the horizontal and vertical plane as suggested by my study may be, at least partly, the result of the fly's specific body shape. The asymmetric mass distribution and shape along the longitudinal and transverse body axes are likely to be deferentially affected by the inertial vector and gravity. An elongated body

provides more stability in yaw and in pitch, but not in roll. So strategies used for chasing in azimuth and elevation would both be affected by an elongated body.

The fact that in one case gravity plays a bigger role (elevation) than in the other (azimuth), is probably a better explanation due to the higher investment of energy required to do PP in the vertical direction. This may impose different dynamics for horizontal and vertical steering which could have facilitated the development of the separate pursuit strategies.

The body orientation of the pursuer: In first experiments on *Lucilia* I focused on body orientation of the male fly during pursuit (see preliminary results in chapter 2). I considered the pursuer as a elliptic body, defined by the position of its center of mass and two angles orientations: the absolute yaw and pitch angles. I observed that the fly's orientation varies with the target's angular velocity.

Horizontal plane: body yaw, heading, and side-slip. Over the range of target velocities we tested, flies always aligned their longitudinal body axis (yaw-orientation) with the line of sight (LoS) to keep the image of the target projected onto their 'love spot'. But we observed that the horizontal component of the LoF is hardly aligned with the LoS at high angular velocities (significant difference between the two angular velocities $p = 0.002$). This difference is likely the result of inertia-based side-slip during fast trajectory changes which, to our knowledge, has not been analysed during chasing flights before. Tested target trajectories included only clockwise rotation components. As a result, the values for the angle θ_E relative to LoS and LoF are always larger than those for θ_{EB} relative to LoS and LoB (Fig. 2.7***h***). This difference is probably the consequence of the animal's side-slip component which is always directed outwards with respect to its turning radius. Had we applied symmetrical clockwise and counter-clockwise rotation components to the dummy trajectories, we could have easily missed the difference as positive and negative values of θ_E would have cancelled out each other.

I think it is important to mention that in case of pursuit, side-slip may result in an uncontrolled coordinated flight. Whereas in cruising flight side-slip are a necessary condition for the ability of *HS*-cell to provide relative distance information (Lindemann, Roland Kern, J H van Hateren, et al. 2005).

Body pitch and the altitude changes. We did not observe significant differences $p = 0.09$ of the angle φ_{e2} (elevation angle formed between LoS and LoF) when the target moved at slow or fast angular velocity. This suggests the absence of vertical-slips in the sagittal plane, in other words there is no inertia dependant offset in the x-z plane. To further study potential adjustments of the elevation component of the LoF, we would have to introduce changes in the z-position of the moving target, which is challenging in the current setup.

4.3 Coordinated flight

Side-slip results in a loss of energy. During coordinated flight the fly controls its centripetal acceleration to avoid side-slip, i.e the fly aligns LoB and LoF (personal observations suggest hoverflies are really good at this). In the same way a fixed-wing aircraft would do, flies have to perform banked turns and adjust their forward speed. During coordinated turns, the change of heading is linked to the roll-angle and forward speed, the latter being linked to body pitch. In this section I will present the complexity and the relationship between body-yaw, body-pitch and body-roll during sharp turns.

4.3.1 Banked turns

In banked turns, to turn left the body performs a counter-clockwise roll rotation around its longitudinal axis. The projection of the lift following this rotation onto the horizontal plane is a force orthogonal to the speed vector creating a change of heading, that is inversely proportional to the forward speed (Eq. 4.1).

$$\Omega_P = \frac{g}{\frac{dxy}{dt}}.tan(\theta_{roll}) \tag{4.1}$$

Banking angle and body-roll: Banking angle or roll-angle have to be defined. Assuming the flight kinematics of the a blowfly are similar to those of a fixed-wing aircraft, the most efficient way of changing flight direction would be the performance of coordinated turns (McClamroch 2011), similar to those honeybees do when loitering around the beehive (Mahadeeswara and Srinivasan 2018). If x_A, y_A and z_A are the axes of a fly- or aircraft-fixed coordinate system, the body roll-angle is defined as the rotation angle around x_A (or the LoB axis). The banking angle is defined as the angle between the aircraft fixed y_A and the horizontal plane, based on a rotation around the LoF. Thus, unlike the body roll-angle which is related to steady fly body orientation, the banking angle is linked to the fly's velocity vector. In coordinated flight, the side-slip angle is zero, so without a side-slip component the LoF is aligned with the LoB and the body roll-angle is equal to the banking angle. But in the presence of side-slip, the body roll- and banking angle are different.

Banked turns in insect flights: Previous studies suggested that fruit flies are able to change their heading direction without banking by generating torque about their yaw-axis (Karl Geokg Götz 1964; Hedrick, B. Cheng, and Deng 2009; Bergou, Ristroph, Guckenheimer, et al. 2010). However, during fast escape manoeuvres they do perform banked turns (Florian T. Muijres, Elzinga, Melis, et al. 2014), which has been implemented in bioinspired flapping wing aerial robots (Karasek, Florian T Muijres, Wagter, et al. 2018). For a blowfly with a significant inertia operating at Reynold number around 600 (Buckholz 1981), banked turns are common during body saccades (Schilstra and J. Hateren 1999). Whether or not blowflies perform banked turns when

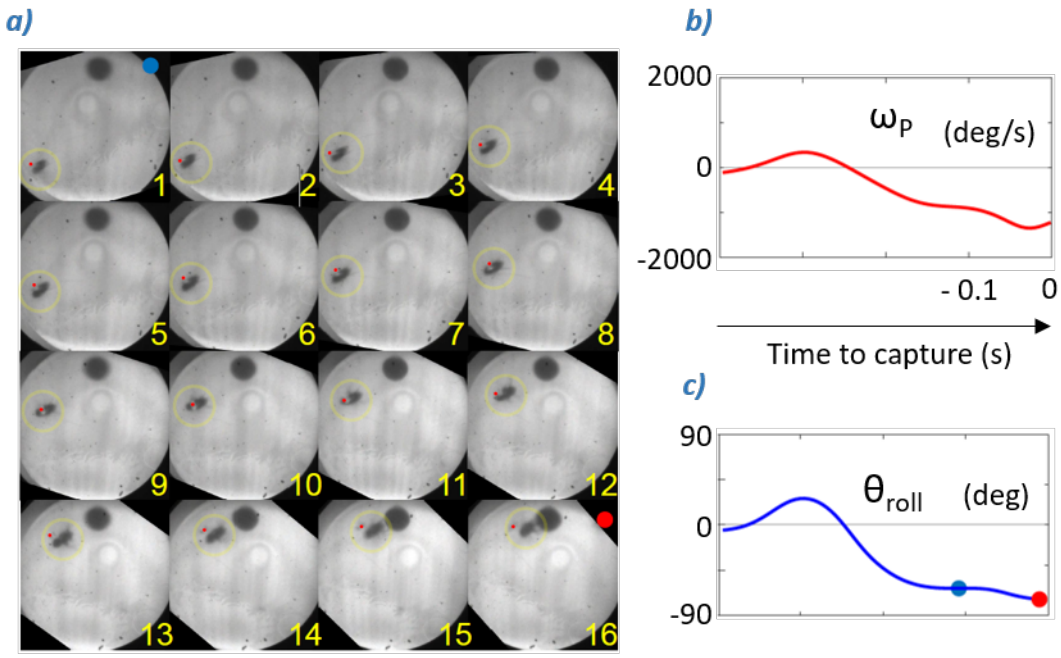

Figure 4.4 – **View from the embedded camera and banked turn** (representation of the pursuit presented in Fig. 2.7***a-b***). ***a)*** Series of the final approach of the pursuer centered in the yellow circle, with a small red point indicating the tip of the dorso-ventral flag. Time between consecutive frames is 5.26 ms. We can identify the capture move with a nose-up manoeuvre to catch the target between frame 13 to 16. ***b)*** Change of heading in the horizontal plane as a function of time. The final approach is a sharp turn ($\omega_P > 1000$ deg/s). ***c)*** Theoretical roll-angle computed with Eq. 4.1 as a function of time (with variables from pursuit in ***a-b***). During the final approach (between blue and red dots frame 1 and 16 in ***a***, respectively), the computed roll-angle is mostly constant around 75 deg which seems to be consistent with observations pictured in ***a***).

engaging on chasing flights has not yet been systematically studied, but our first observations suggest that they do (Fig. 2.8).

4.3.2 Forward speed

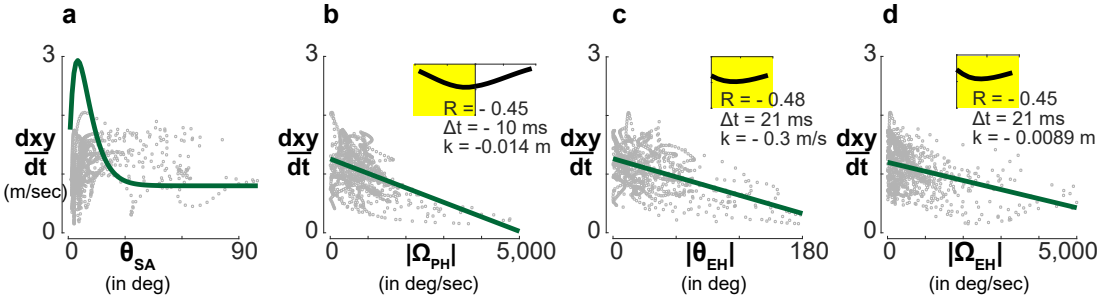

$$s(t) = \begin{cases} S_g & \text{if } \rho \leqslant 0.5^\circ \\ \rho(t-\Delta t)\, S_v e^{-\rho(t-\Delta t)/\rho^*} + S_g & \text{if } \rho > 0.5^\circ \end{cases} \tag{4.2}$$

Figure 4.5 – **Looking for relationships between horizontal speed and other variables.** (**a**) Relationship between pursuer horizontal speed and target angular size. Measured data (gray dots) and control law (green curve) Boeddeker and Martin Egelhaaf 2003 proposed as described in Equation (4.2). The data I obtained in my study are not described well by the proposed control law. (**b**) Relationship between pursuer's horizontal speed and its angular velocity. Fast angular rotations are (weakly) correlated with a lower translational speed, as described for coordinated turns. Cross correlation analysis shows that the best linear fit is observed when deceleration occurs 10ms before the turn. (**c**) Relationship between the horizontal speed and the horizontal target heading angle θ_E (**d**) Relationship between the horizontal speed and the horizontal target heading angular rate Ω_{EH}. In (**b, c, d**) relationships between horizontal speed and angular parameters show a weak linear correlation $R < 0.5$.

Forward speed during sharp turns: To find out whether *Lucilia* performed coordinated turns during its chasing flights I extracted angular rotation peaks - which reached values of up to 7000 deg/sec - and correlated changes in forward speed from the free flight data. I isolated the 6 fastest yaw rotations and yaw speeds higher than 1500 deg/sec. The analysis of these segments demonstrated an expected reduction of the forward speed when the fly performed these spectacular sharp turns. Deceleration of the forward speed, coupled with high yaw rotation describes well coordinated turns.

Forward speed and body pitch: We observed that the elevation coordinate of the error angle between LoS and LoB (see θ_{EB} in Fig 2.7***g***) is significantly different (p = 0.01) when the target moves with slow or high angular velocity. This can be explained by the linear relationship between forward speed and absolute pitch-angle as described in blowfly by Schilstra and J. Hateren 1999.

Forward speed control: Chasing strategies are sometimes limited to the characterisation of 2D or 3D steering without much consideration of forward speed control. I already mentioned that the forward speed controller developed by Boeddeker and Martin Egelhaaf 2003 did not fit with my data (see section 4.2.2 looming stimuli paragraph). So I decided to look for an alternative control law for forward speed and found an average linear correlation of R ~ -0.5 between horizontal speed and θ_{EH} (Fig. 4.5***c***). I found the same linear correlation between horizontal speed and Ω_{EH} (Fig. 4.5***d***). I also found that the forward speed decreases 10 ms before the onset of the yaw rotation (Fig. 4.5***b***), which is in line with what was described in houseflies (Land and Thomas S Collett 1974). The implementation of a forward speed control based on these relationships, however, did not give satisfactory results.

The analysis of experimental results suggests a relationship between retinal target position (not size) and forward speed, through thrust regulation. This is in line with the model developed by Gronenberg and Strausfeld 1991, where the frontal retinal position of the target elicits an increase in thrust (*MLG4* in Fig. 4.1). If a small object appears in the central region of the retina – i.e. love spot –, it increases thrust. In the case that retinal target position is stabilized in this central zone, the prolonged positive thrust will certainly increase the forward speed. I found linear relationships between error θ_{EH} and thrust (R = -0.6), but I prefer to remain careful about this relationship for several reasons. First, this maximum correlation (in absolute value) appears at a zero time delay, which appears to be unrealistic. Second, the coefficient of the proportional controller depends on the mass of the fly. The body size varied between individuals, and I assume that the mass variations would be correlated. Several males are present simultaneously in the arena, and I am not able to identify which one is engaged in the pursuit. Nonetheless I started to develop a dynamic model of the pursuit, in which I estimated fly mass to be 100 mg, and I constrained the possible speed range: maximum forward velocity: 2 m/s, and maximum forward acceleration 15 m/s^2. Preliminary results are encouraging, but the development of an acceptable dynamic model of the pursuit needs more quantitative measurements.

4.3.3 Horizontal steering influences vertical steering

Although only at a low coefficient of $R = 0.5$, there is a correlation between Ω_{PH} and Ω_{PV}. Indeed I found a linear relationship of the form: $\Omega_{PZ(t)} = k.\Omega_{PH(t-\Delta t)} + A$ with $k = -0.25$, Δt = 21 ms and A = 3.85 s^{-1} (Fig. 4.6). A large path change in the horizontal plane – independent of the direction of rotation – is followed by a negative vertical rotation, i.e. a downward rotation. This phenomenon can be explained by the

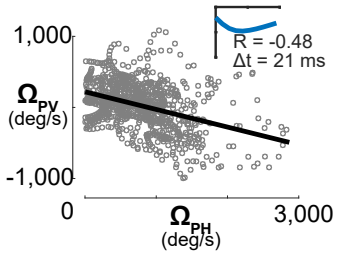

Figure 4.6 – **Relationship between horizontal and vertical steering.** The cross correlation gives a weak maximum ($R = -0.48$) for a 21 ms delay. We can quantify the relationship by a linear regression (black line) of the form: $\Omega_{PV(t)} = -0.25.|\Omega_{PH(t-21ms)}|$ for $0 < |\Omega_{PH}| < 1500$ deg/sec

presence of banked turns. The gain in force due to the yaw rotation is compensated for negative vertical lift resulting in a loss of altitude. However, when the relationship between horizontal and vertical steering is implemented in the vertical steering control, I did not observe any significant improvement of its performance. This needs further investigations.

4.4 Head-body movements while chasing

Movements of the head relative to the body have minimum impact on the general trajectory of the fly when considering a kinematic model of the pursuit. However, as the movement of the head relative to the body significantly affects the retinal position of the target, it plays a major role in pursuit control.

Head-body fixation approximation: *No body-roll, no need for head compensation!* For the different studies presented in this thesis I estimated the retinal target profile (position, velocity, size and expansion rate) without knowing exactly the orientation of the head of the fly. When I studied the orientation of the body in yaw and pitch, I estimated that the head was aligned with the longitudinal body axis. When I studied the kinematics – the displacements of the centers of mass – I estimated that the head and the longitudinal body axis were aligned with the speed vector. In both cases, the compound eyes were always aligned with the external horizon.

When I moved on towards dynamic models of the pursuit integrating the banked turn, the orientation of the head became a real concern. In simple kinematic model, or Cartesian approaches (Fig. 4.7***a***) retinal target position in azimuth controls the fly's motion in horizontal plane (yaw turn, change of the horizontal heading and horizontal speed), and retinal target elevation controls vertical flight parameters (body pitch and vertical heading) (Eqs. 3.4.1 and 3.4.2 and Varennes, Krapp, and Stéphane Viollet 2019).

In banked turns, change in heading is linked to body-roll (Eq. 4.1). If we assume that head and body are fixed, banked turns would rotate the pursuer visual field. Once the target is placed along vertical axis of the retina, the fly does a pitch-rotation to adjust the retinal target elevation (Fig. 4.7***b***).

That would be the case in the absence of gaze stabilization.

4.4.1 Gaze stabilization

The gaze stabilization is an important sensorimotor control task for almost all visually oriented animals. It stabilises the eyes with respect to the external horizon during locomotion. Previous works characterized the gaze stabilisation reflex in blowflies (Strausfeld, Seyan, and Milde 1987; Roland Hengstenberg 1991; Schwyn, Heras, Bolliger, et al. 2011 review: Hardcastle and Krapp 2016), with applications in engineered systems such as MAVs (Kerhuel, S. Viollet, and N. Franceschini 2007; Gremillion, Humbert, and Krapp 2014). The fly uses several visual and mechanosensory cues to stabilize its eyes relative to the surroundings by compensatory head/eye movements. I am not aware of any study about gaze stabilization during aerial pursuit in flies.

During pursuit, corrective head movements are important as the pursuer's pitch and roll manoeuvres could cause extensive retinal target movement, making it hard to perform appropriate compensatory turns. Dragonflies therefore stabilize their gaze towards the target during flight (Mischiati, Lin, Herold, et al. 2015; Robert M. Olberg

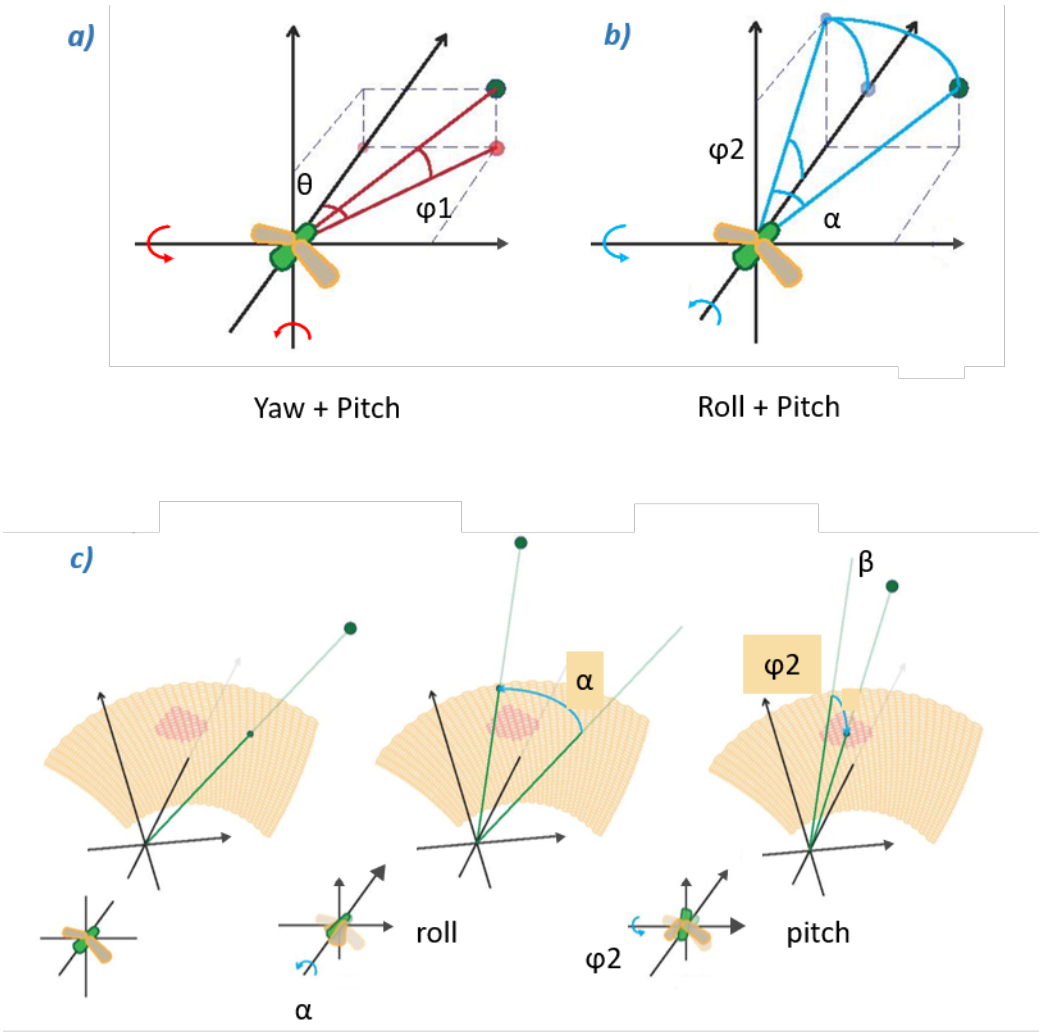

Figure 4.7 – **In head-fixed model, two approaches may bring back the target into the love spot:** ***a)*** What I call Cartesian approach: azimuth and vertical corrections are controlled by yaw and pitch respectively, as described in Chapter 3. ***b)*** Another approach I would call Planar approach may consist of sequential roll then pitch rotations. ***c)*** Detailed sequence presented in ***b)***. To bring the target into the central zone of the visual field first the fly will rotate along its longitudinal axis (body-roll), so that the target is projected into the frontal meridian of the retina, then the fly rotates along transversal axis (body-pitch) to adjust the target's vertical retinal position.

2012), rotating their head via neck muscles against the body axis and also by means of inertial stabilization (Von Holst and Mittelstaedt 1950). Note, that in dragonflies forward models (or efference copies or internal models) may be in place, since this delay has been reported to be as brief as 4 ms (Mischiati, Lin, Herold, et al. 2015).

Roland Hengstenberg 1991 found that with input from the compound eyes alone, the amplitude of compensatory head-roll movement peaks at an angular velocity of around 70 deg/sec in blowflies. Response delays of the gaze stabilisation reflex, when mediated by the compound eyes alone, are around 20 ms in blowflies (Roland Hengstenberg 1991; Parsons, Krapp, and Simon B. Laughlin 2010).

Gaze stabilization is essential in all of the fly's behaviours encountered so far (Roland Hengstenberg 1991). One would expect to find the gaze stabilization reflex still working during pursuit as it is maintained during all flight behaviours, so far. The fly's head would stay stabilized relative to the horizon, while the body would rotate to change the thrust direction, especially along its longitudinal body axis to engage in banked turns.

4.4.2 The head is not locked to horizon

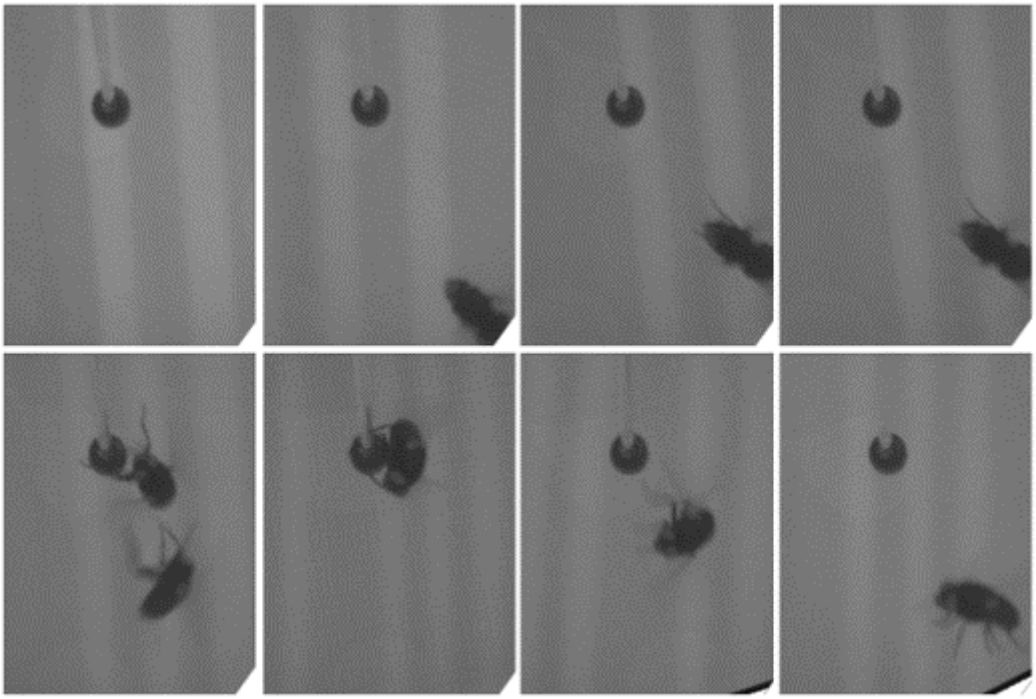

Figure 4.8 – **Capture of the target, recorded by a Awaiba microcamera.** We can clearly see that during approach, landing and take off the head does not align with external horizon.

The embedded module presented in Chapter 2 provided me with qualitative data on head-body rotations. The head of the fly in the video frames appears not to

be horizontally oriented (Fig. 2.8***a*** and Fig. 4.8). Unfortunately, the resolution of implemented recording modules were insufficient to perform quantitative analysis of the head-body coordination. The NanEye camera acquisition speed was too low, and the spatial resolution of the optic fiber bundles (micro-endoscope module version 1 and 2) was not high enough to extract head-body orientations. It leaves me unable to model the gaze stabilization reflex during pursuit. I tried basic image processing such as contrast enhancement and feature extraction on fly's head and body without satisfying results (as explained in Chapter 2).

The extremely fast (10ms) delay time in horizontal steering control during pursuit is the same as the delay time for head compensation. This was measured under tethered conditions with the body rotated against a stationary background (compound eyes and halteres condition) (Roland Hengstenberg 1991). Gaze stabilization is a multisensory reflex, and the visual part shares the same motion vision pathway as the optomotor response: LPTCs (Hardcastle and Krapp 2016). Suppressive action of the pursuit on the optomotor response (Fig. 4.2***c***), has an impact on gaze stabilization reflex. What we assume is that the head angle can also be voluntarily controlled, which requires the use of an efference copy. There are tons of data showing that compensatory head movements are compressed.

5 Conclusion

Sommaire

5.1 Concluding remarks 120
5.2 Future directions 121

5.1 Concluding remarks

In this thesis, behavioural work was presented, aimed towards understanding general principles of sensorimotor control during aerial pursuit in Diptera. An experimental method was implemented which could be applied to characterise the visuomotor pursuit system of different fly species. I experimented this setup with *Lucilia*, *Calliphora*, *Sarcophaga* and *Eristalis*, only *Lucilia* responded to our experimental conditions.

In the introduction, the question was raised whether the pursuit in the blowfly *Lucilia* could be modeled as a visuomotor system. I gave a brief overview of the compound eye and motion vision in Diptera. I also introduced a number of different experimental studies including optomotor responses, responses to looming, object fixation, and other visuomotor behaviors that are related (documented or not) to aerial pursuit. I then described the different phases of pursuit, detection, tracking, capture as well as the questions I address during my project.

A rather complex experimental setup was built for this project, and I upgraded it several times. Its design, tests and upgrades are presented in chapter 2. In chapter 3, I present a kinematic model of the fly based on my behavioural data. The behavioural analysis highlighted a difference in approach strategies on the horizontal and vertical planes. The steering control is quite simple (proportional to the error angle) with a very small time delay 10 ms. I also observed banked turns and side-slip which have not been reported for blowfly chasing a target so far.

In the last chapter I discussed how the neuroanatomy of the pursuer is specialised to perform during the different phases of the pursuit. I also discussed the flight dynamics, and the importance of coordinated turn to to trade off manoeuvribility against energy efficiency. Gaze direction during pursuit is crucial. Indeed head orientation determines the projection of the target onto the pursuer's retina which supports target detection, steering, thrust, landing responses and triggers the final capture phase during a chasing flight. Finally, I discussed the necessity of gaze stabilization during chasing - which, apparently, may be switched off during certain phases of the behaviour. The suppressive model proposed by (Trischler, Roland Kern, and Martin Egelhaaf 2010) may account not only for optomotor response but also for gaze stabilization. The efference copy model may work even as well.

5.2 Future directions

Each single phase of the pursuit is remarkable, and may as well provide the basis for separate dedicated research projects.

Target detection: Detection surface described by Cliff and Bullock 1993 for *Eristalis* (Fig. 1.9 ***g***) was a brilliant idea. One can imagine the same principle for the design of detection volume for every species of aerial chasers, based on anatomy and physiology of the compound eyes. What happens if the target exits this zone during pursuit, is the chase abandoned?

Target tracking: - Chasing behaviour in flies occurs in many different natural environments such as bushes, open fields, forests and even indoor below chandeliers (Land and Thomas S Collett 1974). The presented setup is perfectly suited to investigate how the pursuit trajectory may be affected by external perturbations such as obstacles or wind. This would help to understand interaction between pursuit and other sensorimotor responses highlighting the underlying motion vision pathways.

- It would be interesting to further investigate how the fly maintains the image of the target in the love spot. For that I would recommend to start with tethered fly experiments. When presented with moving targets does the head follows the target? What are the preferred head moves that will bring the target on the frontal meridian of the retina, yaw rotation of roll-rotation (Fig. 4.7 ***a-b***)?

- As suggested earlier, it would be interesting to investigate how the pursuit system "suppresses" the optomotor response. What exactly is affected by the pursuit? Is it inhibiting the responses to wide-field motion? If any modification would already take place at the level of LPTCs this would have an impact in gaze stabilization – not if you take forward models into account. To take this line of arguments even further, if the gaze stabilization reflex is not supported by wide-field motion, would it still be controlled by other modalities including halteres and ocelli?

- Is there a change in functional structure of gaze control during pursuit? Could the presence of a projected image of a target in the love spot change the functional structure of the gaze control? Indeed, the fly changes input-and output configuration of the gaze control system when it alternates between flight and walking (Roland Hengstenberg 1991).

- My behavioural data suggested that the steering may be controlled by θ_E and ω_A. I would suggest to try a control law with fractional derivatives (Bootsma, Ledouit, Remy Casanova, et al. 2016).

- I tried to develop a dynamic model of the pursuer. I managed to achieve a working model controlling thrust. Steering control may require more work to take into account coordinated turns and head-body positions.

Capture: I think there is a link between looming response and pursuit. If presented with the right retinal size and expansion rate, the target may elicit the capture response

(similar to the landing response). If the combination of retinal size, expansion rate, position and velocity do not fit the the pursuer's matched filters, the pursuit would be abandoned (such as during collision avoidance).

Bibliography

[Abd+05] Jellali Abdeljalil, Meziane Hamid, Ouagazzal Abdel-Mouttalib, et al. “The optomotor response: A robust first-line visual screening method for mice”. In: *Vision Research* 45.11 (2005), pp. 1439–1446. ISSN: 00426989. DOI: 10.1016/j.visres.2004.12.015 (cit. on p. 30).

[Ach+19a] Jan M. Ache, Shigehiro Namiki, Allen Lee, et al. “State-dependent decoupling of sensory and motor circuits underlies behavioral flexibility in Drosophila”. In: *Nature Neuroscience* 22.7 (2019), pp. 1132–1139. ISSN: 15461726. DOI: 10.1038/s41593-019-0413-4 (cit. on p. 34).

[Ach+19b] Jan M. Ache, Jason Polsky, Shada Alghailani, et al. “Neural Basis for Looming Size and Velocity Encoding in the Drosophila Giant Fiber Escape Pathway”. In: *Current Biology* 29.6 (2019), 1073–1081.e4. ISSN: 09609822. DOI: 10.1016/j.cub.2019.01.079 (cit. on pp. 34, 35, 108).

[AS19] Lucia de Andres-Bragado and Simon G. Sprecher. “Mechanisms of vision in the fruit fly”. In: *Current Opinion in Insect Science* 36 (2019), pp. 25–32. ISSN: 22145753. DOI: 10.1016/j.cois.2019.06.005 (cit. on p. 26).

[AVG05] Rozi Andretic, Bruno Van Swinderen, and Ralph J. Greenspan. “Dopaminergic modulation of arousal in Drosophila”. In: *Current Biology* 15.13 (2005), pp. 1165–1175. ISSN: 09609822. DOI: 10.1016/j.cub.2005.05.025 (cit. on p. 24).

[AF13] Jacob W. Aptekar and Mark A. Frye. “Higher-order figure discrimination in fly and human vision”. In: *Current Biology* 23.16 (2013), R694–R700. ISSN: 09609822. DOI: 10.1016/j.cub.2013.07.022 (cit. on p. 35).

[AK71] Abdel Aziz and HM Karara. “Direct linear transformation into object space coordinates in close-range photogrammetry”. In: *In Proc. of the Symposium on Close-Range Photogrammetry* (1971), pp. 1–18 (cit. on p. 54).

[Bai+13] Emily Baird, Norbert Boeddeker, Michael R. Ibbotson, et al. “A universal strategy for visually guided landing”. In: *Proceedings of the National Academy of Sciences of the United States of America* 110.46 (2013), pp. 18686–18691. ISSN: 00278424. DOI: 10.1073/pnas.1314311110 (cit. on p. 34).

[BNO07] Paul D. Barnett, Karin Nordström, and David C. O’Carroll. “Retinotopic Organization of Small-Field-Target-Detecting Neurons in the Insect Visual System”. In: *Current Biology* 17.7 (2007), pp. 569–578. ISSN: 09609822. DOI: 10.1016/j.cub.2007.02.039 (cit. on p. 106).

[BD06] John A. Bender and Michael H. Dickinson. "Visual stimulation of saccades in magnetically tethered Drosophila". In: *Journal of Experimental Biology* 209.16 (2006), pp. 3170–3182. ISSN: 00220949. DOI: 10.1242/jeb.02369 (cit. on p. 34).

[Ber+10] Attila J Bergou, Leif Ristroph, John Guckenheimer, et al. "Fruit Flies Modulate Passive Wing Pitching to Generate In-Flight Turns". In: *PHYSICAL REVIEW LETTERS* 104 (2010), pp. 148101–4. DOI: 10.1103/PhysRevLett.104.148101 (cit. on p. 110).

[Bla+14] Kevin Bland, Nicholas P. Revetta, Annette Stowasser, et al. "Unilateral range finding in diving beetle larvae". In: *Journal of Experimental Biology* 217.3 (2014), pp. 327–330. ISSN: 00220949. DOI: 10.1242/jeb.092833 (cit. on p. 38).

[BE03] Norbert Boeddeker and Martin Egelhaaf. "Steering a virtual blowfly: simulation of visual pursuit." In: *Proceedings. Biological sciences / The Royal Society* 270.1527 (2003), pp. 1971–8. ISSN: 0962-8452. DOI: 10.1098/rspb.2003.2463 (cit. on pp. 60, 65, 82, 108, 112, 113).

[BKE03] Norbert Boeddeker, Roland Kern, and Martin Egelhaaf. "Chasing a dummy target: smooth pursuit and velocity control in male blowflies." In: *Proceedings. Biological sciences / The Royal Society* 270.1513 (2003), pp. 393–399. ISSN: 0962-8452. DOI: 10.1098/rspb.2002.2240 (cit. on pp. 44, 47, 49, 59, 85, 108).

[BWT09] Richard J. Bomphrey, Simon M. Walker, and Graham K. Taylor. "The typical flight performance of blowflies: Measuring the normal performance envelope of Calliphora vicina using a novel corner-cube arena". In: *PLoS ONE* 4.11 (2009). Ed. by Stuart Humphries, e7852. ISSN: 19326203. DOI: 10.1371/journal.pone.0007852 (cit. on p. 85).

[Boo+16] Reinoud J Bootsma, Simon Ledouit, Remy Casanova, et al. "Fractional-order information in the visual control of lateral locomotor interception". In: *Journal of Experimental Psychology: Human Perception and Performance* 42.4 (2016), pp. 517–529. ISSN: 19391277. DOI: 10.1037/xhp0000162 (cit. on pp. 80, 121).

[Bor09] Alexander Borst. "Drosophila's View on Insect Vision". In: *Current Biology* 19.1 (2009), R36–R47. ISSN: 09609822. DOI: 10.1016/j.cub.2008.11.001 (cit. on p. 26).

[Bor14a] Alexander Borst. "Fly visual course control: behaviour, algorithms and circuits." In: *Nature reviews. Neuroscience* 15.9 (2014), pp. 590–599. ISSN: 1471-0048. DOI: 10.1038/nrn3799 (cit. on p. 30).

[Bor14b] Alexander Borst. *In search of the holy grail of fly motion vision*. 2014. DOI: 10.1111/ejn.12731 (cit. on p. 29).

[BB86] Alexander Borst and S. Bahde. "What kind of movement detector is triggering the landing response of the housefly?" In: *Biological Cybernetics* 55.1 (1986), pp. 59–69. ISSN: 03401200. DOI: 10.1007/BF00363978 (cit. on pp. 34, 108).

[Bra86] Valentino. Braitenberg. *Vehicles : experiments in synthetic psychology*. MIT Press, 1986, p. 152. ISBN: 0262521121 (cit. on p. 24).

[BF66] Valentino. Braitenberg and Cloe Ferretti. "Landing Reaction of Musca Domestica Induced by Visual Stimuli". In: *Naturwissenschaften* (1966), pp. 1966–1966 (cit. on p. 34).

[BT19] Caroline H. Brighton and Graham K. Taylor. "Hawks steer attacks using a guidance system tuned for close pursuit of erratically manoeuvring targets". In: *Nature Communications* 10.1 (2019). ISSN: 20411723. DOI: 10.1038/s41467-019-10454-z (cit. on pp. 5, 84, 88).

[Bri+17] Caroline H. Brighton, Adrian L.R. Thomas, Graham K. Taylor, et al. "Terminal attack trajectories of peregrine falcons are described by the proportional navigation guidance law of missiles". In: *Proceedings of the National Academy of Sciences of the United States of America* 114.51 (2017), pp. 13495–13500. ISSN: 10916490. DOI: 10.1073/pnas.1714532114 (cit. on p. 84).

[Buc81] Richard H Buckholz. "Measurements of unsteady periodic forces generated by the blowfly flying in a wind tunnel". In: *The Journal of Experimental Biology* 90 (1981), pp. 163–173. DOI: 90:163-173 (cit. on p. 110).

[BTL01] Brian G Burton, Ben W Tatler, and Simon B Laughlin. "Variations in photoreceptor response dynamics across the fly retina." In: *Journal of neurophysiology* 86.2 (2001), pp. 950–960. ISSN: 0022-3077. DOI: 11495963 (cit. on p. 42).

[BL03] Brian G. Burton and Simon B. Laughlin. "Neural images of pursuit targets in the photoreceptor arrays of male and female houseflies Musca domestica". In: *Journal of Experimental Biology* 206.22 (2003), pp. 3963–3977. ISSN: 0022-0949, 1477-9145. DOI: 10.1242/jeb.00600 (cit. on pp. 41, 42, 64).

[BS96] Elke K. Buschbeck and Nicholas J. Strausfeld. "Visual motion-detection circuits in flies: Small-field retinotopic elements responding to motion are evolutionarily conserved across taxa". In: *Journal of Neuroscience* 16.15 (1996), pp. 4563–4578. ISSN: 02706474. DOI: 10.1523/jneurosci.16-15-04563.1996 (cit. on p. 104).

[BS97] Elke K. Buschbeck and Nicholas J. Strausfeld. "The relevance of neural architecture to visual performance: Phylogenetic conservation and variation in dipteran visual systems". In: *Journal of Comparative Neurology* 383.3 (1997), pp. 282–304. ISSN: 00219967. DOI: 10.1002/(SICI)1096-9861(19970707)383:3<282::AID-CNE2>3.0.CO;2-# (cit. on p. 104).

[But16] Patrick J. Butler. "The physiological basis of bird flight". In: *Philosophical Transactions of the Royal Society B: Biological Sciences* 371.1704 (2016). ISSN: 14712970. DOI: 10.1098/rstb.2015.0384 (cit. on p. 24).

[CD08] Gwyneth Card and Michael H. Dickinson. "Visually Mediated Motor Planning in the Escape Response of Drosophila". In: *Current Biology* 18.17 (2008), pp. 1300–1307. ISSN: 09609822. DOI: 10.1016/j.cub.2008.07.094 (cit. on pp. 32, 34, 35).

[Cen+13] Andrea Censi, Andrew D. Straw, Rosalyn W. Sayaman, et al. "Discriminating External and Internal Causes for Heading Changes in Freely Flying Drosophila". In: *PLoS Computational Biology* 9.2 (2013). ISSN: 1553734X. DOI: 10.1371/journal.pcbi.1002891 (cit. on p. 25).

[CPD98] Wai Pang Chan, Frederick Prete, and Michael H. Dickinson. "Visual input to the efferent control system of a fly's 'gyroscope'". In: *Science* 280.5361 (1998), pp. 289–292. ISSN: 00368075. DOI: 10.1126/science.280.5361.289 (cit. on p. 97).

[Chi16] Lars Chittka. "Editorial overview: Behavioural ecology - Molecular and neural mechanisms underpinning adaptive behaviour in insects". In: *Current Opinion in Insect Science* 15 (2016), pp. vii–ix. ISSN: 22145745. DOI: 10.1016/j.cois.2016.05.002 (cit. on p. 24).

[CS88] Charles Chubb and George Sperling. "Drift-balanced random stimuli: a general basis for studying non-Fourier motion perception". In: *Journal of the Optical Society of America A* 5.11 (1988), p. 1986. ISSN: 1084-7529. DOI: 10.1364/josaa.5.001986 (cit. on p. 37).

[CB93] Dave Cliff and Seth Bullock. "Adding "Foveal Vision" to Wilson's Animat". In: *Adaptive Behavior* 2.1 (1993), pp. 49–72. ISSN: 17412633. DOI: 10.1177/105971239300200103 (cit. on pp. 41, 121).

[Col71] T. S. Collett. "visual neurones for tracking moving targets". In: *Nature* 232 (1971), pp. 127–130. ISSN: 0028-0836. DOI: 10.1038/232127a0 (cit. on p. 106).

[Col78] T. S. Collett. "Peering-A Locust Behaviour Pattern for Obtaining Motion Parallax Information". In: *The Journal of Experimental Biology* 76.1 (1978), pp. 237–241. ISSN: 0022-0949 (cit. on p. 82).

[Col80] T. S. Collett. “Angular tracking and the optomotor response an analysis of visual reflex interaction in a hoverfly”. In: *Journal of Comparative Physiology A* 140.2 (1980), pp. 145–158. ISSN: 03407594. DOI: 10.1007/BF00606306 (cit. on pp. 31, 32, 35, 37).

[CL75] Thomas S Collett and Michael F. Land. “Visual control of flight behaviour in the hoverfly Syritta pipiens L.” In: *Journal of Comparative Physiology A* 99.1 (1975), pp. 1–66. ISSN: 0340-7594. DOI: 10.1007/BF01464710 (cit. on pp. 35, 64).

[CL78] Thomas S Collett and Michael F. Land. “How hoverflies compute interception courses”. In: *Journal of Comparative Physiology A* 125.3 (1978), pp. 191–204. ISSN: 03407594. DOI: 10.1007/BF00656597 (cit. on pp. 47, 65).

[DC12] Saskia E.J. De Vries and Thomas R. Clandinin. “Loom-sensitive neurons link computation to action in the Drosophila visual system”. In: *Current Biology* 22.5 (2012), pp. 353–362. ISSN: 09609822. DOI: 10.1016/j.cub.2012.01.007 (cit. on p. 34).

[DL95] Michael H. Dickinson and John R.B. Lighton. “Muscle efficiency and elastic storage in the flight motor of Drosophila”. In: *Science* 268.5207 (1995), pp. 87–90. ISSN: 00368075. DOI: 10.1126/science.7701346 (cit. on p. 32).

[DM16] Michael H. Dickinson and Florian T. Muijres. “The aerodynamics and control of free flight maneuvers in Drosophila”. In: *Philosophical transactions of the Royal Society of London B: Biological Sciences* 371 (2016), p. 20150388. ISSN: 14712970. DOI: 10.1098/rstb.2015.0388 (cit. on p. 32).

[Ege87] Martin Egelhaaf. “Dynamic properties of two control systems underlying visually guided turning in house-flies”. In: *Journal of Comparative Physiology A* 161.6 (1987), pp. 777–783. ISSN: 03407594. DOI: 10.1007/BF00610219 (cit. on p. 37).

[Ege+12] Martin Egelhaaf, Norbert Boeddeker, Roland Kern, et al. “Spatial vision in insects is facilitated by shaping the dynamics of visual input through behavioral action.” In: *Frontiers in neural circuits* 6.December (2012), p. 108. ISSN: 1662-5110. DOI: 10.3389/fncir.2012.00108 (cit. on p. 26).

[EB93] Martin Egelhaaf and Alexander Borst. “A look into the cockpit of the fly: visual orientation, algorithms, and identified neurons”. In: *J Neurosci* 13.11 (1993), pp. 4563–4574. ISSN: 0270-6474. DOI: 10.1523/JNEUROSCI.13-11-04563.1993 (cit. on p. 32).

[Ege+88] Martin Egelhaaf, Klaus Hausen, Werner Reichardt, et al. "Visual course control in flies relies on neuronal computation of object and background motion". In: *Trends in Neurosciences* 11.8 (1988), pp. 351–358. ISSN: 01662236. DOI: 10.1016/0166-2236(88)90057-4 (cit. on pp. 36, 37).

[Eic+17] Courtney Eichorn, Michael Hrabar, Emma C. Van Ryn, et al. "How flies are flirting on the fly". In: *BMC Biology* 15.1 (2017), p. 2. ISSN: 1741-7007. DOI: 10.1186/s12915-016-0342-6 (cit. on p. 43).

[Enn89] B Y A Roland Ennos. "The kinematics and aerodynamics of the free flight of some Diptera." In: *J. exp. Biol* 85 (1989), pp. 49–85. URL: http://jeb.biologists.org/content/jexbio/142/1/49.full.pdf (cit. on p. 65).

[Fab+18] Samuel T. Fabian, Mary E. Sumner, Trevor J. Wardill, et al. "Interception by two predatory fly species is explained by a proportional navigation feedback controller". In: *Journal of the Royal Society, Interface* 15.147 (2018). ISSN: 17425662. DOI: 10.1098/rsif.2018.0466 (cit. on pp. 84, 85, 90).

[FW07] Brett R. Fajen and William H. Warren. "Behavioral dynamics of intercepting a moving target". In: *Experimental Brain Research* 180.2 (2007), pp. 303–319. ISSN: 00144819. DOI: 10.1007/s00221-007-0859-6 (cit. on pp. 64, 80).

[FN06] Valerie C. Fleisch and Stephan C.F. Neuhauss. *Visual behavior in zebrafish*. 2006. DOI: 10.1089/zeb.2006.3.191 (cit. on p. 30).

[Fra14] Nicolas Franceschini. "Small brains, smart machines: From fly vision to robot vision and back again". In: *Proceedings of the IEEE* 102.5 (2014), pp. 751–781. ISSN: 00189219. DOI: 10.1109/JPROC.2014.2312916 (cit. on p. 24).

[Fra+81] Nicolas Franceschini, R. Hardie, W. Ribi, et al. "Sexual dimorphism in a photoreceptor". In: *Nature* 291.5812 (1981), pp. 241–44. ISSN: 1098-6596. DOI: 10.1017/CBO9781107415324.004. arXiv: arXiv:1011.1669v3 (cit. on p. 38).

[FK00] Matthias O. Franz and Holger G. Krapp. "Wide- field , motion-sensitive neurons and matched filters for optic flow fields". In: *Biological Cybernetics* 197 (2000), pp. 185–197 (cit. on pp. 29, 104).

[FD04] Mark A. Frye and Michael H. Dickinson. "Closing the loop between neurobiology and flight behavior in Drosophila". In: *Current Opinion in Neurobiology* 14.6 (2004), pp. 729–736. ISSN: 09594388. DOI: 10.1016/j.conb.2004.10.004 (cit. on p. 33).

[Gab+04] Fabrizio Gabbiani, Holger G. Krapp, Nicholas Hatsopoulos, et al. "Multiplication and stimulus invariance in a looming-sensitive neuron". In: *Journal of Physiology Paris* 98.1-3 SPEC. ISS. (2004), pp. 19–34. ISSN: 09284257. DOI: 10.1016/j.jphysparis.2004.03.001 (cit. on p. 34).

[GKE12] Bart R.H. Geurten, Roland Kern, and Martin Egelhaaf. "Species-specific flight styles of flies are reflected in the response dynamics of a homolog motion-sensitive neuron". In: *Frontiers in Integrative Neuroscience* 6.MARCH (2012), pp. 1–15. ISSN: 16625145. DOI: 10.3389/fnint.2012.00011 (cit. on p. 104).

[Gho06] K. Ghose. "Steering by Hearing: A Bat's Acoustic Gaze Is Linked to Its Flight Motor Output by a Delayed, Adaptive Linear Law". In: *Journal of Neuroscience* 26.6 (2006), pp. 1704–1710. ISSN: 0270-6474. DOI: 10.1523/JNEUROSCI.4315-05.2006 (cit. on p. 84).

[Gib51] James J. Gibson. "The Perception of the Visual World." In: *The Philosophical Review* 60.4 (1951), p. 594. ISSN: 00318108. DOI: 10.2307/2181436 (cit. on pp. 27, 28).

[GS91a] Cole Gilbert and Nicholas J. Strausfeld. "The functional organization of male-specific visual neurons in flies". In: *Journal of Comparative Physiology A* 169.4 (1991), pp. 395–411. ISSN: 03407594. DOI: 10.1007/BF00197653 (cit. on p. 102).

[GFN16] Paloma T. Gonzalez-Bellido, Samuel T Fabian, and Karin Nordström. "Target detection in insects: optical, neural and behavioral optimizations". In: *Current Opinion in Neurobiology* 41 (2016), pp. 122–128. ISSN: 09594388. DOI: 10.1016/j.conb.2016.09.001 (cit. on pp. 35, 64).

[Gon+13] Paloma T. Gonzalez-Bellido, Hanchuan Peng, Jinzhu Yang, et al. "Cozzarelli Prize Winner: Eight pairs of descending visual neurons in the dragonfly give wing motor centers accurate population vector of prey direction". In: *Proceedings of the National Academy of Sciences* 110.2 (2013), pp. 696–701. ISSN: 0027-8424. DOI: 10.1073/pnas.1210489109 (cit. on p. 106).

[GCB16] E. Axel Gorostiza, Julien Colomb, and Bjorn Brembs. "A decision underlies phototaxis in an insect". In: *Open Biology* 6.12 (2016). ISSN: 20462441. DOI: 10.1098/rsob.160229 (cit. on p. 24).

[Göt64] Karl Geokg Götz. "0ptomotorische Untersuchung des visuellen Systems einiger Augenmutanten der Fruehtfliege Drosophila". In: *Kybernetik* 2.2 (1964), pp. 77–92. ISSN: 03401200. DOI: 10.1007/BF00288561 (cit. on p. 110).

[Göt68] Karl Georg Götz. "Flight control in Drosophila by visual perception of motion". In: *Kybernetik* 4.6 (1968), pp. 199–208. ISSN: 14320770. DOI: 10.1007/BF00272517 (cit. on p. 30).

[Göt75] Karl Georg Götz. "The optomotor equilibrium of the Drosophila navigation system". In: *Journal of Comparative Physiology A* 99.3 (1975), pp. 187–210. ISSN: 03407594. DOI: 10.1007/BF00613835 (cit. on pp. 35, 37).

[GHK14] Gregory Gremillion, J. Sean Humbert, and Holger G. Krapp. "Bio-inspired modeling and implementation of the ocelli visual system of flying insects". In: *Biological Cybernetics* 108.6 (2014), pp. 735–746. ISSN: 14320770. DOI: 10.1007/s00422-014-0610-x (cit. on p. 115).

[GS91b] Wulfila Gronenberg and Nicholas J. Strausfeld. "Descending pathways connecting the male-specific visual system of flies to the neck and flight motor". In: *Journal of Comparative Physiology A* 169.4 (1991), pp. 413–426. ISSN: 03407594. DOI: 10.1007/BF00197654 (cit. on pp. 42, 103, 113).

[GRR18] Eyal Gruntman, Sandro Romani, and Michael B. Reiser. "Simple integration of fast excitation and offset, delayed inhibition computes directional selectivity in Drosophila". In: *Nature Neuroscience* 21.2 (2018), pp. 250–257. ISSN: 15461726. DOI: 10.1038/s41593-017-0046-4 (cit. on p. 29).

[Hai+13] Väinö Haikala, Maximilian Joesch, Alexander Borst, et al. "Optogenetic control of fly optomotor responses". In: *Journal of Neuroscience* 33.34 (2013), pp. 13927–13934. ISSN: 02706474. DOI: 10.1523/JNEUROSCI.0340-13.2013 (cit. on pp. 32, 104).

[HK16] Ben J. Hardcastle and Holger G. Krapp. "Evolution of Biological Image Stabilization". In: *Current biology : CB* 26.20 (2016), R1010–R1021. ISSN: 09609822. DOI: 10.1016/j.cub.2016.08.059 (cit. on pp. 105, 106, 115, 118).

[Har+81] R.C. Hardie, Nicolas Franceschini, W. Ribi, et al. "Distribution and properties of sex-specific photoreceptors in the fly Musca domestica". In: *Journal of Comparative Physiology A: Neuroethology, Sensory, Neural, and Behavioral Physiology* 145.2 (1981), pp. 139–152. ISSN: 0340-7594. DOI: 10.1007/BF00605029 (cit. on p. 38).

[Har85] Roger C Hardie. *Functional Organization of the Fly Retina*. 1985. DOI: 10.1007/978-3-642-70408-6_1 (cit. on p. 25).

[HSW76] William A Harris, William S Stark, and John A Walker. "Genetic dissection of the photoreceptor system in the compound eye of Drosophila melanogaster". In: *J. Physiol* 256 (1976), pp. 415–439. URL: https://www.ncbi.nlm.nih.gov/pmc/articles/PMC1309314/pdf/jphysiol00854-0161.pdf (cit. on p. 49).

[HGW14] Andreas F Haselsteiner, Cole Gilbert, and Z Jane Wang. "Tiger beetles pursue prey using a proportional control law with a delay of one half-stride". In: *Journal of The Royal Society Interface* 11.95 (2014), p. 20140216. ISSN: 1742-5689, 1742-5662. DOI: 10.1098/rsif.2014.0216 (cit. on p. 82).

[HR53] Bernhard Hassenstein and Werner Reichardt. “Der Schluß von Reiz-Reaktions-Funktionen auf System-Strukturen”. In: *Zeitschrift fur Naturforschung - Section B Journal of Chemical Sciences* 8.9 (1953), pp. 518–524. ISSN: 18657117. DOI: 10.1515/znb-1953-0910 (cit. on p. 104).

[HR56] Bernhard Hassenstein and Werner Reichardt. “Systemtheoretische Analyse der Zeit-, Reihenfolgen- und Vorzeichenauswertung bei der Bewegungsperzeption des Rüsselkäfers”. In: *Z. Naturforschg.* 11B (1956), pp. 513–524 (cit. on p. 29).

[Hat+89] J. H. van Hateren, R. C. Hardie, A. Rudolph, et al. “The bright zone, a specialized dorsal eye region in the male blowfly Chrysomyia megacephala”. In: *Journal of Comparative Physiology A* 164.3 (1989), pp. 297–308. ISSN: 03407594. DOI: 10.1007/BF00612990 (cit. on p. 64).

[HS80] K. Hausen and Nicholas J. Strausfeld. “Sexually Dimorphic Interneuron Arrangements in the Fly Visual System”. In: *Proceedings of the Royal Society of London B* 208.1170 (1980), pp. 57–71. ISSN: 0962-8452. DOI: 10.1098/rspb.1980.0042 (cit. on p. 102).

[Hau82] Klaus Hausen. “Motion sensitive interneurons in the optomotor system of the fly - I. The horizontal cells: Structure and signals”. In: *Biological Cybernetics* 45.2 (1982), pp. 143–156. ISSN: 03401200. DOI: 10.1007/BF00335241 (cit. on p. 104).

[Hau93] Klaus Hausen. “Decoding of retinal image flow in insects.” In: *Rev. Oculomot. Res.* 5 (1993), pp. 203–235 (cit. on p. 29).

[Hed08] Tyson L Hedrick. “Software techniques for two- and three-dimensional kinematic measurements of biological and biomimetic systems.” In: *Bioinspiration & biomimetics* 3.3 (2008), p. 034001. ISSN: 1748-3190. DOI: 10.1088/1748-3182/3/3/034001 (cit. on pp. 54, 59).

[HCD09] Tyson L Hedrick, Bo Cheng, and Xinyan Deng. “Wingbeat time and the scaling of passive rotational damping in flapping flight”. In: *Science* 324.5924 (2009), pp. 252–255. ISSN: 00368075. DOI: 10.1126/science.1168431 (cit. on p. 110).

[HW84] M. Heisenberg and R. Wolf. *Vision in Drosophila*. Springer-Verlag Berlin Heidelberg, 1984 (cit. on p. 37).

[Hen82] R Hengstenberg. “of Giant Vertical Cells in the Lobula Plate of the Blowfly CMliphora”. In: *Journal Of Comparative Physiology* (1982), pp. 179–193 (cit. on p. 104).

[Hen91] Roland Hengstenberg. “Gaze control in the blowfly Calliphora: a multisensory, two-stage integration process”. In: *Seminars in Neuroscience* 3.1 (1991), pp. 19–29. ISSN: 10445765. DOI: 10.1016/1044-5765(91)90063-T (cit. on pp. 115, 117, 118, 121).

[Hor+00] E P Hornstein, David C. O'Carroll, J C Anderson, et al. "Sexual dimorphism matches photoreceptor performance to behavioural requirements." In: *Proceedings. Biological sciences / The Royal Society* 267.1457 (2000), pp. 2111–7. ISSN: 0962-8452. DOI: 10.1098/rspb.2000.1257 (cit. on pp. 38, 42, 64).

[How74] Howard C. Howland. "Optimal strategies for predator avoidance: The relative importance of speed and manoeuvrability". In: *Journal of Theoretical Biology* 47.2 (1974), pp. 333–350. ISSN: 10958541. DOI: 10.1016/0022-5193(74)90202-1 (cit. on p. 65).

[Ila12] Ilan E. Mayer. *corexy.com*. 2012 (cit. on pp. 49, 50).

[Ji+20] Xiaoxiao Ji, Deliang Yuan, Hongying Wei, et al. "Differentiation of Theta Visual Motion from Fourier Motion Requires LC16 and R18C12 Neurons in Drosophila". In: *iScience* 23.4 (2020), p. 101041. ISSN: 25890042. DOI: 10.1016/j.isci.2020.101041 (cit. on p. 37).

[Joe+10] Maximilian Joesch, Bettina Schnell, Shamprasad Varija Raghu, et al. "ON and off pathways in Drosophila motion vision". In: *Nature* 468.7321 (2010), pp. 300–304. ISSN: 00280836. DOI: 10.1038/nature09545 (cit. on p. 29).

[JBH11] Sarah Nicola Jung, Alexander Borst, and Juergen Haag. "Flight activity alters velocity tuning of fly motion-sensitive neurons". In: *Journal of Neuroscience* 31.25 (2011), pp. 9231–9237. ISSN: 02706474. DOI: 10.1523/JNEUROSCI.1138-11.2011 (cit. on p. 29).

[Juu+17] Mikko Juusola, An Dau, Zhuoyi Song, et al. "Microsaccadic sampling of moving image information provides Drosophila hyperacute vision". In: *eLife* 6 (2017), pp. 1–149. ISSN: 2050084X. DOI: 10.7554/eLife.26117 (cit. on p. 42).

[KFR15] Suzanne Amador Kane, Andrew H Fulton, and Lee J Rosenthal. "When hawks attack: animal-borne video studies of goshawk pursuit and prey-evasion strategies." In: *The Journal of experimental biology* 218.Pt 2 (2015), pp. 212–22. ISSN: 1477-9145. DOI: 10.1242/jeb.108597 (cit. on p. 63).

[Kar+18] Matej Karasek, Florian T Muijres, Christophe De Wagter, et al. "A tailless aerial robotic flapper reveals that flies use torque coupling in rapid banked turns". In: *Science* 2.September (2018), pp. 1089–1094 (cit. on p. 110).

[KVF07] L. Kerhuel, S. Viollet, and N. Franceschini. "A sighted aerial robot with fast gaze and heading stabilization". In: *IEEE International Conference on Intelligent Robots and Systems* (2007), pp. 2634–2641. DOI: 10.1109/IROS.2007.4399497 (cit. on p. 115).

[KFM15] Anmo J Kim, Jamie K Fitzgerald, and Gaby Maimon. "Cellular evidence for efference copy in Drosophila visuomotor processing." In: *Nature neuroscience* 18.9 (2015), pp. 1247–1255. ISSN: 1546-1726. DOI: 10.1038/nn.4083 (cit. on p. 106).

[KH17] Michiyo Kinoshita and Uwe Homberg. "Insect Brains: Minute Structures Controlling Complex Behaviors". In: *Brain Evolution by Design: From Neural Origin to Cognitive Architecture*. Ed. by Shigeno Shuichi, Yasunori Murakami, and Tadashi Nomura. Springer, Tokyo, 2017. Chap. 6, pp. 123–151. DOI: 10.1007/978-4-431-56469-0_6 (cit. on p. 24).

[Kla+17] Nathan C. Klapoetke, Aljoscha Nern, Martin Y. Peek, et al. "Ultra-selective looming detection from radial motion opponency". In: *Nature* 551.7679 (2017), pp. 237–241. ISSN: 14764687. DOI: 10.1038/nature24626. URL: http://dx.doi.org/10.1038/nature24626 (cit. on p. 34).

[Kla98] Roberta L. Klatzky. "Allocentric and Egocentric Spatial Representations: Definitions, Distinctions, and Interconnections". In: *Conference on Raumkognition, Trier, Germany, September 1997*. Springer, Berlin, Heidelberg, 1998, pp. 1–17. DOI: 10.1007/3-540-69342-4_1 (cit. on p. 80).

[KV87] J J Koenderink and A.J. Van Doorn. "Representation of Local Geometry in the Visual System". In: *Biological Cybernetics* 362375.55 (1987), pp. 367–375 (cit. on p. 27).

[Kra00] Holger G. Krapp. *Neuronal matched filters for optic flow processing in flying insects*. Vol. 44. Elsevier Masson SAS, 2000, pp. 93–120. DOI: 10.1016/s0074-7742(08)60739-4 (cit. on p. 29).

[Kra+98] Holger G. Krapp, Bärbel Hengstenberg, Roland Hengstenberg, et al. "Dendritic Structure and Receptive-Field Organization of Optic Flow Processing Interneurons in the Fly". In: *Journal of Neurophysiology* 79.4 (1998), pp. 1902–1917. ISSN: 00223077. DOI: 10.1152/jn.1998.79.4.1902 (cit. on p. 28).

[KH96] Holger G. Krapp and Roland Hengstenberg. "Estimation of self-motion by optic flow processing in single visual interneurons". In: *Nature* 384.December (1996), pp. 463–466. ISSN: 00280836. DOI: 10.1038/384463a0 (cit. on pp. 29, 104).

[KH97] Holger G. Krapp and Roland Hengstenberg. "A fast stimulus procedure to determine local receptive field properties of motion-sensitive visual interneurons". In: *Vision Research* 37.2 (1997), pp. 225–234. ISSN: 00426989. DOI: 10.1016/S0042-6989(96)00114-9 (cit. on p. 105).

[KTH12] Holger G. Krapp, Graham K. Taylor, and J. Sean Humbert. "The mode-sensing hypothesis: Matching sensors, actuators and flight dynamics". In: *Frontiers in Sensing: From Biology to Engineering*. Vol. 9783211997. Vienna: Springer Vienna, 2012, pp. 101–114. ISBN: 9783211997499. DOI: 10.1007/978-3-211-99749-9_7 (cit. on p. 104).

[LN95] T. Labhart and D. E. Nilsson. "The dorsal eye of the dragonfly Sympetrum: specializations for prey detection against the blue sky". In: *Journal of Comparative Physiology A* 176.4 (1995), pp. 437–453. ISSN: 03407594. DOI: 10.1007/BF00196410 (cit. on p. 82).

[Lan+19] Benjamin H. Lancer, Bernard J.E. Evans, Joseph M. Fabian, et al. "A Target-Detecting Visual Neuron in the Dragonfly Locks on to Selectively Attended Targets". In: *The Journal of neuroscience : the official journal of the Society for Neuroscience* 39.43 (2019), pp. 8497–8509. ISSN: 15292401. DOI: 10.1523/JNEUROSCI.1431-19.2019 (cit. on p. 24).

[Lan93] Michael F. Land. "Chasing and pursuit in the dolichopodid fly Poecilobothrus nobilitatus". In: *Journal of Comparative Physiology A* 173.5 (1993), pp. 605–613. ISSN: 03407594. DOI: 10.1007/BF00197768 (cit. on p. 88).

[Lan97] Michael F. Land. "Visual Acuity in Insects". In: *Annual Review of Entomology* 42.1 (1997), pp. 147–177. ISSN: 0066-4170. DOI: 10.1146/annurev.ento.42.1.147 (cit. on p. 25).

[Lan19] Michael F. Land. "Eye movements in man and other animals". In: *Vision Research* 162.June (2019), pp. 1–7. ISSN: 18785646. DOI: 10.1016/j.visres.2019.06.004 (cit. on p. 30).

[LC74] Michael F. Land and Thomas S Collett. "Chasing behaviour of houseflies (Fannia canicularis)". In: *Journal of Comparative Physiology* 89.4 (1974), pp. 331–357. ISSN: 0340-7594. DOI: 10.1007/BF00695351 (cit. on pp. 35, 64, 65, 82, 88, 102, 103, 113, 121).

[LE85] Michael F. Land and H. Eckert. "Maps of the acute zones of fly eyes". In: *Journal of Comparative Physiology A* 156.4 (1985), pp. 525–538. ISSN: 03407594. DOI: 10.1007/BF00613976 (cit. on pp. 38, 41, 64, 102).

[LN12] Michael F. Land and Dan-Eric Nilsson. *Animal eyes*. 2nd ed. Oxford Animal Biology Series, 2012, p. 221. ISBN: 0-19-850968-5. DOI: DOI:10.1111/j.1463-6395.2012.00570.x (cit. on pp. 24, 25, 64).

[LW93] S B Laughlin and M. Weckström. "Fast and slow photoreceptors - a comparative study of the functional diversity of coding and conductances in the Diptera". In: *Journal of Comparative Physiology A* 172.5 (1993), pp. 593–609. ISSN: 03407594. DOI: 10.1007/BF00213682 (cit. on p. 27).

[LD97] Fritz Olaf Lehmann and Michael H. Dickinson. "The changes in power requirements and muscle efficiency during elevated force production in the fruit fly Drosophila melanogaster". In: *Journal of Experimental Biology* 200.7 (1997), pp. 1133–1143. ISSN: 00220949 (cit. on p. 32).

[Lin+03] J. P. Lindemann, R. Kern, C. Michaelis, et al. "FliMax, a novel stimulus device for panoramic and highspeed presentation of behaviourally generated optic flow". In: *Vision Research* 43.7 (2003), pp. 779–791. ISSN: 00426989. DOI: 10.1016/S0042-6989(03)00039-7 (cit. on p. 32).

[Lin+05] J. P. Lindemann, Roland Kern, J H van Hateren, et al. "On the Computations Analyzing Natural Optic Flow: Quantitative Model Analysis of the Blowfly Motion Vision Pathway". In: *Journal of Neuroscience* 25.27 (2005), pp. 6435–6448. ISSN: 0270-6474. DOI: 10.1523/JNEUROSCI.1132-05.2005 (cit. on pp. 101, 109).

[Liu+19] Pan Liu, Sanjay P. Sane, Jean Michel Mongeau, et al. "Flies land upside down on a ceiling using rapid visually mediated rotational maneuvers". In: *Science Advances* 5.10 (2019). ISSN: 23752548. DOI: 10.1126/sciadv.aax1877 (cit. on p. 44).

[Loa92] Dimitrios Loannis Peppas. "Proportional Navigation and Command To Line of Sight of a Command Guided Missile for a Point Defence System". PhD thesis. Naval postgraduate school Monterey, California, 1992 (cit. on p. 84).

[LK10] Kit D. Longden and Holger G. Krapp. "Octopaminergic modulation of temporal frequency coding in an identified optic flow-processing interneuron". In: *Frontiers in Systems Neuroscience* 4.November (2010), pp. 1–12. ISSN: 16625137. DOI: 10.3389/fnsys.2010.00153 (cit. on p. 29).

[Lon+14] Kit D. Longden, Tomaso Muzzu, Daniel J. Cook, et al. "Nutritional state modulates the neural processing of visual motion". In: *Current Biology* 24.8 (2014), pp. 890–895. ISSN: 09609822. DOI: 10.1016/j.cub.2014.03.005 (cit. on p. 24).

[MS18] Mandiyam Y. Mahadeeswara and Mandyam V. Srinivasan. "Coordinated Turning Behaviour of Loitering Honeybees". In: *Scientific Reports* 8 (2018), pp. 1–14. ISSN: 20452322. DOI: 10.1038/s41598-018-35307-5 (cit. on p. 110).

[MSD10] Gaby Maimon, Andrew D. Straw, and Michael H. Dickinson. "Active flight increases the gain of visual motion processing in Drosophila". In: *Nature Neuroscience* 13.3 (2010), pp. 393–399. ISSN: 10976256. DOI: 10.1038/nn.2492 (cit. on p. 24).

[McC11] N. Harris McClamroch. *Steady Aircraft Flight and Performance*. Princeton University Press, 2011, p. 417. ISBN: 1400839068 (cit. on p. 110).

[McH+19] Matthew J. McHenry, Jacob L. Johansen, Alberto P. Soto, et al. "The pursuit strategy of predatory bluefish (Pomatomus saltatrix)". In: *Proceedings of the Royal Society B: Biological Sciences* 286.1897 (2019), pp. 1–6. ISSN: 14712954. DOI: 10.1098/rspb.2018.2934 (cit. on p. 82).

[MB91] R Menzel and W Backhaus. "Colour vision in insects". In: *Gouras P (ed) Vision and visual dysfunction. The perception of colour*. MacMillan, London, 1991, pp. 262–288 (cit. on p. 49).

[MW92] FA Miles and J. Wallmab. *Visual Motion and its Role in the Stabilization of Gaze: Reviews of Oculamotor Research*. Elsevier Science Ltd, 1992. ISBN: 978-0444811950 (cit. on p. 30).

[Mis+15] Matteo Mischiati, Huai-Ti Lin, Paul Herold, et al. "Internal models direct dragonfly interception steering". In: *Nature* 517.7534 (2015), pp. 333–338. ISSN: 0028-0836. DOI: 10.1038/nature14045 (cit. on pp. 47, 90, 115, 117).

[Mon+19] Jean Michel Mongeau, Karen Y. Cheng, Jacob Aptekar, et al. "Visuomotor strategies for object approach and aversion in Drosophila melanogaster". In: *Journal of Experimental Biology* 222.3 (2019). ISSN: 00220949. DOI: 10.1242/jeb.193730 (cit. on p. 37).

[MF17] Jean Michel Mongeau and Mark A. Frye. "Drosophila Spatiotemporally Integrates Visual Signals to Control Saccades". In: *Current Biology* 27.19 (2017), 2901–2914.e2. ISSN: 09609822. DOI: 10.1016/j.cub.2017.08.035 (cit. on p. 37).

[ML08] Markus Mronz and Fritz Olaf Lehmann. "The free-flight response of Drosophila to motion of the visual environment". In: *Journal of Experimental Biology* 211.13 (2008), pp. 2026–2045. ISSN: 00220949. DOI: 10.1242/jeb.008268 (cit. on pp. 31, 32).

[Mui+14] Florian T. Muijres, Michael J. Elzinga, Johan M. Melis, et al. "Flies Evade Looming Targets by Executing Rapid Visually Directed Banked Turns". In: *Science* 344.4 (2014), pp. 172–177. ISSN: 15481433. DOI: 10.1111/aman.12147 (cit. on pp. 32, 34, 67, 110).

[Nah12] Paul J. Nahin. *Chases and escapes : the mathematics of pursuit and evasion*. Princeton University Press, 2012, p. 253. ISBN: 1400842069 (cit. on p. 82).

[NH94] Gerbera Nalbach and Roland Hengstenberg. "The halteres of the blowfly Calliphora - II. Three-dimensional organization of compensatory reactions to real and simulated rotations". In: *Journal of Comparative Physiology A* 175.6 (1994), pp. 695–708. ISSN: 03407594. DOI: 10.1007/BF00191842 (cit. on p. 84).

[Nil89] Dan-Eric Nilsson. "Optics and Evolution of the Compound Eye". In: *Facets of Vision*. Springer Berlin Heidelberg, 1989, pp. 30–73. DOI: 10.1007/978-3-642-74082-4_3 (cit. on p. 42).

[Nit+18] Vivek Nityananda, Ghaith Tarawneh, Sid Henriksen, et al. "A Novel Form of Stereo Vision in the Praying Mantis Current Biology Report A Novel Form of Stereo Vision in the Praying Mantis". In: *Current Biology* 28 (2018), pp. 1–6. DOI: 10.1016/j.cub.2018.01.012. URL: https://doi.org/10.1016/j.cub.2018.01.012 (cit. on p. 38).

[Nor12] Karin Nordström. "Neural specializations for small target detection in insects". In: *Current Opinion in Neurobiology* 22.2 (2012), pp. 272–278. ISSN: 09594388. DOI: 10.1016/j.conb.2011.12.013 (cit. on p. 106).

[NBO06] Karin Nordström, Paul D. Barnett, and David C. O'Carroll. "Insect detection of small targets moving in visual clutter". In: *PLoS Biology* 4.3 (2006), pp. 0378–0386. ISSN: 15457885. DOI: 10.1371/journal.pbio.0040054 (cit. on pp. 42, 106).

[OCa93] David C. O'Carroll. "Feature-detecting neurons in dragonflies". In: *Nature* 362.6420 (1993), pp. 541–543. ISSN: 00280836. DOI: 10.1038/362541a0 (cit. on p. 106).

[OCa+96] David C. O'Carroll, N. J. Bidwell, S. B. Laughlin, et al. "Insect motion detectors matched to visual ecology". In: *Nature* 382.6586 (1996), pp. 63–66. ISSN: 00280836. DOI: 10.1038/382063a0 (cit. on p. 104).

[Olb+07] R. M. Olberg, R. C. Seaman, M. I. Coats, et al. "Eye movements and target fixation during dragonfly prey-interception flights". In: *Journal of Comparative Physiology A: Neuroethology, Sensory, Neural, and Behavioral Physiology* 193.7 (2007), pp. 685–693. ISSN: 03407594. DOI: 10.1007/s00359-007-0223-0 (cit. on pp. 47, 82).

[OWV00] RM M Olberg, AH H Worthington, and KR R Venator. "Prey pursuit and interception in dragonflies." In: *Journal of comparative physiology. A, Sensory, neural, and behavioral physiology* 186.2 (2000), pp. 155–162. ISSN: 0340-7594. DOI: 10.1007/s003590050015 (cit. on pp. 38, 86).

[Olb12] Robert M. Olberg. "Visual control of prey-capture flight in dragonflies". In: *Current Opinion in Neurobiology* 22.2 (2012), pp. 267–271. ISSN: 09594388. DOI: 10.1016/j.conb.2011.11.015 (cit. on p. 115).

[Pal15] S. Pal. "Dynamics of aerial target pursuit". In: *The European Physical Journal Special Topics* 224.17-18 (2015), pp. 3295–3309. ISSN: 1951-6355. DOI: 10.1140/epjst/e2015-50084-6 (cit. on pp. 43, 65).

[PZG20] Rachel H. Parkinson, Sinan Zhang, and John R. Gray. "Neonicotinoid and sulfoximine pesticides differentially impair insect escape behavior and motion detection". In: *Proceedings of the National Academy of Sciences of the United States of America* 117.10 (2020), pp. 5510–5515. ISSN: 10916490. DOI: 10.1073/pnas.1916432117 (cit. on p. 24).

[PKL10] Matthew M. Parsons, Holger G. Krapp, and Simon B. Laughlin. "Sensor fusion in identified visual interneurons." In: *Current biology : CB* 20.7 (2010), pp. 624–8. ISSN: 1879-0445. DOI: 10.1016/j.cub.2010.01.064 (cit. on p. 117).

[Pet+00] Ralf Petrowitz, Hansjürgen Dahmen, Martin Egelhaaf, et al. "Arrangement of optical axes and spatial resolution in the compound eye of the female blowfly Calliphora". In: *Journal of Comparative Physiology - A Sensory, Neural, and Behavioral Physiology* 186.7-8 (2000), pp. 737–746. ISSN: 03407594. DOI: 10.1007/s003590000127 (cit. on p. 25).

[PYR11] Mark Pierce, Dihua Yu, and Rebecca Richards-Kortum. "High-resolution Fiber-optic Microendoscopy for in situ Cellular Imaging". In: *Journal of vision experiment* 47 (2011), e2306. ISSN: 1940-087X. DOI: doi:10.3791/2306 (cit. on p. 67).

[Pin79] B Y Robert B Pinter. "Inhibition and Excitation in the Locust DCMD Receptive Field: Spatial Frequency, Temporal and Spatial Characteristics". In: *Journal of Experimental Biology* 80.1 (1979), pp. 191–216. ISSN: 0022-0949 (cit. on p. 34).

[PR76] Tomaso Poggio and Werner Reichardt. "Visual control of orientation behaviour in the fly: Part II. Towards the underlying neural interactions". In: *Quarterly Reviews of Biophysics* 9.03 (1976), p. 377. ISSN: 0033-5835. DOI: 10.1017/S0033583500002535 (cit. on pp. 32, 37).

[PRF10] Geoffrey Portelli, Franck Ruffier, and Nicolas Franceschini. "Honeybees change their height to restore their optic flow". In: *Journal of Comparative Physiology A: Neuroethology, Sensory, Neural, and Behavioral Physiology* 196.4 (2010), pp. 307–313. ISSN: 03407594. DOI: 10.1007/s00359-010-0510-z (cit. on p. 49).

[Pra+80] J. P. van Praagh, W Ribi, C Wehrhahn, et al. "Drone bees fixate the queen with the dorsal frontal part of their compound eyes". In: *Journal of Comparative Physiology A* 136.3 (1980), pp. 263–266. ISSN: 03407594. DOI: 10.1007/BF00657542 (cit. on p. 90).

[RJ16] Nadine Randel and Gáspár Jékely. "Phototaxis and the origin of visual eyes". In: *Philosophical Transactions of the Royal Society B: Biological Sciences* 371.1685 (2016). ISSN: 14712970. DOI: 10.1098/rstb.2015.0042 (cit. on p. 25).

[RP76] Werner R. Reichardt and Tomaso Poggio. "Visual control of orientation behaviour in the fly. Part I. A quantitative analysis". In: *Quarterly Reviews of Biophysics* 9.3 (1976), pp. 311–375. ISSN: 0033-5835. DOI: 10.1017/S0033583500002523 (cit. on p. 35).

[Rey+17] Catherine R. von Reyn, Aljoscha Nern, W. Ryan Williamson, et al. "Feature Integration Drives Probabilistic Behavior in the Drosophila Escape Response". In: *Neuron* 94.6 (2017), 1190–1204.e6. ISSN: 10974199. DOI: 10.1016/j.neuron.2017.05.036 (cit. on p. 35).

[RF84] A. Riehle and Nicolas Franceschini. "Motion detection in flies: Parametric control over ON-OFF pathways". In: *Experimental Brain Research* 54.2 (1984), pp. 390–394. ISSN: 00144819. DOI: 10.1007/BF00236243 (cit. on pp. 29, 42, 104).

[RWO17] Elisa Rigosi, Steven D. Wiederman, and David C. O'Carroll. "Visual acuity of the honey bee retina and the limits for feature detection". In: *Scientific Reports* 7 (2017), pp. 1–7. ISSN: 20452322. DOI: 10.1038/srep45972 (cit. on p. 42).

[Rin+20] F Claire Rind, Lisa Jones, Ghaith Tarawneh, et al. "Target tracking behaviour of the praying mantis Sphrodromantis lineola (Linnaeus) is driven by looming-type motion-detectors . Key words". In: *bioRxiv* (2020) (cit. on p. 106).

[Ris+09] Leif Ristroph, Gordon J Berman, Attila J Bergou, et al. "Automated hull reconstruction motion tracking (HRMT) applied to sideways maneuvers of free-flying insects." In: *The Journal of experimental biology* 212 (2009), pp. 1324–1335. ISSN: 0022-0949. DOI: 10.1242/jeb.025502 (cit. on p. 67).

[Ros+09] R. Rosner, M. Egelhaaf, J. Grewe, et al. "Variability of blowfly head optomotor responses". In: *Journal of Experimental Biology* 212.8 (2009), pp. 1170–1184. ISSN: 00220949. DOI: 10.1242/jeb.027060 (cit. on p. 24).

[SB15] Tabea Schilling and Alexander Borst. "Local motion detectors are required for the computation of expansion Flow-Fields". In: *Biology Open* 4.9 (2015), pp. 1105–1108. ISSN: 20466390. DOI: 10.1242/bio.012690 (cit. on p. 34).

[SH99] C. Schilstra and J.H. Hateren. "Blowfly flight and optic flow. I. Thorax kinematics and flight dynamics". In: *J. Exp. Biol.* 202.11 (1999), pp. 1481–1490. ISSN: 14779145 (cit. on pp. 85, 110, 113).

[SV98] C. Schilstra and J. H. Van Hateren. "Using miniature sensor coils for simultaneous measurement of orientation and position of small, fast-moving animals". In: *Journal of Neuroscience Methods* 83.2 (1998), pp. 125–131. ISSN: 01650270. DOI: 10.1016/S0165-0270(98)00069-7 (cit. on p. 67).

[SSG02] Stefan Schuster, Roland Strauss, and Karl G. Götz. "Virtual-reality techniques resolve the visual cues used by fruit flies to evaluate object distances". In: *Current Biology* 12.18 (2002), pp. 1591–1594. ISSN: 09609822. DOI: 10.1016/S0960-9822(02)01141-7 (cit. on p. 37).

[Sch+11] Daniel A. Schwyn, Francisco J.H. H Heras, Gino Bolliger, et al. “Interplay between feedback and feedforward control in fly gaze stabilization”. In: *IFAC Proceedings Volumes (IFAC-PapersOnline)*. Vol. 18. 2011, pp. 9674–9679. ISBN: 9783902661937. DOI: 10.3182/20110828-6-IT-1002.03809 (cit. on p. 115).

[She78] Truman E. Sherk. “Development of the compound eyes of dragonflies (odonata). III. Adult compound eyes”. In: *Journal of Experimental Zoology* 203.1 (1978), pp. 61–79. ISSN: 1097010X. DOI: 10.1002/jez.1402030107 (cit. on p. 64).

[Shn98] N.A. Shneydor. “Mechanization of Proportional Navigation”. In: *Missile Guidance and Pursuit* x.x (1998), pp. 129–163 (cit. on pp. 43, 84).

[SJL10] Klaus S. Sollmann, Musa K. Jouaneh, and David Lavender. “Dynamic modeling of a two-axis, parallel, H-frame-type XY positioning system”. In: *IEEE/ASME Transactions on Mechatronics* 15.2 (2010), pp. 280–290. ISSN: 10834435. DOI: 10.1109/TMECH.2009.2020823 (cit. on p. 49).

[Str76] Nicholas J. Strausfeld. *Atlas of an Insect Brain*. Springer Berlin Heidelberg, 1976. DOI: 10.1007/978-3-642-66179-2 (cit. on pp. 24, 27).

[Str80] Nicholas J. Strausfeld. “Male and female visual neurons in Dipterous insects”. In: *Nature* 283.5745 (1980), pp. 381–383. ISSN: 00280836. DOI: 10.1038/283381a0 (cit. on p. 102).

[Str91] Nicholas J. Strausfeld. “Structural organization of male-specific visual neurons in calliphorid optic lobes.” In: *Journal of comparative physiology. A, Sensory, neural, and behavioral physiology* 169.4 (1991), pp. 379–93. ISSN: 0340-7594. DOI: 10.1007/BF00197652 (cit. on p. 42).

[Str12] Nicholas J. Strausfeld. *Arthropod Brains*. Press, Harvard University, 2012, p. 848. ISBN: 9780674046337 (cit. on p. 102).

[SSM87] Nicholas J. Strausfeld, H. S. Seyan, and J. J. Milde. “The neck motor system of the fly Calliphora erythrocephala I. Muscles and motor neurons”. In: *Journal of Comparative Physiology A* 160.2 (1987), pp. 205–224. ISSN: 03407594. DOI: 10.1007/BF00609727 (cit. on p. 115).

[Str+11] Andrew D Straw, Kristin Branson, Titus R Neumann, et al. “Multi-camera real-time three-dimensional tracking of multiple flying animals.” In: *Journal of the Royal Society, Interface* 8.56 (2011), pp. 395–409. ISSN: 1742-5662. DOI: 10.1098/rsif.2010.0230. arXiv: 1001.4297 (cit. on p. 67).

[SSS15] Reuben Strydom, Surya P.N. N. Singh, and Mandyam V. Srinivasan. “Biologically inspired interception: A comparison of pursuit and constant bearing strategies in the presence of sensorimotor delay”. In: *2015 IEEE International Conference on Robotics and Biomimetics (ROBIO)* (2015), pp. 2442–2448. DOI: 10.1109/ROBIO.2015.7419705 (cit. on p. 94).

[Suk+08] Kom Kabkaew L. Sukontason, Tarinee Chaiwong, Somsak Piangjai, et al. "Ommatidia of blow fly, house fly, and flesh fly: Implication of their vision efficiency". In: *Parasitology Research* 103.1 (2008), pp. 123–131. ISSN: 09320113. DOI: 10.1007/s00436-008-0939-y (cit. on p. 41).

[Sup+20] Jack A Supple, Daniel Pinto-Benito, Christopher Khoo, et al. "Binocular Encoding in the Damselfly Pre-motor Target Tracking System". In: *Current Biology* (2020), pp. 1–12. ISSN: 09609822. DOI: 10.1016/j.cub.2019.12.031 (cit. on p. 38).

[Suv+16] Marie P Suver, Ainul Huda, Nicole Iwasaki, et al. "An Array of Descending Visual Interneurons Encoding Self-Motion in Drosophila". In: *The Journal of Neuroscience* 36.Xx (2016), pp. 1–13. ISSN: 0270-6474. DOI: 10.1523/JNEUROSCI.2277-16.2016 (cit. on p. 24).

[TD02] Lance F. Tammero and Michael H. Dickinson. "Collision-avoidance and landing responses are mediated by separate pathways in the fruit fly, Drosophila melanogaster." In: *The Journal of experimental biology* 205.Pt 18 (2002), pp. 2785–2798. ISSN: 0022-0949. DOI: 10.1007/BF01139758 (cit. on pp. 33, 34, 67, 108).

[TK07] Graham K. Taylor and Holger G. Krapp. *Sensory Systems and Flight Stability: What do Insects Measure and Why?* Vol. 34. Elsevier Ltd, 2007, pp. 231–316. ISBN: 9780123737144. DOI: 10.1016/S0065-2806(07)34005-8 (cit. on p. 104).

[TRF10] Jamie C Theobald, Dario L Ringach, and Mark A. Frye. "Visual stabilization dynamics are enhanced by standing flight velocity." In: *Biology letters* 6.3 (2010), pp. 410–3. ISSN: 1744-957X. DOI: 10.1098/rsbl.2009.0845 (cit. on p. 32).

[The+08] Jamie Carroll Theobald, Brian J Duistermars, Dario L Ringach, et al. "Flies see second- order motion". In: *Cell* 18.11 (2008), pp. 464–465. ISSN: 0960-9822. DOI: 10.1016/j.cub.2008.03.050 (cit. on p. 37).

[Thy+18] Malin Thyselius, Paloma T. Gonzalez-Bellido, Trevor J. Wardill, et al. "Visual approach computation in feeding hoverflies". In: *Journal of Experimental Biology* 221.10 (2018). ISSN: 00220949. DOI: 10.1242/jeb.177162 (cit. on p. 43).

[TP78] V. Torre and T. Poggio. "A synaptic mechanism possibly underlying directional selectivity to motion". In: *Proceedings of the Royal Society of London - Biological Sciences* 202.1148 (1978), pp. 409–416. ISSN: 09628452. DOI: 10.1098/rspb.1978.0075 (cit. on p. 29).

[TBE07] Christine Trischler, Norbert Boeddeker, and Martin Egelhaaf. "Characterisation of a blowfly male-specific neuron using behaviourally generated visual stimuli". In: *Journal of Comparative Physiology A: Neuroethology, Sensory, Neural, and Behavioral Physiology* 193.5 (2007), pp. 559–572. ISSN: 03407594. DOI: 10.1007/s00359-007-0212-3 (cit. on pp. 84, 102).

[TKE10] Christine Trischler, Roland Kern, and Martin Egelhaaf. "Chasing behavior and optomotor following in free-flying male blowflies: flight performance and interactions of the underlying control systems." In: *Frontiers in behavioral neuroscience* 4.May (2010), p. 20. ISSN: 1662-5153. DOI: 10.3389/fnbeh.2010.00020 (cit. on pp. 32, 38, 105, 106, 120).

[VD12] Floris Van Breugel and Michael H. Dickinson. "The visual control of landing and obstacle avoidance in the fruit fly Drosophila melanogaster". In: *Journal of Experimental Biology* 215.11 (2012), pp. 1783–1798. ISSN: 00220949. DOI: 10.1242/jeb.066498 (cit. on p. 34).

[VKV19] Léandre P. Varennes, Holger G. Krapp, and Stéphane Viollet. "A novel setup for 3D chasing behavior analysis in free flying flies". In: *Journal of Neuroscience Methods* 321.April (2019), pp. 28–38. ISSN: 1872678X. DOI: 10.1016/j.jneumeth.2019.04.006 (cit. on pp. 47, 50, 51, 53, 55, 57, 60, 62, 66, 68, 75–77, 94, 115).

[Vio14] Stéphane Viollet. "Vibrating makes for better seeing: From the fly's micro-eye movements to hyperacute visual sensors". In: *Frontiers in Bioengineering and Biotechnology* 2.APR (2014), p. 9. ISSN: 22964185. DOI: 10.3389/fbioe.2014.00009 (cit. on p. 42).

[VM50] E Von Holst and H Mittelstaedt. "The principle of reafference: Interactions between the central nervous system and the peripheral organs". In: *PC Dodwell (Ed. and Trans.), Perceptual processing: Stimulus equivalence and pattern recognition* (1950), pp. 41–72 (cit. on pp. 106, 117).

[Wag86a] H Wagner. "Flight performance and visual control of flight of the free-flying housefly (musca domestical L.) III. Interactions between angular movement induced by wide- and smallfield stimuli". In: *Philosophical Transactions of the Royal Society of London. B, Biological Sciences* 312.1158 (1986), pp. 581–595. ISSN: 0080-4622. DOI: 10.1098/rstb.1986.0019 (cit. on pp. 37, 63).

[Wag86b] H. Wagner. "Flight performance and visual control of flight of the free-flying housefly (Musca domestica l.) II. Pursuit of targets". In: *Philosophical Transactions of the Royal Society B: Biological Sciences* 312.1158 (1986), pp. 527–551. ISSN: 0962-8436. DOI: 10.1098/rstb.1986.0018 (cit. on p. 35).

[War+17] Trevor J Wardill, Samuel T Fabian, Ann C Pettigrew, et al. "A Novel Interception Strategy in a Miniature Robber Fly with Extreme Visual Acuity". In: *Current Biology* 27.6 (2017), pp. 854–859. ISSN: 09609822. DOI: 10.1016/j.cub.2017.01.050 (cit. on pp. 38, 42, 47, 63, 64, 82, 84, 90).

[War+15] Trevor J. Wardill, Katie Knowles, Laura Barlow, et al. "The killer fly hunger games: Target size and speed predict decision to pursuit". In: *Brain, Behavior and Evolution* 86.October (2015), pp. 28–37. ISSN: 00068977. DOI: 10.1159/000435944 (cit. on pp. 38, 42, 43, 47).

[War16] Eric J Warrant. *Sensory matched filters*. 2016. DOI: 10.1016/j.cub.2016.05.042 (cit. on p. 41).

[Weh87] Rüdiger Wehner. "'Matched filters' - neural models of the external world". In: *Journal of Comparative Physiology A* 161.4 (1987), pp. 511–531. ISSN: 03407594. DOI: 10.1007/BF00603659 (cit. on pp. 25, 43).

[WS00] Martina Wicklein and Nicholas J. Strausfeld. "Organization and significance of neurons that detect change of visual depth in the hawk moth Manduca sexta". In: *Journal of Comparative Neurology* 424.2 (2000), pp. 356–376. ISSN: 00219967. DOI: 10.1002/1096-9861(20000821)424:2<356::AID-CNE12>3.0.CO;2-T (cit. on p. 34).

[Wie+17] Steven D. Wiederman, Joseph M. Fabian, James R. Dunbier, et al. "A predictive focus of gain modulation encodes target trajectories in insect vision". In: *eLife* 6 (2017), pp. 1–19. ISSN: 2050084X. DOI: 10.7554/eLife.26478 (cit. on p. 106).

[WO13] Steven D. Wiederman and David C. O'Carroll. "Selective attention in an insect visual neuron". In: *Current Biology* 23.2 (2013), pp. 156–161. ISSN: 09609822. DOI: 10.1016/j.cub.2012.11.048 (cit. on p. 24).

[WSO08] Steven D. Wiederman, Patrick A. Shoemaker, and David C. O'Carroll. "A model for the detection of moving targets in visual clutter inspired by insect physiology". In: *PLoS ONE* 3.7 (2008), pp. 1–11. ISSN: 19326203. DOI: 10.1371/journal.pone.0002784 (cit. on p. 106).

[YDH10] Satoko Yamaguchi, Claude Desplan, and Martin Heisenberg. "Contribution of photoreceptor subtypes to spectral wavelength preference in Drosophila". In: *Proceedings of the National Academy of Sciences of the United States of America* 107.12 (2010), pp. 5634–5639. ISSN: 00278424. DOI: 10.1073/pnas.0809398107 (cit. on p. 27).

[Zha+90] S. W. Zhang, Wang Xiang, Liu I U Zili, et al. "Visual tracking of moving targets by freely flying honeybees". In: *Visual neuroscience* 4.04 (1990), pp. 379–386. ISSN: 0952-5238. DOI: 10.1017/S0952523800004582 (cit. on pp. 37, 82, 88).

[Zha+13] Xiaonan Zhang, He Liu, Zhengchang Lei, et al. “Lobula-specific visual projection neurons are involved in perception of motiondefined second-order motion in Drosophila”. In: *Journal of Experimental Biology* 216.3 (2013), pp. 524–534. ISSN: 00220949. DOI: 10.1242/jeb.079095 (cit. on p. 37).

[Zhu+18] Ying Zhu, Richard B. Dewell, Hongxia Wang, et al. “Pre-synaptic Muscarinic Excitation Enhances the Discrimination of Looming Stimuli in a Collision-Detection Neuron”. In: *Cell Reports* 23.8 (2018), pp. 2365–2378. ISSN: 22111247. DOI: 10.1016/j.celrep.2018.04.079 (cit. on p. 34).

ANNEXE

The programmes and raw data will be made available at the following address https://github.com/veandre/chasing-arena